2020

# Throughput Maximization in Unmanned Aerial Vehicle Networks

Saadullah Kalwar

# Throughput Maximization in Unmanned Aerial Vehicle Networks

A thesis submitted in partial fulfilment of the requirements for the award of the degree

Doctor of Philosophy

from

UNIVERSITY OF WOLLONGONG

by

Saadullah Kalwar

Masters of Engineering (Telecommunications)

Bachelor of Engineering (Telecommunications)

School of Electrical, Computer and Telecommunications Engineering

February 2020

# Statement of Originality

I, Saadullah Kalwar, declare that this thesis, submitted in partial fulfilment of the requirements for the award of Doctor of Philosophy, in the School of Electrical, Computer and Telecommunications Engineering, University of Wollongong, is wholly my own work unless otherwise referenced or acknowledged. The document has not been submitted for qualifications at any other academic institutions.

Signed

Saadullah Kalwar

February, 2020

# Abstract

The use of Unmanned Aerial Vehicles (UAVs) swarms in civilian applications such as surveillance, agriculture, search and rescue, and border patrol is becoming popular. UAVs have also found use as mobile or portable base stations. In these applications, communication requirements for UAVs are generally stricter as compared to conventional aircrafts. Hence, there needs to be an efficient Medium Access Control (MAC) protocol that ensures UAVs experience low channel access delays and high throughput. Some challenges when designing UAVs MAC protocols include interference and rapidly changing channel states, which require a UAV to adapt its data rate to ensure data transmission success. Other challenges include Quality of Service (QoS) requirements and multiple contending UAVs that result in collisions and channel access delays.

To this end, this thesis aims to utilize Multi-Packet Reception (MPR) technology. In particular, it considers nodes that are equipped with a Successive Interference Cancellation (SIC) radio, and thereby, allowing them to receive multiple transmissions simultaneously. A key problem is to identify a suitable a Time Division Multiple Access (TDMA) transmission schedule that allows UAVs to transmit successfully and frequently. Moreover, in order for SIC to operate, there must be a sufficient difference in received power. However, in practice, due to the location and orientation of nodes, the received power of simultaneously transmitting nodes

may cause SIC decoding to fail at a receiver. Consequently, a key problem concerns the placement and orientation of UAVs to ensure there is diversity in received signal strength at a receiving node. Lastly, interference between UAVs serving as base station is a critical issue. In particular, their respective location may have excessive interference or cause interference to other UAVs; all of which have an impact on the schedule used by these UAVs to serve their respective users.

To address the first problem, this thesis adopts a discrete optimization approach to select a transmission schedule that yields the highest expected number of successes over random channel gains. In addition, it proposes a novel heuristic approach to generate a subset of transmission schedules for use in large-scale UAV networks. The results show both proposed approaches yield high throughput under various network conditions. The average number of successful transmissions for schedules generated by the proposed solutions is greater than 70%. In contrast, a competing approach only has an average success rate of less than 50%. The work also includes a trace-based simulation using data from a test-bed with three static or mobile UAVs. The results show that using a transmission schedule where at most two UAVs transmit yields more transmission successes.

As for the second problem, this thesis introduces a novel Learning Medium Access Control (L-MAC) for multi-rate UAVs. The ground station uses L-MAC to learn a TDMA schedule length that yields the highest throughput. UAVs, on the other hand, use L-MAC to learn the best transmission slot and data rate for a given frame length. In addition, UAVs can also use L-MAC to learn the optimal orientation that yields the highest transmission success. Extensive simulation results show that L-MAC achieves up to five times higher throughput as compared to the well-known Aloha protocol. Specifically, L-MAC achieves a throughput of 500 kbps as compared to 100 kbps for Aloha. In comparison, Aloha with SIC achieves a throughput of 300 kbps for the same network scenario. The results also show that the frame length is always set to around 60% to 75% of the total number of UAVs.

Finally, this thesis considers optimizing the location of UAVs in order to improve

network capacity. A key challenge is the interference caused by transmitting ground devices in neighboring cells. This problem is solved using a Gibbs sampling approach where UAVs sample discrete locations to find the optimal location that leads to the minimal schedule length. Simulation results show that the proposed approach results in schedule lengths that are up to 17% shorter as compared to simply placing UAVs at equidistant to all ground nodes. Results also show that the optimal schedule length is 110 time slots per frame in case of 250 ground devices, which equates to approximately 44% of the total number of ground devices.

# Acknowledgments

First and foremost, I would like to thank my principal supervisor, Associate Professor Kwan-Wu Chin for his guidance and utmost patience. He spent a lot of time working with me on my writing and technical skills. Despite being overly busy, he always responded to my queries in a short time and always provided quick feedback. Without his constant support, I would not be able to finish this project.

I like to thank all anonymous reviewers at conferences and journals for their time and efforts they spend in giving valuable comments. Their suggestions have certainly raised the quality of my publications.

I would like to say special thanks to my friends and lab mates in building 39A.201, Mr. Zeeshan Sarwar, Ms. Yishun Wang and other friends, for countless discussions and pleasant working environment.

In the end, I would like to thank my family for always supporting and encouraging me. Specially, my mother for countless prayers. Without their support, I could not be at this stage.

# Contents

# List of Figures

# List of Tables

# Abbreviations

| | |
|---|---|
| **UAV** | Unmanned Aerial Vehicle |
| **MAC** | Medium Access Control |
| **VTOL** | Vertical Take-Off and Landing |
| **LiDAR** | Light Detection and Ranging |
| **ATC** | Air Traffic Controller |
| **GPS** | Global Positioning System |
| **MANET** | Mobile Ad-hoc Network |
| **VANET** | Vehicular Ad-hoc Network |
| **FANET** | Flying Ad-hoc Network |
| **DSR** | Dynamic Source Routing |
| **GPSR** | Greedy Perimeter Stateless Routing |
| **MPR** | Multi-Packet Reception |
| **CDMA** | Code Division Multiple Access |
| **CSI** | Channel State Information |
| **WSN** | Wireless Sensor Network |
| **TDMA** | Time Division Multiple Access |
| **CSMA-CA** | Carrier Sense Multiple Access with Collision Avoidance |
| **BER** | Bit Error Rate |
| **RLC** | Random Linear Combination |

| | |
|---|---|
| **RTS** | Request to Send |
| **CTS** | Clear to Send |
| **RTP** | Request to Pair |
| **CMA** | Cyclic Multiple Access |
| **GDC** | Geometric Disk Cover |
| **SIC** | Successive Interference Cancellation |
| **MBS** | Mobile Base Station |
| **AP** | Access Point |
| **CCR** | Channel Condition Request |
| **NOMA** | Non-Orthogonal Multiple Access |
| **WLAN** | Wireless Local Area Network |
| **MIMO** | Multiple Input Multiple Output |
| **CW** | Contention Window |
| **DCF** | Distributed Coordination Function |
| **SINR** | Signal to Interference and Noise Ratio |
| **DIFS** | Distributed Inter-Frame Space |
| **SG** | Simultaneity Graph |
| **RAS** | Random Access SIC |
| **SAM** | Slotted Aloha-NOMA |
| **MU-MIMO** | Multi-User MIMO |
| **SDMA** | Space Division Multiple Access |
| **CCMA** | Carrier Counting Multiple Access |
| **RSS** | Received Signal Strength |
| **PMF** | Probability Mass Function |
| **LoRa** | Long Range |
| **L-MAC** | Learning MAC |
| **MCS** | Modulation and Coding Schemes |
| **MCMC** | Markov Chain Monte Carlo |

Chapter 1

# Introduction

Unmanned Aerial Vehicles (UAVs) or drones have a myriad of applications that can be classified broadly into two categories: military and civil. Both can further be subdivided as shown in Figure 1.1. Military applications include drones capable of performing reconnaissance and combat missions. One example is the Predator drone, which has a satellite link for sending real-time images to ground stations. The Predator drone is now used in various countries for reconnaissance as well as for destroying targets [12] [13].

Drones have many civil applications; see Figure 1.1. Companies such as Amazon and Google have been working on drone based delivery services [14]. Drones are also envisioned as flying taxis [15], and to date, these taxis have been trialed successfully in Dubai [16]. Apart from that, drones are used frequently by the general public for photography and by hobbyists [17]. They have become an ideal choice for journalists [3], where they are frequently used to capture live events. They are cheaper than helicopters due to their low cost, and portability. Drones have also found use in fields such as agriculture and wildlife monitoring [18]. For example, UAVs can be equipped with thermal sensors to monitor and track one or more animals [19].

A UAV swarm can also be employed for border surveillance and to monitor border crossings [20]. In these applications, UAVs are expected to remain in the

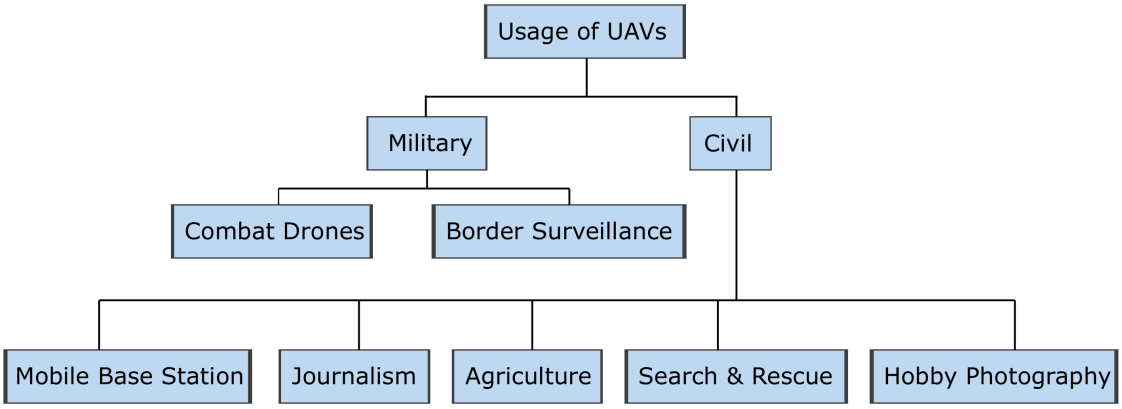


Figure 1.1: Applications of UAVs [1][2][3][4] [5].

air for a prolonged period of time, which is not possible due to their limited fuel. Algorithms can be designed to activate and fly UAVs only when certain conditions occur. For example, in [21], UAVs equipped with motion sensors continuously sense the environment and alert the operator whenever there is a target. If an operator believes an event requires attention, it deploys an UAV [22]. Precision agriculture is also beginning to rely on drones for monitoring soil and crops [23].

UAVs have also found applications in communication systems. They can function as remote base stations to extend the coverage or capacity of a cellular network [24]. They are more cost effective as compared to deploying femto-cells [25], and they are able to change their position and orientation to meet changing traffic and user distribution [4, 26]. Besides that, UAVs acting as base stations are particularly useful after a natural disaster [27].

Drones can be equipped with one or more sensors. Examples include gyroscope, accelerometer, magnetometer, pressure and navigation sensors [28]. These sensors are used for different purposes including drone control and data collection. The uses of these sensors are shown in Table 1.2. For example, UAVs equipped with a light detection and ranging or LiDAR sensor can be used as a remote sensing device to generate a map of a disaster area and to estimate damages [9]. LiDAR equipped UAVs can also be used for 3D modeling of buildings [29, 30].

UAVs can be classified as follows:

Table 1.1: Classification of applications.

| **Area** | **Drone Type** | **Number of Drones** | **Applications** | **Examples** |
|---|---|---|---|---|
| Military/Combat | Fixed wing jet | Single | Missile or intelligence gathering | [1], [31] |
| Surveillance | Fixed wing, multi-rotor, single rotor | Single / Multiple (Depending on area to cover) | Wildlife monitoring, border surveillance, and geo-mapping | [2], [19], [21], [32], [23] |
| Photography | Multi-rotor | Single | Hobby photography, events reporting, journalism, and 3D modeling | [33], [34], [35], [36], [30] |
| Mobile Networks | Multi-rotor, single rotor | Swarm | Ad-hoc communication infrastructure, improve coverage and capacity of a cellular network | [4, 27, 37], [25] |

Table 1.2: List of sensors on board UAVs [6][7][8][9].

| **Sensor Category** | **Sensor** | **Uses** |
|---|---|---|
| Gesture Control | Gyroscope<br>Accelerometer<br>Magnetometer<br>Pressure | To stabilize drone motion<br>Detects changes in drone orientation<br>Acts as a compass and helps decide directions<br>Detects altitude |
| Navigation | Global Positioning System (GPS), GLONASS, BeiDou, Galileo | Satellite navigation of drone |
| Communication | Camera<br>Telemetry radio station | Used for remote operation of drone and recording<br>Communication & Control from ground stations |
| Obstacle avoidance | Ultrasonic range sensor<br>Electronic Speed Control (ESC)<br>LiDAR | Obstacle avoidance<br>Automatic varying of speed<br><br>Laser mapping, 3D modeling |

1. *Fixed wing drones.* They look similar to normal commercial or fighter jets except they do not have a cockpit. Fixed wing drones can be sub-divided into two categories:

   (a) High Altitude and Long Endurance (HALE). These are mainly military drones. Examples include Aquila and Predator drones. They typically need a long runway; for instance, Predator drones need a runway with a length of 1500 meters [38]. HALE drones offer great flying time because they are built similar to conventional jets and have sufficient fuel to sustain long flights. For example, RQ-4 global Hawk drones can fly up to 24-hours [31] whereas a Predator drone can fly up to 40-hours without re-fueling [1].

   (b) Low Altitude and Short Endurance (LASE). These are smaller drones with short flying time typically ranging from 40 to 70 minutes [11]. They are normally battery operated and weigh below five kilogram. These drones fly at low altitudes, making them suitable for aerial surveillance and monitoring applications [2].

2. *Multi rotor drones.* They use multiple rotating blades as a lifting mechanism. Common designs include quadcopters [39], hexacopters [40] and octacopters [28]. Multiple rotors tend to produce varying thrust and thus requires electronic stabilizers [41]. As compared to fixed wing drones, multi rotor drones are much cheaper and easier to operate [42]. Also, they do not require any command center. Instead they can be operated by a single person using a laptop or a smart phone. A shortcoming is their short flying time because they are powered by a battery. Their flying time normally ranges from thirty minutes to two hours. Bigger batteries can be used at the expense of a higher weight, which affects lift [39, 43].

3. *Single rotor drones.* Single rotor drones are also known as Helicopter-based UAVs (H-UAVs). They utilize one rotary blade, have one main rotor and a

Table 1.3: A comparison of different UAVs and their capabilities [10][11].

| UAV Type | Flying Difficulty | Flying Time | Applications | Cost | Comments |
|---|---|---|---|---|---|
| Fixed Wing | Expert | Very high (up to 40 hours) | Mapping large areas | Very high, starting from USD $1300 | Professional use, not suitable for hobbyists or small companies. Need a runway. |
| Multi Rotor | Amateur | Low (up to two hours) | Photography, surveillance, delivery | Cheap, starting from USD $100 | Simple and cheap design |
| Single Rotor | Moderate | High | Heavy payloads, mapping larger areas | Very high, starting from USD $2500 | Stable by design, hover flight |
| Fixed Wing Hybrid | Expert | Medium (up to seven hours with a gas engine) | Delivery systems | In development | Not yet available in the market |

tail rotor. They are more stable as compared to multi rotor drones. H-UAVs use a lifting mechanism that is very similar to helicopters; the combination of two rotors help facilitate lift and maneuver. This complex lifting technique results in higher cost [44, 45].

4. *Fixed-wing hybrid.* These drones are also known as Vertical Take-off and Landing (VTOL) aircrafts. Their design combines the benefits of rotary drones and fixed-wing drones, meaning they can land vertically and take-off similar to fixed wings drones. These capabilities offer more speed and endurance. For example Boeing's X-50 has a maximum speed of 400 kilometers per hour with five hours of flying time [46, 47].

## 1.1 Communications

Conventional aircrafts are required to communicate with Air Traffic Controllers (ATCs). However, UAVs have additional communication requirements. They have to be in contact with an operator who remotely pilots an aircraft [48]. A UAV may also have to transmit different sensor values to a ground station. The communication requirements of UAVs can be divided into three categories:

1. *Platform safety.* The aim is to ensure flight safety. It includes communication with an ATC, and between drones for collision avoidance [49]. ATC traffic is similar to those generated by conventional aircrafts. Typical bandwidth requirement is 10 Kbps per aircraft [50]. It is only required for large drones; i.e., those with a maximum takeoff weight greater than 150 Kg and a maximum range higher than 30 Km [51].

2. *Remote piloting.* This requires communication between an UAV and a ground station for the purpose of operating an UAV. Video transmissions between an UAV to an operator may require 1 Mbps [48]. Remote Control (RC) can be of different types. The simplest type is controlling an aircraft through a joystick. It requires very low delay as an UAV needs to be operated in real time. This kind of link requires 10 Kbps of data rate and less than 10 ms delay [49]. RC can also be indirect where flight path instructions such as coordinates are sent to a drone [52]. A satellite link can be used in this case as delay is not a critical issue. An Iridium link, for instance, offers 2.1 Kbps with delays in the range of one to seven seconds [53]; e.g., this satellite link is sufficient for flying a Predator drone.

3. *Sensor data.* The sensor type dictates the amount of data. For example, an IMU sensor sends data typically at 200 Hz. An altimeter on the other hand transmits at a rate of 25 Hz [54]. Sensor data may require links with several megabits per second; e.g., sensor data generated by HALE drones can exceed 250 Mbps [55].

A multi-UAV system can be centralized or decentralized. In a centralized system, all UAVs are connected to a ground station. In a decentralized system, UAVs communicate with each other and each UAV acts as a router. In a multi-UAVs environment, UAVs may have to coordinate and act as a routing node to relay information for other UAVs. Consequently, each UAV has to maintain topology and routing information. As shown in Figure 1.2, a UAV can relay sensed information

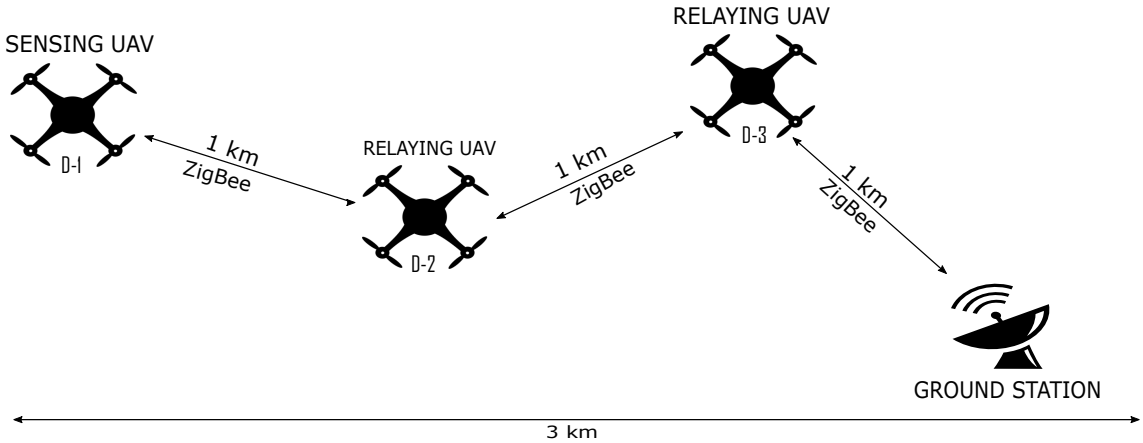


Figure 1.2: Communications among UAVs

through other UAVs when a destination is not within range.

Communication links between UAVs and to ground stations can be realized using Wi-Fi [56], ZigBee [43] or Bluetooth [57]. For long range links, UAVs can be connected to a cellular network, or a satellite. These communications links can be divided into four categories:

1. *Direct link.* This can be realized using ZigBee and Wi-Fi, and it is typically used by UAVs operating over short distances; i.e., less than 1.5 Km. ZigBee [58] and Wi-Fi [59] are ideal choices because of their high availability, inexpensive hardware modules and use of unlicensed spectrum [49]. ZigBee can be used for non-real-time applications. The data rate needs to be under 250 Kbps. ZigBee can provide a range of about 200 meters for a ground to air link and about 500 meter for an air-to-air link [60]. The range is extended to 1.5 Km in case of ZigBee Pro [61], and thus making it an ideal choice for applications such as control and coordination of UAVs because these do not require high bandwidth [62]. IEEE 802.11 [59] is ideal for transmitting images and videos. A Wi-Fi link is only viable for short distances with a maximum range of 500 meter [52]. Both ZigBee and Wi-Fi can be used on a single drone [63]. In such cases, Wi-Fi can be used for more bandwidth demanding applications such as sensor data while ZigBee can be used for control and coordination [62].

2. *Cellular.* This is suitable for UAVs operating over long distances [48]. Along

with increased range, cellular networks also provide data rates as high as 1 Gbps; see Table 1.4.

3. *Satellite*. Military drones are usually connected to ground stations through satellite links when they operate beyond Line-of-Sight (LoS). An aircraft receives instructions and transmits sensor data over a satellite data link [64]. The data can be a few kilobits per second for remote control of aircraft but it can be several megabits per second for transmission of sensor data [55]. The satellite link can connect a ground station to an UAV as well as serve a link between UAVs. Satellites can also be used as a backhaul in emergency situations, especially when UAVs are deployed during a disaster [65, 66].

The coverage of a UAV network can be extended using mesh technology [67, 68]. Each node in a mesh network can relay information to a ground station via one or more UAVs. This eliminates the requirement for each UAV to be in the range of a ground station. Figure 1.2 shows a typical mesh network scenario. Each UAV is equipped with ZigBee Pro [61] for communication. Only UAV D-3 is in the communication range of the ground station. UAV D-1 is at a destination site and it has to transmit information to a ground station. It cannot directly reach the ground station as it is out of range. UAV D-1 can relay sensed data to the ground station via D-2 and D-3.

Understanding the UAV propagation channel is important for the design and performance evaluation of UAV based communication systems. To date, most works have focused on Air-to-Ground (AG) communication channel. This is reasonable given that regulating bodies only allow LoS communications due to safety concerns. However, researchers are now shifting their focus towards safe operation of UAVs without LoS. Past works that characterize AG communication channels include [69–71] and [72]. Reference [73] and [74] investigate the effects of antenna height and orientation on the Received Signal Strength (RSS) and throughput of a IEEE 802.11a system based UAV network. The authors found that with suitable

antenna orientation, height differences can be alleviated. The authors also investigated RSS and throughput changes with a fixed height and distance by changing antenna orientation. The study in [74] shows that the best result is achieved when a horizontally oriented dipole antenna on a UAV communicates with a horizontally oriented dipole antenna on an elevated ground node. The characteristics of IEEE 802.11 air-to-air channel are discussed in [75]. The authors use a number of flight campaigns to investigate channel characteristics with respect to changing distance, antenna orientation and height of a UAV. For air-to-air channel, the results show a strong signal variance and multi-path effects when a UAV flies at a low altitude. Radio propagation conditions are also quite different for air-to-air communications as compared to air-to-ground communications. UAVs usually have LoS [76]. Unlike conventional propagation models, error statistics are also non-stationary for UAVs because of constantly changing distance [77]. UAV-to-UAV communications also offer better reception because both the transmitter and receiver are in the air. Experiments conducted in [62] show that packet reception rates are much better for air-to-air links as compared to air-to-ground or ground-to-air links [77].

## 1.2 Problem Space and Motivation

A key challenge when designing a Medium Access Control (MAC) for multi-UAV networks is to ensure quick channel access. This is particularly important when UAVs have limited energy and memory. Moreover, they may waste energy when contending for the channel and when they have to retransmit lost packets.

Figure 1.3 shows example scenarios with multiple UAVs communicating with a single ground station and also multiple ground stations communicating with a UAV. These UAVs are usually equipped with one or more sensors because they are required to communicate with the ground station periodically for remote piloting and transmission of sensed data. Moreover, depending on the application, there may be Quality of Service (QoS) requirements in terms of delay or bandwidth [93]. In

Table 1.4: Comparison of different link types.

| Type of Link | Spectrum Type | Distance | Throughput | Application | Application examples |
|---|---|---|---|---|---|
| **Direct Wi-Fi (802.11)** | Unlicensed | Short Distance 500 m | Up to 54 Mbps (802.11 a,b,g) 600 Mbps 802.11n [78] | Sensor data, video surveillance | Sensor data [43, 79] |
| **Direct Zigbee (802.15.4)** | Unlicensed | Short Distance 1.5 km | 250 Kbps [59] | Control and coordination, agriculture, delivery of goods | [80] |
| **Satellite** | Licensed | Long distance | - | Military and disaster relief | [81], [66] |
| **Cellular** | Licensed | Long distance | General Packet Radio Service (GPRS) 115 Kbps [82]<br><br>Enhanced Data GSM Environment (EDGE) 384 Kbps [87]<br>Wideband Code Division Multiple Access (WCDMA) (3G) [88]<br>High Speed Packet Access (HSPA) 42 Mbps [89]<br>Long Term Evolution (LTE) 150 Mbps [90]<br>LTE-Advanced 1 Gbps [91] | Rapidly deployable base stations, agriculture, and video surveillance | [83], [66], [84], [85], [86] |
| **Mesh** | - | Multi hop | - | Search & rescue, and network coverage | [48] [68], [79], [67] [92] |

particular, the communication between UAVs and ground stations may have have a certain data rate requirement; e.g., video transmissions require at least 1 Mbps [94]. On the other hand, simple LoS control of a UAV through a joy stick requires only 10 Kbps data rate and less than 10 ms delay [95].

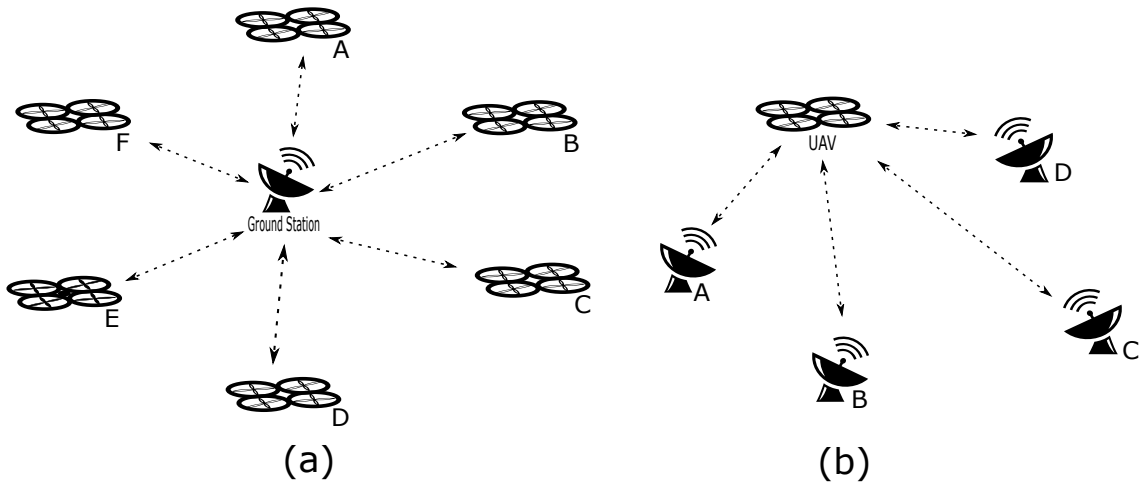


Figure 1.3: Example UAV networks (a) Multiple UAVs communicating with a ground station (b) Multiple ground stations communicating with a UAV

Guaranteeing these requirements, however, is challenging as there may be transmission errors due to collisions or interference, and channel access delays, especially when multiple UAVs or ground stations contend for channel access. In this respect, the channel access protocol used by UAVs and ground stations has a significant impact on performance. In particular, it must ensure transmissions are collision-free. One approach to guarantee collision-free channel access is to employ Time Division Multiple Access (TDMA). This means each UAV is allowed to transmit in a fixed and periodic transmission slot without channel contention. An example transmission schedule for use by the network in Figure 1.3(a) is shown in Figure 1.4(a). We see that each UAV transmits one after another. In any given time, there is only one transmitting node; hence, UAVs do not experience any collisions. Also, as the schedule repeats, each UAV is able to transmit periodically. This means if a schedule is short, a UAV has a high link capacity to the ground station.

An approach to improve network capacity is to employ Multi-Packet Reception (MPR) capability at ground stations. Specifically, they can be equipped with a

Successive Interference Cancellation (SIC) radio [96], which then allows them to decode multiple simultaneous transmissions. Figure 1.4 shows two possible schedules for the topology shown in Figure 1.3(a). In particular, without a SIC radio, the schedule length is six slots in length. However, with a SIC radio, the ground station only needs a schedule with three slots. As the schedule repeats, a shorter schedule means each UAV is able to transmit more frequently to the ground station.

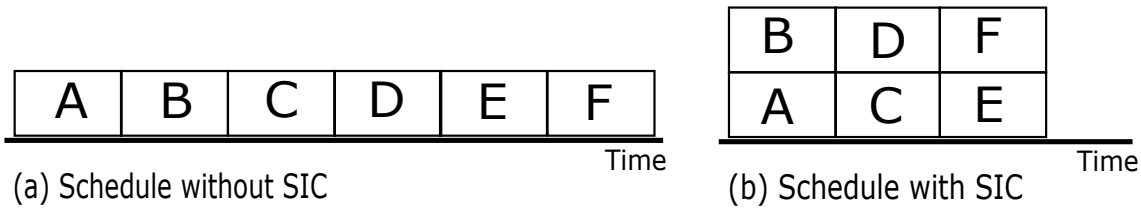


Figure 1.4: Schedule with and without SIC.

A challenging aspect when operating UAVs is random channel gains. As shown in [56], UAVs and ground stations can experience rapid fading. Yanmaz et al. [73] showed that the Received Signal Strength (RSS) of a UAV-ground link experiences rapid fluctuations due to multipath fading and variable UAV orientation. Moreover, LoS communications may be blocked occasionally due to terrain or buildings [97]. Apart from that, signals are affected by air-frame shadowing during aircraft manoeuvre [98]. This means for a given schedule, transmissions may fail. For example, in the first slot depicted in Figure 1.4(b), transmitting UAVs may experience a decoding error due to random channel gains. Consequently, although the transmission schedule with SIC is short, the number of decoding failures can be high. Hence, a transmission schedule without SIC may be preferred.

To combat the vagaries of the wireless channel, estimating or obtaining Channel State Information (CSI) may be necessary. This allows a transmitter to ascertain the best Modulation Coding Scheme (MCS) or data rate that ensures minimum transmission errors. However, obtaining perfect CSI in UAV networks is not practical due to dynamic channel conditions. Hence, a solution that does not require a ground station to first gather CSI will be advantageous.

Henceforth, this thesis aims to tackle the above challenges. Specifically, it con-

siders multi-UAV networks that employ a TDMA schedule where ground stations have a SIC radio. The main research problems of interest include:

1. How to identify the best TDMA schedule out of all possible schedules that works well over imperfect CSI?
2. How to determine a TDMA schedule in a centralized and distributed manner?
3. How to determine the optimal TDMA schedule length?
4. How to optimize a UAV base station's placement in single and multiple cells scenario?

The first question relates to user or TDMA schedule selection. As shown in Figure 1.4, a TDMA transmission schedule with SIC is preferable as it results in a higher network capacity. However, the total number of possible transmission schedules increases exponentially as the number of UAVs increases. In particular, the total number of possible transmission schedules for a network with $n$ UAVs will be $2^n$. Compounding to this challenge is that a network operator has to select a schedule that works across all channel conditions given imperfect CSI.

A MAC or link scheduler can run at a ground station in a centralized manner, where it has complete information of the network. However, collecting information such as CSI and the set of UAVs with data to transmit incurs a high overhead. To this end, a distributed MAC is preferred, meaning each node has to make decisions based on local information. For example, a UAV does not know the CSI to its ground stations or/and the number of contending UAVs. Moreover, it may not know the transmission power or data rate employed by these contending UAVs. The problem at hand is to select a transmission slot without using the said information.

Another key problem is determining the best schedule length. If the schedule length is too short, too many UAVs will occupy each time slot. Consequently, UAVs may experience a high number of collisions and transmission failures. On the other hand, if the schedule length is too large, then some slots will be idle. Therefore,

it is crucial to have the optimal schedule length in order to maximize the overall throughput.

Lastly, when a UAV operates as a Mobile Base Station (MBS), its placement and orientation are critical to ensure good coverage to/from users in its cell. In particular, the optimal placement or/and orientation of a UAV may reduce the length of the TDMA schedule used to provide transmission opportunities to UAVs. In particular, the optimal location may facilitate more simultaneous transmissions in a given slot, and thus leads to a shorter TDMA schedule. Another issue of interest is that a UAV may operate in a multi-cell network. This means each UAV may experience interference from adjacent cells. Moreover, it may cause interference to other UAVs or users operating in these adjacent cells. In this respect, it is important to identify a UAV location in which it does not experience high interference or cause excessive interference to neighbouring cells.

## 1.3 Contributions

The main contributions of this thesis are as follows.

### 1.3.1 Discrete Stochastic Optimization

The goal is to maximize the throughput in a multi-UAV network. The chapter proposes a TDMA MAC where ground stations are equipped with SIC radio, and operate over random channel gains. The MAC relies on discrete optimization [99], which allows a ground station to learn over time the best transmission schedule that has a high expected number of successes. In addition, this chapter also contains a heuristic approach that can be used to generate a subset of transmission schedules. This heuristic allows the proposed discrete optimization solution to be applied in large scale UAV networks. Both solutions are verified in small and large scale UAV networks. The results show that with SIC, up to four UAVs can be scheduled in each time slot. In comparison to the $\epsilon$-greedy algorithm [100], the average transmission

success rate of the proposed solutions is 70% whereas schedules generated by the $\epsilon$-greedy algorithm have an average transmission success rate of 50%.

### 1.3.2 Learning MAC (L-MAC)

This part of the thesis proposes a novel distributed solution called L-MAC, whereby UAVs learn the best time slot for a given frame or schedule size. This means once a UAV learns of the best slot and data rate, it continues to use them for the given frame size. Lastly, the derived schedule can serve as a capacity upper-bound for any random channel access protocols. Once all UAVs have learned the best time slot and data rate, the frame size is repeated until the ground station finds that it causes too many collisions and idle slots. It then sets a new frame size. The results show that the proposed L-MAC has a throughput of 500 Kbps as compared to Aloha without SIC that only achieved 50 Kbps, and Aloha with SIC has a throughput of 300 Kbps.

### 1.3.3 Orientation-aware L-MAC

Orientation aware L-MAC is an extension to L-MAC and it addresses the following problem: given a UAVs network with a ground station that has SIC capability, determine the shortest possible transmission schedule for UAVs. Each UAV is tasked with learning the best transmission policy, i.e., to determine the best time slot and antenna orientation. Changing the antenna orientation of UAVs can result in different channel gains. Therefore, if a transmission from a set of UAVs causes SIC decoding to fail, one or more UAVs can change their antenna orientation. This will result in different channel gains, which may better facilitate SIC decoding at a ground station. A Mixed Integer Linear Program (MILP) is formulated for the said problem. Simulation results show that the proposed approach achieves a throughput that is 59% higher than the well-known Aloha protocol (without SIC) and 28% higher than Aloha with SIC.

### 1.3.4 Placement Optimization MAC

Lastly, this thesis proposes a placement optimization approach for a SIC-enabled UAV base station. The work considers the problem of base station placement in order to exploit SIC. It adopts a Gibbs sampling based approach, which allows each UAV to learn of its optimal placement. In addition, it also considers a multiple cells scenario where each base station may experience interference from adjacent cells. Therefore, placing a UAV becomes even more challenging since the optimal position in one cell may interfere with another base station. The simulation results show that the schedule length is up to 17% shorter at the optimal location.

## 1.4 Publications

The work in each chapter has been reported in the following publications:

1. **S. Kalwar**, K-W Chin and Z.H Yuan. *Downlink Throughput Maximization in Multi-UAVs Networks using Discrete Optimization*, Springer Journal of Network and Systems Management, 2020. *To Appear.*

2. **S. Kalwar**, K-W Chin and L.Y Wang. *An Orientation Aware Learning MAC for Multi-UAVs Networks*, IEEE International Telecommunications and Applications Conference (ITNAC), Auckland, NZ, November, 2019.

3. **S. Kalwar**, K-W Chin and Z.H Yuan. *A Learning MAC for Multi-Rate UAV Networks*, Springer Wireless Networks, 2020 *Under review*

4. **S. Kalwar**, and K-W Chin. *Minimizing Schedule Length via UAV Placement: A Gibbs Sampling Approach*, *Under preparation*.

## 1.5 Thesis Structure

1. *Chapter 2.* This chapter surveys works on channel access strategies for multi-to-one systems, and placement optimization of UAVs. It also surveys works

related to MPR, SIC and Multi-Use Multiple Input Multipe Output (MU-MIMO).

2. *Chapter 3.* This chapter presents the aforementioned discrete stochastic optimization algorithm for identifying the TDMA best transmission set, and also a heuristic algorithm to generate a subset of transmission sets for use in large-scale UAV networks.

3. *Chapter 4.* This chapter presents a MAC that allows multiple UAVs to learn the best transmission slot in a distributed manner.

4. *Chapter 5.* This chapter proposes an extension to L-MAC by allowing UAVs to learn the best orientation to communicate with a ground station.

5. *Chapter 6.* This chapter outlines the said Gibbs sampling based solution for placing UAV in single and multi cells UAV networks.

6. *Chapter 7.* This chapter concludes the thesis and list some future works.

Chapter 2

# Literature Review

This chapter presents a survey of prior works that consider medium access strategies for UAVs. In addition, it also includes a review of works related to MPR, and works focusing on placement optimization of UAVs. Figure 2.1 depicts the structure of this chapter. A summary of all relevant works is presented in Section 2.5.

## 2.1 Channel Access in UAVs Networks

### 2.1.1 Single Hop

Many prior works have focused on the connection between UAVs and ground stations/sensors where multiple sensors communicate with a single UAV. Some challenges in UAV based ad-hoc networks include interference and high mobility of UAVs, which cause the channel state to change rapidly [101]. The section focuses on works related to connectivity and packet loss.

To minimize packet loss, the authors of [101] adopt full-duplex radios and MPR capability. Each UAV supports MPR and employs a Code Division Multiple Access (CDMA) transceiver with a matched filter for reception. The system uses a token based MAC to exchange codes, determine channel gains and obtain delay requirements. The token contains information such as code, channel gain and delay

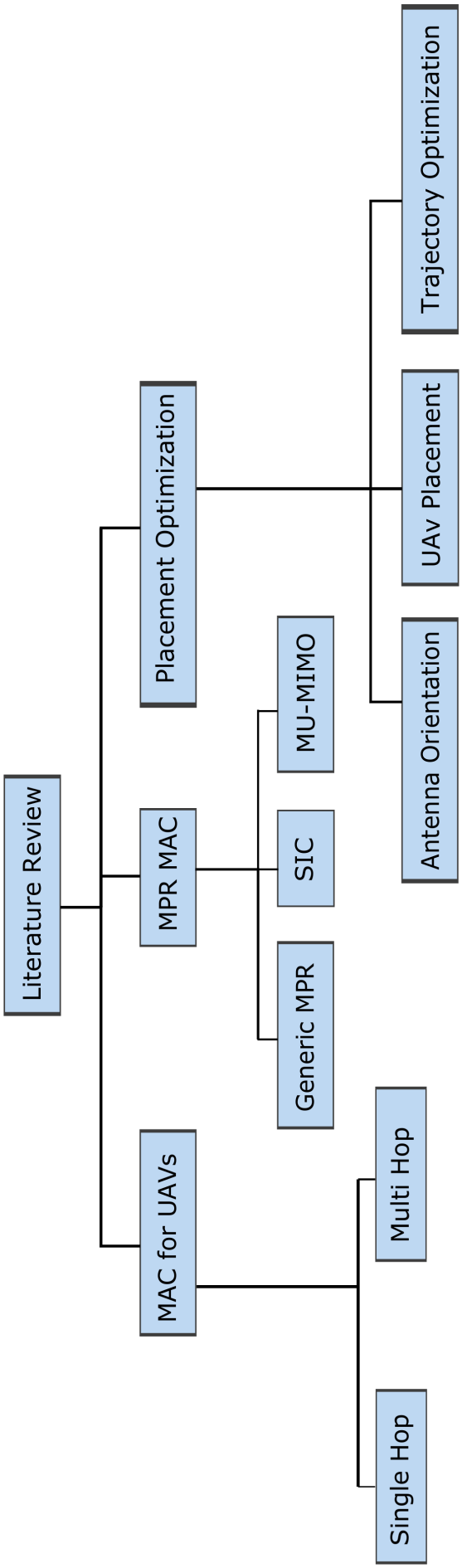


Figure 2.1: Chapter 2's structure

requirement. When a node has data, it selects a code included in the token and immediately passes the token to the next node. It also updates channel gains and the waiting time of its head-of-line packet. The authors consider two cases: perfect channel knowledge and imperfect Channel State Information (CSI). In the first case, each node decides whether it will transmit based on CSI and delay requirements. The objective is to maximize throughput and delay. This multi-objective optimization problem is formulated as a combinatorial optimization problem where the decision variable is which nodes are allowed to transmit in each time slot. As for the imperfect channel information case, the authors formulated a combinatorial and discrete stochastic optimization problem. The objective is to estimate the best transmission set given varying channel gains that maximize the expected throughput.

One of the key considerations while designing MAC for UAVs is the loss of connectivity due to a UAV's flight. Many works have proposed priority based MAC to deal with this issue. For example, the work presented in [102] considers a UAV aided Wireless Sensor Network (WSN) system and propose a hybrid priority based transmission scheme. The proposed MAC works in the following manner. The UAV which is flying above sensors, transmits a beacon periodically. All those sensors that receive the beacon contend for transmission. Then, the UAV transmits a second beacon, which broadcasts the transmission schedule for the registered sensors that contended in the first round. Lastly, sensors transmit based on the TDMA schedule broadcasted by the UAV. Yang et al. in [103] address the issue of energy and time consumption due to a UAV's path. They work on finding the optimal path to minimize energy and time consumption. The authors in [104] also propose a priority based UAV MAC called Advanced Prioritized MAC (AP-MAC). The proposed MAC works in four steps. In the first step, an UAV sends a beacon to all the sensors in its LoS. In the second step, sensors that receive the beacon and do not already have a transmission slot attempt to register for a slot. In step 3, the UAV generates a TDMA schedule and transmits to all registered sensors. Lastly, in step 4, sensors

transmit in TDMA based slots and the process repeats. Works that focus on priority based MAC include [105], [106] and [107]. Both of these works consider a system where sensors and UAV are mobile. Reference [106] proposes a prioritized MAC where the UAV broadcasts a beacon and sensors that receive the beacon are eligible for contention. All these sensors transmit based on CSMA with Collision Avoidance (CSMA/CA). The authors in [105] propose a contention-free MAC that guarantees fairness. The MAC works by taking into account the contact duration between sensors and the UAV. Therefore, a sensor is assigned a slot to transmit only when there is sufficient contact duration between both. The authors in [107] propose a priority-based contention-free MAC. The system considers a number of sensors on the ground and a UAV flying above them. The sensors are divided into sub-groups based on their location. Then, each sub-group is allowed to transmit in TDMA based schedules when the UAV is approaching them. The authors show that TDMA based approach is more suitable due to having a large number of sensors. The proposed solution also proposes the optimal number of sub-groups and the UAV speed.

Energy consumption is an important issue for UAVs and wireless sensors. Tazibt et al. in [108] focus on minimizing the energy consumption of sensors and an UAV. A simple approach is to fly the UAV above all sensors and collect data. However, this approach will result in sub-optimal path. Therefore, the authors propose nominating a cluster head for a set of sensors that acts as a sink for those sensors. Therefore, the UAV only needs to fly above the cluster heads and collect data. This approach significantly reduces the path followed by UAV, resulting in energy efficiency. The authors of [109] also propose a cluster-based transmission scheme. Their aim is to minimize energy consumption, UAV travel time and Bit Error Rate (BER) by optimizing the UAV's path. The proposed scheme is known as Low Energy Adaptive Clustering Hierarchy Centralized (LEACH-C). A UAV base station collects the information about location and energy capacity of all nodes before the flight. Based on this information, the UAV nominates Cluster Heads (CHs). Then, all remaining nodes identify the closest CH to send their data. The authors in

[110] also aim to minimize the energy consumption of a UAV and sensors. They achieve this objective by jointly optimizing an UAV's trajectory and sensor nodes wake up schedule. Therefore, sensors only wake up when an UAV passes close by, minimizing their energy consumption. The proposed approach also minimizes the UAV's energy consumption by optimizing its trajectory and altitude. The authors in [111] propose a priority-based MAC where nodes remain idle until they receive a beacon from UAV. At that point, nodes transmit their location. Based on the location data, UAV decides the priority levels for all nodes. Li at al. [112] propose a slotted Aloha based approach for UAV aided WSN system. The sensors remain idle until they receive a beacon from UAV. All sensors which receive the beacon, send their sensor head packet to the UAV. The sensor head packet includes the sensor's location. Then, the UAV assigns priority to each sensor based on its location and put it in a queue for transmission. The UAV also assigns a CDMA code to each sensor in the queue. Then, all sensors in the queue transmit based on CDMA to minimize the collisions.

One of the challenges for UAV MACs is to deal with varying traffic requirements of UAVs during different flight phases. For example, the authors of [113] classify a UAV flight into two phases: flight and data gathering. During the flight phase, communication between UAVs is mainly related to platform safety and remote piloting, which has a high delay but low network traffic requirements. However, during a data gathering phase, network traffic is extremely high because all UAVs start transmitting reconnaissance data to a ground station. To this end, the authors propose to automatically select an appropriate MAC protocol based on parameters such as network traffic, queue length or location. The proposed protocol can shift between Carrier Sense Multiple Access (CSMA) and TDMA, hence it is known as CT-MAC. UAVs use CSMA during the flight phase and switch to TDMA when they reach a reconnaissance area.

The authors of [114] focus on increasing throughput and providing a greater reception range under adverse channel conditions between a ground station and an

UAV. They introduce a technique called Flowcode that uses multiple transmitters and receivers. It also exploits antenna beam diversity to extend the reception range. In particular, when a spatial channel is incoherent, another antenna orientation may allow a better reception. Random linear network coding [115] is employed to exploit diversity gains by allowing opportunistic packet delivery over any link. In the first step, Flowcode groups $k$ number of packets together. Each group is known as a generation and they all have a unique generation ID. Each generation is then coded by generating Random Linear Combinations (RLCs) based on random coefficients. All nodes transmit these coded frames for each generation. Flowcode uses an Automatic Repeat Query (ARQ) scheme to ensure that each generation is received at the destination. It acknowledges a received generation through a link layer acknowledgment broadcast frame that contains the received generation ID. This acknowledgment is relayed through the receiver and transmitter nodes to the source. If the source does not receive an acknowledgment within a timeout period, it retransmits the generation and keeps repeating for $kr$ number of times, where $r$ is the maximum number of generation retries. Flowcode automatically sets the timeout period based on the maximum link rate and frame transmission time.

Table 2.1 compares prior works from six aspects: objective, problem, MAC type and the mobility of UAVs and nodes. Specifically, in terms of objective, references [103, 108–111, 116, 117] and [112] aim to minimize the energy consumption of sensors and/or UAVs. Works such as [116, 116] and [102] focus on identifying priority levels of different sensor. References [103],[109] and [110] consider the problem of UAV trajectory optimization. With respect to mobility, only papers [106] and [105] consider mobile nodes. All other works assume stationary nodes. However, none of these works assume SIC capable receivers. Moreover, none of them consider equipping nodes with learning capability to decide the best time slots. Also, none of these works consider adjusting a TDMA schedule length dynamically in order to improve throughput or to minimize collision and idle slots.

Table 2.1: A summary of UAV MAC papers.

| **Paper** | **Objective** | **Problem** | **MAC** | **Mobile UAV?** | **Mobile Sensors?** |
|---|---|---|---|---|---|
| [116] | To minimize energy consumption | To find optimal number of priority groups | CDMA | Yes | No |
| [116] | To minimize collisions | To find priority level for each sensor | CSMA/CA | Yes | No |
| [102] | To provide connectivity to all sensors in limited time | To find priority level for each sensor and optimal group size | Hybrid (CSMA / TDMA) | Yes | No |
| [103] | To minimize energy and time consumption | To find the optimal flight path | N/A | Yes | No |
| [104] | To maximize throughput in WSN-UAV environment | To find optimal schedule for sensors to guarantee fairness | TDMA | Yes | No |
| [106] | To maximize throughput in mobile WSN-UAV environment | To guarantee connection for each mobile node | CSMA/CA | Yes | Yes |
| [105] | To guarantee fairness for mobile sensors | To find optimal UAV parameters such as height, velocity | TDMA | Yes | Yes |
| [107] | To maximize throughput in WSN-UAV environment | To find the optimal number of priority groups, data packet size and UAV altitude | TDMA | Yes | No |
| [108] | Minimizing energy consumption of sensors and UAV and minimize UAV path | To find the optimal number of cluster heads | TDMA | Yes | No |
| [109] | Minimizing energy consumption of sensors and UAV | To find optimal UAV path | N/A | Yes | No |
| [110] | Minimizing energy consumption of sensors and UAV | To optimize UAV's trajectory and sensors wake up schedule | TDMA | Yes | No |
| [111] | Minimizing energy consumption of sensors | To find priority levels for all sensors | TDMA | Yes | No |
| [112] | Minimizing energy consumption of sensors | To find priority levels for all sensors based on their location | CDMA / Slotted Aloha | Yes | No |
| [113] | To propose a hybrid MAC that automatically switches between CSMA and TDMA | When to switch between TDMA and CSMA | CSMA / TDMA | Yes | no |

### 2.1.2 Multi Hop

The capabilities of UAVs can be exploited even further if they work in a multi-hop manner; doing so helps extend their coverage. Apart from that, multi-UAV networks need to be autonomous and collaborative. They may have strict timing requirements for command and control messages due to coordination among UAVs. The key problems addressed are related to the coordination of UAVs. That is, how multiple UAVs communicate with each other given that an UAV is already communicating with a central node. Another problem is to maintain and update the list of neighbors frequently. UAVs need to have information about one and two-hop neighbors. The challenge is the ever-changing network topology.

Some works that are based on multi-hop UAVs include [118] and [119]. Both papers consider a swarm of UAVs. UAVs can communicate with ground stations through multiple hops if a direct connection is not available. There are two types of UAVs in [119]. There is a master and actor UAVs. The master UAV is used as a gateway for data dissemination towards a remote data center. Actor UAVs are located inside the communication range of a master UAV. The proposed protocol is a hybrid collision coordination protocol that partially adopts IEEE 802.11 and TDMA protocols. The master UAV is responsible for scheduling transmission for all actor UAVs. The master UAV allocates TDMA slots to all actor UAVs to transmit their Request to Send (RTS) message. Actor UAVs with data to transmit reply with an RTS frame in their assigned slot. The master UAV then sends a Clear to Send (CTS) in reply to these UAVs which also includes their transmission order. During this transmission period, other idling UAVs have an opportunity to exchange data by directing their antenna towards each other. Specifically, idle UAVs that are closer to each other as per Received Signal Strength Indicator (RSSI) can pair up by sending control frames called Request to Pair (RTP) and Clear to Pair (CTP). Both RTP and CTP contain an RSSI and location field. Thus, while busy nodes are transmitting towards a master UAV, idle UAVs are able to exchange data.

MACs for UAVs require quick access guarantee due to strict timing requirements. Jiang et al. in [118] introduce a Collision Free MAC; aka CF-MAC. It is designed for transmitting command and control messages with strict timing requirements. All UAVs are equipped with an omni-directional antenna. The protocol divides all nodes into different communication zones. Every node maintains its one or two-hop neighbors. Frame information transmitted by each node contains information about all one-hop neighbors. CF-MAC is a slot based protocol. Every node has to transmit frame information in its particular slot even if it has no data. Each node receives information about its neighbors by listening to the channel and analyzing frame information from its neighbors. CF-MAC avoids collisions using CSMA. If any node senses the channel and knows another node is accessing the channel, it defers its transmission. The node will choose a free slot in the next time frame. If the node obtains a free slot successfully, it will directly transmit its data without back off.

Most research works to date assume UAVs have an omni-directional antenna. This limits the capacity of UAVs and also makes UAVs susceptible to jamming. Consequently, researchers have equipped UAVs with directional antennas. As a result, UAVs have a longer transmission range, experience less delay and spatial reuse improves. Reference [120] and [121] outline a MAC protocol that can steer the antenna reference point of the UAV based on changes in a destination's position to maintain a high received signal strength. Each UAV uses four antennas. Two of them are directional and are located above and below the aircraft. In idle mode, a UAV listens to other UAVs using omni-directional antennas. Each UAV creates a target information table by exchanging control messages that contain the position of neighboring UAVs. The target information table includes latitude, longitude, altitude and the position of destination UAVs. When an UAV wants to send data, it needs the position of the destination UAV. Transmitting UAVs send an RTS over their omni-directional antenna. The message includes the position of the UAV and the transmission duration. The destination node responds with a CTS packet

that includes its location. Each node that hears the CTS or RTS will store the information in the target information table for future use. If there is no activity for one second, each UAV sends a heartbeat message using an omni-directional antenna. This message causes other UAVs to update their target information table and respond with a similar heartbeat message.

## 2.2 Placement Optimization and Antenna Orientation of UAVs

One of the key issues when establishing a communication link with a single or multiple UAVs is placement optimization. The idea is to choose a position for the UAV and its antenna orientation that maximizes throughput. In some cases this is achieved centrally; a central node estimates the location and heading angle of an UAV and positions it. In some cases, each UAV estimates the location and antenna orientation based on a predefined algorithm. In such cases, the UAV chooses its position by checking the link quality at multiple positions and selecting the best available position and antenna orientation.

Changing a UAV's position or antenna orientation can result in better signal reception and system performance. Many research works have focused on the task of optimizing system performance by positioning UAVs. The authors in [122] propose an algorithm for optimizing the performance of ground to UAV links by controlling an UAV heading angle. The protocol aims to maximize the uplink data rate while ensuring the individual data rate of each link is above a certain threshold. The authors in [123] consider a system with multiple single antenna ground nodes and a multiple-antenna UAV. The UAV communicates with multiple nodes at a time by using Space Division Multiple Access (SDMA). The UAV aims to improve link quality and number of on-going transmissions by adjusting its antenna orientation. The authors in [124] and [125] propose a mobility control algorithm for the forma-

tion and maintenance of a chain of UAVs acting as communication relays. Each UAV estimates its location and aims to improve the capacity of the communication chain by optimizing its location. The location estimate is derived using RSSI measurements taken along during the flight of aircraft.

Distributed control of UAVs working collaboratively to achieve a task has also been a focus in recent years. Gil et al. in [126] consider UAVs serving as a communication backbone for a number of ground vehicles located over a large area. UAVs position themselves at a location that optimize the link quality amongst all ground based vehicles. The work presented in [127] also focuses on a wireless node that can automatically seek and adjust to the best reception position. Neighboring nodes can cooperatively form a relay network. Nodes use a measurement protocol that measures wireless link quality over a deployment area. Based on these measurements, each node autonomously adjusts its position to meet network requirements. The authors in [128] work on the optimal placement of a UAV acting as a flying relay to fill coverage gaps. They consider the fact that most of existing methods rely on air-to-ground channel models and therefore fail to fully utilize the air-to-air potential. They propose an algorithm to optimize the UAV relay position based on LoS conditions.

The use of UAVs as mobile base stations has been gaining popularity recently. A UAV base station can be deployed quickly when required. In case of natural disasters, they can be used for rapid deployment in the absence of traditional cellular networks. Lyu et al. in [129] consider a system where UAV functions as a mobile base station to provide connectivity to a group of ground stations. The authors propose an algorithm to allocate time to different ground stations based on a UAV's position to maximize the throughput. Each node has the highest rate when a UAV is close to its position. Hence, a time slot is assigned to the closest node so as to maximize the throughput of all nodes. A Cyclic Multiple Access (CMA) scheme is proposed to schedule the communications between a UAV and ground stations in a cyclic time division manner. The channel between the nodes and the mobile UAV is

known perfectly. In another work, Lyu et al. [130] consider placement optimization for UAV based base stations. The placement algorithm works by placing all UAVs sequentially, starting from the perimeter of the area boundary until all ground stations are covered. The authors formulate this problem as a Geometric Disk Cover (GDC) problem, whose objective is to cover a set of ground stations in a region with the minimum number of UAVs. The authors in [131] also work on the positioning of UAVs as cellular relays. A swarm of UAVs equipped with cellular technology is used to temporarily offload traffic into neighboring cells. They propose a design called fly-hover-communicate which works as follows. Ground nodes are divided into a set of locations and a ground node at each location is nominated as the corresponding node. Then, the UAV hovers over each corresponding node to transfer the data quickly. The authors propose an algorithm to optimize hovering locations, communication duration and also the UAV's trajectory connecting these corresponding nodes. The authors in [132] aim to minimize a UAV's mission competition time by optimizing its trajectory. Specifically, they consider a UAV communicating with fixed cellular infrastructure. The aim is to travel from one location to another while maintaining the reliable communication.

The authors in [133] consider a UAV aided WSN where the UAV also employs wireless power transfer to charge the ground sensors. Therefore, the authors aim to design the optimal UAV trajectory which offers maximum charging time for sensors and also offers the maximum uplink throughput. The solution in [133] ensures the UAV hovers over a certain number of nodes for wireless power transfer. In addition, the UAV also needs to hover over each node to offer time for uplink communication. Shi et al. in [134] and [135] aim to minimize a SIC equipped UAV base station's data collection time by optimizing its trajectory. They achieve this by finding a set of suitable points in the cell where the base station offers maximum connectivity. Based on these points, they build the optimal trajectory. The authors in [136] design a distributed trajectory control mechanism. The aim is to offload traffic from fixed base stations to improve network performance. The work presented in [137] aims to

provide coverage to all users in a given area while minimizing total number of required UAVs. The authors in [138] also consider a similar objective. However, they also take into account the charging requirement of UAVs. They solve this problem by building a cascaded chain of UAVs. In this way, they provide coverage to all users while ensuring each UAV gets sufficient time for charging. Mozaffari et al. in [139] aim to optimize a UAV BS's altitude and transmit power to maximize the coverage area. They also consider a scenario with two Mobile Base Stations (MBSs) and optimize distance between the two base stations to maximize the coverage. The authors in [140] aim to improve Non-Orthogonal Multiple Access (NOMA) enabled UAV's performance by optimizing its altitude, antenna beam width and power allocation. The authors in [141] aim to complement existing fixed base stations by placing UAV BSs between them to offload traffic. They prove that UAV BSs offer better throughout and RSS due to their ability to position near actual users as compared to the nano-cells. The authors in [138] consider a network where multiple UAVs are used to provide continuous wireless coverage over a large area. In such a situation, the UAVs need to return periodically to a charging station and other UAVs replace them. The authors aim to find the minimum number of UAVs required to continuously cover the given area considering the charging requirement.

Another key issue for UAVs is energy efficiency. Many works have considered optimizing UAV placement/trajectory to efficiently utilize the UAV's limited energy. The authors in [142] aim to minimize the total required transmit power of multiple UAVs working as MBSs while maintaining the data rate requirements of the users. The authors divide the placement problem into two sub-problems. In the first sub-problem, they fix the cell boundaries for each UAV base station and optimize the UAV placement in each cell. In the second sub-problem, they fix the UAV's positions and optimize cell boundaries. They show that the total required transmit power can significantly be reduced by optimizing these two parameters. Zeng et al. in [143] also focus on a similar goal; i.e., to optimize UAV placement to minimize energy consumption while ensuring throughput requirements of users. They aim to

minimize the power consumption of UAV due to the propulsion system and also due to the communication. They solve this problem by jointly optimizing UAV trajectory and communication time. Zeng et al. in [144] also work on the energy efficiency of UAVs and aim to optimize a UAV's trajectory to minimize the energy consumption. They show that the optimal energy efficiency can be obtained using a circular trajectory by optimizing the flight radius and speed. The authors in [145] consider a solar power UAV and aim to maximize its run time by jointly optimizing its trajectory and resource allocation. The works presented in [110] and [146] consider a UAV aided WSN and aim to improve the energy efficiency of UAV and sensors to maximize the network lifetime. The authors in [110] jointly optimize the sensors wake up time and UAV trajectory to minimize the energy consumption. Therefore, sensors remain in sleep mode and wake up only when they receive a beacon from UAV when it is passing nearby. Their proposed approach ensures that the trajectory is properly designed to ensure successful transmission in the presence of dynamic channel conditions. The authors in [146] note that the uplink energy consumption of WSN nodes can be minimized if the UAV flies closer to the ground. However, flying close to the ground requires high propulsion energy for the UAV. The authors jointly optimize this problem by proposing circular and straight trajectories for the UAV. The authors in [147] aim to improve a NOMA capable UAV's energy efficiency by placing it at the optimal position. The authors in [148] also work on a similar aim and optimize UAV's altitude and transmission power.

Table 2.2 summarizes the UAV placement works discussed above. The table shows that most of the existing works do not consider SIC. Moreover, only references [131] and [136] consider interference between multiple UAVs.

Table 2.2: A summary of of UAV Placement Works.

| **Paper** | **System** | **Aim** | **Problem** | **Uplink / Downlink** | **SIC?** | **Interference between UAVs** |
|---|---|---|---|---|---|---|
| [122] | Multiple UAVs acting as relays | To maximize uplink throughout | To optimize the UAV's heading angle | Uplink | No | No |
| [142] | Multiple MBSs | To minimize the total required transmit power of multiple MBSs while maintaining the data rate requirements of the users | Placement of UAVs | Downlink | No | No |
| [137] | Multiple MBSs | To provide coverage to all users | To find minimum number of MBSs to cover all users | Downlink | No | No |
| [139] | Single and multiple MBSs | Cover a given geographical area by placing one and two UAVs | To find minimum altitude and power for coverage of given area | Downlink | No | Yes |
| [138] | Multiple MBSs | Minimizing number of required UAVs for continues coverage of a given area | To find minimum number of UAVs for continues coverage given the recharging requirement | Downlink | No | No |
| [130] | Multiple MBs | Minimizing required number of UAVs | Placement of MBSs | Downlink | No | No |
| [141] | Multiple MBSs | To improve network performance by placing MBS between actual base station | Placement of MBSs | Downlink | No | No |
| [134] | Single MBS | To utilize SIC and UAV's movement to minimize transmission time | To find optimal trajectory | Uplink | Yes | No |
| [136] | Multiple MBSs | To provide emergency coverage to a large area | To find optimal trajectory | Uplink | No | Yes |
| [126] | Multiple MBSs | To improve overall link quality | Optimal UAV placement | Uplink | No | No |
| [127] | Multiple UAVs as relays | To form a relay network by forming a cascading chain of UAVs | To find optimal position for each UAV in the relay | Uplink | No | No |
| [128] | Multiple UAVs as relays | To fill network coverage gaps by using UAVs | Optimal UAV position | Uplink | No | No |
| [129] | Single MBS | To provide wireless connectivity to distributed ground users | To find optimal transmission slot for each ground user | Uplink | No | No |
| [131] | Multiple MBS | To offload cellular traffic to neighboring cells | Finding optimal trajectory and hovering locations | Uplink | No | yes |
| [132] | Single MBS | To minimize a UAV's mission completion time | Finding optimal trajectory | Uplink | No | No |

## 2.3 WLANs MAC Protocols

A UAV network is similar to a Wireless Local Area Network (WLAN). In both networks, multiple stations or UAVs attempt to transmit to a single receiver or AP or ground station. The nodes in both networks also experience high delays with increasing number of nodes. This is due to increased collisions which lead to higher back-off ranges that result in delays and channel wastage. The key approaches to overcome collisions include redesigning back-off mechanisms, using Multiple-Input Multiple Output (MIMO) techniques and equipping the Access Points (APs) with MPR techniques [149].

The work presented in [150, 151] and [152] aims to improve channel access delays due to high back-off ranges. Gowda et al. in [150] solve this problem by proposing a hierarchical back-off mechanism and changing the value of Contention Window (CW). It groups all nodes into some smaller sets. A two-round contention scheme works in the following way. In the first round (R1), all nodes contend and choose a back-off number. The chosen back-off number is much smaller as compared to conventional schemes. If the back-off range is $[0, CW]$ in the case of Wi-Fi, it is set to $[0, \sqrt{CW}]$ in the proposed scheme. When the back-off range is set to a smaller value, many nodes will choose the same counter. Then, the group of nodes with the smallest counter will be the winner in the first round R1 and will proceed to the second round (R2). Winner nodes will again contend by choosing a new back-off and all nodes in round two transmit based on their chosen back-off. During this time, losers in round R1 will freeze their counter until round R2 completes. Nodes in round R2 transmit a busy signal while they count down, so that the nodes in R1 do not start their counters. Once all nodes in round R2 have completed their transmission and no busy signal is detected by the losers of round R1, they advance to the second round and the procedure repeats. The two-round contention procedure can be extended to more rounds depending on node density.

In traditional IEEE 802.11 Distributed Coordination Function (DCF), the value

of CW is set to a minimum value and it is doubled after each collision. After each successful transmission, the CW is reset to a minimum value regardless of network load. Resetting CW to a minimum value increases the probability of collision especially when the number of competing nodes is high. Ksentini et al. in [152] aim to reduce the collision probability due to high load by dividing the overall back-off range into multiple smaller ranges. Each back off sub-range is associated to a particular collision resolution stage. In other words, unlike DCF that increases only the upper range with each collision, Deterministic Contention Window Algorithm (DCWA) increases both upper and lower bounds of the back off range. As a result, during each contention stage, every station draws a back-off interval from a distinct back off range that does not overlap with the other back off range associated to other contention stages. In case of a successful transmission, instead of resetting CW to a minimum value, DCWA sets the CW range with an intermediate value that depends upon the network load. Edalat et al. in [153] also work on contention window adjustment. They propose a machine learning based approach to find the optimal contention window size. The proposed approach works by taking into account recent network contention along with the last packet transmission status. The authors in [154] propose an Intelligent-CW (ICW) algorithm that utilizes machine learning to learn the minimum CW value for each node. They aim to guarantee fairness for each node by setting a minimum CW size. They equip each node with a machine learning module. Using this module, each node observes the activities of other nodes and set their minimum CW accordingly.

## 2.4 MAC for Multi-Packet Reception Nodes

Traditional single user nodes are capable of receiving data only from a single transmitter at a time. With recent advances in communication technologies, receivers are now capable of MPR [155]. This capability, on one hand, enhances system performance but on the other hand, it introduces many problems due to multiple

transmitting stations. An MPR capable node can communicate with multiple nodes concurrently as opposed to conventional nodes which can communicate with only one node at a time. A conventional IEEE 802.11 AP is designed to restrict other nodes while a node is communicating. This scenario is not applicable if the AP is MPR enabled. The Signal to Interference and Noise Ratio (SINR) threshold requirement of nodes also becomes greater due to a number of simultaneous transmissions. An MPR enabled AP allows only spatial-compatible stations to communicate simultaneously, i.e., those with least inter-user interference, to transmit simultaneously.

Relevant works that consider MPR include [151, 155, 156] and [157]. They assume that the AP supports MPR and is able to decode up to $L$ simultaneous transmissions. In [151], nodes are able to estimate whether the number of ongoing transmissions on the channel is less than or greater than $L$. Each node in a WLAN waits for a constant duration of Short Inter Frame Space (SIFS) for an ACK in single packet scenarios. The ACK can be further delayed in case of MPR because a node may have to wait longer for the channel to be free before it receives an ACK. The protocol works in the following way. A node freezes its back-off timer once it senses the number of ongoing transmissions is equal to $L$. When the channel remains idle for Distributed Inter-Frame Space (DIFS), then it resumes decrementing its timer. Thus, no new transmissions can start once the number of concurrent transmissions is greater than or equal to $L$ or once a node completes transmission. This reduces the delay incurred in receiving an acknowledgment. The authors in [156] also implement MPR in a WLAN. A collision happens when more than $L$ transmitters try to access the channel at the same time. If a node senses the number of ongoing transmissions is greater than $L$, its back-off counter cannot be decreased. The counter will decrease once there are fewer than $L$ active transmissions. When it reaches zero, a contending node is allowed to transmit. The authors in [158] consider a simple Aloha based network with MPR capability. The authors show that simple Aloha based random access offers significant throughput improvements in congested traffic scenarios. Zheng et al. in [155] also consider a similar MPR

model that closely follows IEEE 802.11 DCF. A station with data to transmit sends an RTS frame to the AP. The AP can successfully detect multiple RTS messages if the number of RTS frames is not greater then $L$. When the AP detects RTS frames successfully, it responds with a CTS frame to all requesting stations. Then the stations will start transmitting data frames after a SIFS. If all data frames are received correctly, the AP sends an ACK frame. Zheng et al. in another paper [157] work on a collision resolution scheme for MPR networks. The paper considers a non-carrier sensing model where a station with data to transmit randomly selects an initial back-off time before transmitting a packet. Every time a transmission is unsuccessful, the contention window is multiplied by a back-off factor of $r$. It is assumed that exponential back-off is used at each station.

The author of [159] observe that the MPR channel of [155] is underutilized. The main reason being that the current MAC protocols have only one contention round for each data transmission phase. Hence, the channel is under-utilized when there are fewer than $L$ stations contending for transmission simultaneously. To solve this problem, reference [159] presents a novel multi-round contention random access protocol as an extension to [155]. In this approach, if the number of transmitting stations is small after a contention process then more contention rounds can be completed before data transmission begins. The results show that with more contention rounds, the probability that the channel is fully utilized with $L$ concurrent packet transmissions, increases. The authors of [160] and [161] also present two-round channel contention mechanisms and divide total time into two rounds; random access and transmission time. The random access time finishes when the AP receives $L$ successful RTS messages. During this time, the AP responds with two kinds of CTS messages: Pending CTS (PCTS) and Final CTS (FCTS). PCTS works as an acknowledgment of RTS for a station while FCTS informs all stations the start of a data transmission phase. Compared to [160], reference [161] has a shorter second contention round, where a single message is used to reply to all successfully received RTS messages.

Huang et al. in [162] introduce a CSI based random access MAC protocol for WLAN with MPR capability. In the proposed approach, when the back-off counter of a node reaches zero, the node decides whether to transmit by considering network population and current channel state. Each node estimates the CSI from downlink transmissions and transmits based on a given SNR threshold between itself and the AP. Barghi et al. also introduce an MPR scheme for WLANs in [149]. The proposed scheme allows two concurrent transmissions towards the AP by introducing a waiting time window at the AP. When the AP receives a RTS message, it waits for a time equal to the waiting time window to receive another RTS from any other station. CTS and acknowledgment messages use an extra address field to accommodate two stations. Zheng et al. in [163] propose CSMA based MAC for MPR capable networks. The proposed approach allows $L$ simultaneous transmissions and each node is capable of sensing the channel for the number of ongoing transmissions. The proposed scheme follows CSMA protocol and nodes choose back-off in the same way. However, when the back-off timer reaches zero, the nodes sense the channel. If the number of ongoing transmissions is less than $L$, they will transmit. If the number of ongoing transmissions is greater than $L$, they delay the transmission for a random number of slots. Zheng et al. in another paper [164] propose an MPR MAC based on p-persistent scheme. They consider a similar system where each node is able to sense the channel for the number of ongoing transmissions. The nodes sense the channel at the beginning of a slot. If the number of ongoing transmissions is less than the MPR limit $L$, the node transmits with a probability $p$. Paper [165] also proposes a similar approach where nodes can no longer transmit a packet when the number of ongoing packets reaches the MPR limit i.e., $L$ packets. The authors in [166] also propose a DCF based MAC to incorporate MPR. The nodes in this proposed approach freeze their back-off counter when the number of ongoing transmissions reach the MPR limit $L$.

Zhang et al. in [167] propose a scheme that eliminates collisions by using multi-user detection technology. Each node is assumed to be equipped with a half-duplex

CDMA multi-user detector. Each multi-user detector can detect all signals in a node's neighborhood. The proposed framework is based on a synchronous time division CDMA (TD-CDMA) structure where each frame is divided into two control slots and a continuous data transmission slot. Collisions can occur in the proposed approach only when two signals use the same code. The framework introduces a protocol for assignment of codes and ensures that there is no code repetition within two hops. When a node enters the system, it is assigned a dedicated unused code from a set of predefined codes. The frame structure of proposed synchronous TD-CDMA has three slots. The first two slots are associated with control functions and are called *connectivity update* and *scheduling slots*, respectively. The third slot is used for data transmission. In the *connectivity update slot*, each node broadcasts its identity information on a common signaling channel. This allows neighboring nodes to detect each other. In the *scheduling slot*, senders contend for the channel by taking into account packet priority, access fairness and throughput objectives. The protocol uses dedicated channels for data transmission which are established during the connectivity update phase.

Zhang et al. in their next paper [168] propose a novel receiver initiated MAC protocol. Each node is equipped with a half-duplex CDMA multi-user detector. In the IEEE 802.11 standard [169], nodes use a RTS/CTS handshake to reserve a channel before data transmission. The basic idea is to reduce signaling overhead by initiating the transmission process from receivers rather than transmitters. The authors introduce a Ready-to-Receive (RTR) message. At the beginning of each scheduling slot, each potential receiver uses its dedicated code to broadcast an RTR message at the maximum transmission power. Potential transmitters collect RTR messages in their neighborhood. A receiver list is then formed at each potential transmitter. Based on design objectives such as fairness or throughput maximization, potential transmitters select their associated receivers. Here, a transmission priority is given to a waiting packet with the highest priority. This priority is calculated via a distributive Generic Additive Increase Multiplicative Decrease (GAIMD)

fair scheduling scheme where each node decides to transmit based on the candidate packets waiting at this node and contending packets destined to this node. GAIMD is distributed and window size is adjusted based on local information only.

The authors in [170] note that the traditional channel access mechanisms such as CSMA/CA can be unfair for nodes that are far from the AP. This is due to the fact that in networks with spatially distributed nodes, the channel may be captured by nodes that are near the AP for most of the time. The authors propose a scheme known as Generic Distributed Probabilistic (GDP) protocol. Under this scheme, each node selects one of two possible probabilities after each transmission. All nodes reduce their transmission probability after each transmission success and increase the probability after a failure. In this way, nodes near the AP do not capture the channel for long duration.

Table 2.3 summarizes above papers with respect to considered aim, problem, type of MAC scheme and MPR technology.

Table 2.3: A comparison of MPR papers

| **Paper** | **System** | **Aim** | **Problem** | **MPR Technology** | **Centralized / Distributed** | TPC (Yes / No) | **MAC** | **Saturated / Unsaturated** |
|---|---|---|---|---|---|---|---|---|
| [171] | WLAN | To maximize the channel throughput while satisfying the access delay bounds of different classes of real-time services such as voice and video | To find the maximum number of packets a slot can accommodate based on packet loss ratio for different classes of multimedia traffic | DS-CDMA | Centralized | Yes | TD-CDMA | Unsaturated |
| [172] | WANET | Improve throughput and access fairness in MPR networks with spatially distributed nodes | To decide whether a node should transmit or not based on its transmission probability | Generic | Distributed | No | GDP (Two state Aloha) | Saturated |
| [173] | WANET | To propose a partitioned CDMA approach to enable MPR in WANETs | To find the maximum achievable system load for a given probability of detection success | CDMA | Distributed | Yes | CDMA | Saturated |
| [158] | WANET | To analyze performance of a simple Aloha based random access network with MPR | To find the optima packet length for MPR capable system | CDMA | Distributed | Yes | Aloha | Saturated |
| [151] | WLAN | To redesign traditional MAC and consider the problem of acknowledgment delays in MPR networks | To decide when a node should freeze its back-off timer | Generic | Distributed | No | CSMA | Saturated |
| [174] | WANET | To study the performance of slotted non-persistent CSMA using the Poisson random traffic model in MPR network | To find the optimal MPR capability for throughput maximization | Generic | Distributed | N0 | CSMA | Unsaturated |
| [175] | FANET | To jointly consider full-duplex radio and MPR in UAV ad-hoc networks | To find the set of MPR compatible UAVs to transmit concurrently | CDMA | Centralized | No | Token based MAC | Unsaturated |

### 2.4.1 SIC

Recently, researchers have started considering nodes with Successive Interference Cancellation (SIC) radios [96]. SIC uses the fact that a composite received signal from multiple transmitters should not be considered as random noise. Instead, data of each user can be iteratively extracted. This capability allows a receiver to decode multiple transmissions at a time. SIC enabled receivers are much simpler than other MPR enabled systems [176]. This is because they use the same decoder to decode the composite received signal at different stages.

One of the main objectives of SIC MACs is to redesign existing MAC schemes to allow multiple concurrent transmissions. These works aim to improve the efficiency of existing MAC protocols by exploiting SIC. For example, the work presented in [177] considers a Wireless Ad-hoc NETwork (WANET) and proposes a MAC scheme based on the traditional IEEE 802.11 DCF with SIC. Instead of being silent for a NAV period, a subset of neighboring nodes that received an RTS or CTS message transmit a Channel Condition Request (CCR) message. The source and destination node of the main link that exchanged RTS/CTS decode the CCR transmissions using SIC. If the decoded signals have an SINR greater than a required threshold, the corresponding nodes are allowed to transmit. Otherwise, a busy tone is sent to stop these nodes from concurrent transmissions. References [178] and [179] also use SIC and propose link scheduling algorithms. The authors in [178] propose a new graph model called Simultaneity Graph (SG) to capture the link correlation introduced by SIC. The authors propose two alternative approaches. A slot oriented scheme that assigns a maximal feasible link set to a time slot and a link oriented scheme that assigns each link a sufficient number of slots. The authors in [179] propose a scheme known as Scheduling with SIC (SSIC). The scheme schedules links by checking for SIC opportunities at each step. The result is a schedule of length $T$, where in each time slot all transmissions can be decoded successfully.

The authors in [176] consider a random access MAC protocol with a SIC enabled

receiver. The proposed scheme, called Random Access SIC (RAS-MAC), splits all users into two groups based on their received power: a set of high power users and a set of low power users. The authors assume that all nodes in a group transmit with an equal probability. The AP is capable of decoding only two transmissions at a time, one from each set. When two users transmit, the AP decodes the transmission from the high power user first. The authors in [180] propose a MAC scheme known as k-SIC. The term $k$ indicates that the receiver performs up to $k$ stages of SIC. The protocol assumes a time-slotted system. Each slot includes a small initial signaling phase followed by a larger transmission phase. All the stations contend for medium access during the signaling phase. During the transmission phase, only those links are allowed to transmit that gained access during the signaling phase. The receiver is capable of decoding up to $k$ transmissions.

Uddin et al. in [181] consider a single channel uplink WLAN system with a SIC enabled AP that can decode $M$ packets from at most $M$ users iteratively. The total time is divided into mini-slots. A node with data first senses the medium in each mini-slot. When the channel is free, the node transmits an RTS message. At the same time, other nodes can also start transmitting their RTS messages in the same mini-slot. The AP does not use SIC for receiving RTS packets. The AP updates the CSI of nodes when it receives an RTS. When the AP receives an RTS from a node, it sends an Acceptance Notification (AN) to that node. After receiving the AN, the node waits for the reception of CTS or not CTS (NCTS). The waiting time can be sufficiently large since the AP can receive up to $M$ RTS packets. After receiving the RTS from $M$ users, the AP selects a set of nodes from which it can receive data simultaneously using SIC. The set of nodes is selected based on the SINR model. After selecting the users, the AP sends a common CTS/NCTS packet to all nodes. The CTS/NCTS message identifies the nodes are allowed to transmit and the ones which are not out of $M$ nodes. Uddin et al. in another paper [182] also propose a SIC based approach for existing WLANs. In the proposed approach, MPR is only enabled in the downlink. In the uplink, each node senses the medium

and transmit if the medium is free. The main objective is to find the optimal set of users for transmission from AP using NOMA. In order to find the optimal set of users, the AP transmits a request packet to a set of randomly chosen nodes. After receiving the request packet, nodes transmit an acceptance notification (AN) back to the AP. AN packet contains the channel information. Based on the channel information of all nodes, the PA estimates the optimal set of users for simultaneous transmissions. Uddin et al. in another paper [183] propose SIC based scheduling approach for cellular networks. In this work, they aim to find the optimal set of nodes and transmit power to meet certain minimum throughput requirements.

References [184] and [185] consider the problem of transmit power allocation to nodes such that SIC is successful. The proposed scheme in [184] called Aloha-NOMA allows all connected IoT devices to transmit in term of frames. At the start of each frame, a ground station transmits a beacon. Then, all the nodes with some data to transfer, send a dummy packet to the ground station. After receiving all dummy packets, the ground station estimates the required power level for each node. In the next step, all nodes transmit with the estimated power and the ground station decodes their transmissions using SIC. The authors in [186] propose a similar approach with slotted Aloha known as Slotted Aloha-NOMA (SAM). Mazin et al. in [187] compare SAM with CSMA/CA and show that SAM offers higher throughput at the cost of higher delay due to the power level selection mechanism of SIC.

The authors in [188] consider different traffic requirements of multiple devices in M2M networks. They propose a reconfigurable MAC that works in distributed as well as in a centralized resource allocation manner. In particular, each frame in the proposed scheme is split into two parts: TDMA and CSMA. The TDMA part is further split into NOMA and OMA parts. At the start of each frame, the AP transmits a beacon that includes devices that can transmit based on TDMA in NOMA or OMA part. In the NOMA part, two devices are scheduled to transmit in each time slot. All those devices which are not given any slot in TDMA, can transmit in contention based part.

The authors in [189] aim to improve existing WLANs by using Software Defined Network (SDN) technology along with SIC. They work on two major drawbacks of SIC based WLANs. The first problem arises due to the sequential contention and transmission phase, which leads to low channel utilization. Another problem is due to the different packet lengths of concurrent transmitters. If two nodes have been scheduled for concurrent transmission and they have different packet lengths, it will result in channel wastage due to the shorter packet. To address the first problem, the proposed approach splits the channel into two sub-channels, one for contention and the other for transmission. In the contention phase, each node sends an RTS packet that includes the length of the packet. In order to address the second problem, the authors introduce multiple contention queues, each for different packet size. Based on the packet size, the AP schedules each node, so that the channel wastage is minimum.

Table 2.4 provides a comparison of SIC papers with respect to their system, aims, problems and link access mechanism. Works such as [184, 186] and [185] focus on the problem of transmit power allocation to different nodes. On the other hand, works such as [179, 188] and [183] consider the problem of identifying the optimal set of nodes for concurrent transmissions. However, none of these works consider multiple data rates.

Table 2.4: A summary of SIC MAC papers.

| **Paper** | **System** | **Aim** | **Problem** | **Centralized / Distributed** | TPC (Yes / No) | **MAC** | **Saturated / Unsaturated** | **Data Rates (Fixed or multiple)** |
|---|---|---|---|---|---|---|---|---|
| [177] | WANET | To enable Successive Interference Cancellation (SIC) in a distributed MAC scheme | To determine whether the concurrent transmission of randomly selected subset of neighboring nodes will interfere with a given transmitter | Distributed | No | CSMA | Unsaturated | Fixed |
| [176] | WANET | To improve throughput in SIC networks | To find the achievable rates for concurrently transmitting nodes | Distributed | Yes | Aloha | Saturated | Fixed |
| [178] | WANET | To characterize the link correlation introduced by SIC | To determine the maximum number of feasible links to assign to a time slot, and to determine a sufficient number of slots to assign to each link in a link oriented scheme | Centralized | No | TDMA | Saturated | Fixed |
| [179] | WANET | To propose a polynomial-time scheduling algorithm that uses SIC to compute short schedules | To determine which subset of links should be scheduled concurrently such that they can be decoded successfully | Centralized | No | TDMA | Unsaturated | Fixed |
| [181] | WLAN | To improve the efficiency of CSMA using SIC | For a given node, whether it should transmit or remain silent in a given time slot | Distributed | No | CSMA | Unsaturated | Fixed |
| [180] | WLAN | To propose a carrier sensing based network protocol to exploit SIC | To determine the maximum number of concurrent transmitters | Distributed | No | CSMA | Saturated | Fixed |
| [183] | Cellular | To maximize energy efficiency in downlink NOMA network | To find optimal set of nodes and their transmit power | Centralized | Yes | N/A | Unsaturated | Fixed |
| [184] | M2M IoT | To improve throughput and energy efficiency in IoT network | To estimate optimal transmit power for each node | Centralized | Yes | Aloha | Unsaturated | Fixed |
| [186] | M2M IoT | To improve throughput and energy efficiency in IoT network | To estimate optimal transmit power for each node | Distributed | Yes | Slotted Aloha | Unsaturated | Fixed |
| [185] | IoT | To propose a MIMO-NOMA scheme for users based on their QoS requirements | To estimate optimal transmit power for each node | Centralized | Yes | TDMA | Saturated | Fixed |
| [188] | M2M IoT | To address varying traffic requirements of different nodes | To find an optimal list of devices for transmission with NOMA | Hybrid | No | Hybrid (TDMA / CSMA) | Unsaturated | Fixed |
| [189] | WLAN | To improve existing WLANs by using SDN and SIC | To decide a contention queue for each node | Hybrid | No | Hybrid (TDMA / CSMA) | Unsaturated | Fixed |

### 2.4.2 Multi User-MIMO

Multi-User MIMO (MU-MIMO) is a very promising technique to improve network capacity. In particular, it allows simultaneous transmissions or receptions. One of the main problems in uplink MU-MIMO is the synchronization among transmitting stations. Another problem in multi-user systems is inter-user interference. It occurs because multiple stations access the AP simultaneously. Hence, a key problem is to determine spatially compatible stations. Tandai et al. in [190] aim to solve these problems. The proposed scheme works in the following way. In the first step, a station transmits an RTS frame to initiate an uplink transmission phase to the AP. If the AP agrees, it broadcasts an Asking-CTS (A-CTS) message to stations. If another station has data to send, it transmits an Applying-RTS (A-RTS) frame. The AP identifies a data transmission request from stations by detecting their subcarrier signals. Then, the AP requests these stations to transmit pilot signals in a TDMA manner. The AP calculates the CSI between each station upon receiving the pilot signal. Then, it notifies stations that are spatially-compatible to transmit and their capable transmission rate. After that, these stations transmit their data to the AP. Ettefagh et al. in [191] aim to minimize inter-user interference by allocating all nodes into different clusters. Nodes that belong to the same cluster are allowed to simultaneously transmit. A cluster can also receive several simultaneous streams if the multi-user interference can be cancelled, either directly at the destination or by setting proper gain factors at transmitters. Hence, from a MAC point of view, clusters replace individual nodes. Specifically, nodes belonging to the same cluster look like a single node.

In MU-MIMO LAN, the achievable throughput of a node also depends on other simultaneous transmissions. In traditional IEEE 802.11 MU-MIMO contention protocols, users join concurrent transmissions without considering their impact on other nodes and spatial diversity. Such protocols not only waste time during contention but also fail to fully utilize gains of MU-MIMO. To deal with this issue, Kuo et al.

in [192] present MIMOMate, a leader based MAC protocol for uplink MU-MIMO transmissions. The proposed scheme groups transmitters based on their channel characteristics. The AP groups a number of nodes by learning the uplink channel of all clients from their association frames when they join the network. The AP announces all groups based on their channel characteristics and also elects a leader for each group. Only the leader contends for transmission and all the nodes in that group transmit along with the leader concurrently. The AP needs to re-group the nodes only when it detects that the channel of any node has changed due to channel variations or user mobility.

Tan et al. in [193] present a Spatial Multiple Access (SAM) scheme for WLAN. Mobile stations can coordinate their transmissions in a fully distributed fashion. The authors propose a distributed MAC scheme known as Carrier Counting Multiple Access (CCMA) to allow asynchronous concurrent transmissions. CCMA uses a chain decoding technique to decode simultaneously received data from multiple stations. Each station maintains a transmission counter by detecting other station's frame preambles and decides whether to contend for the channel. Wu et al. in [194] propose a CSMA/CA based MAC protocol for MU-MIMO WLANs. The maximum number of simultaneous transmissions towards the AP depend on the number of antennas at the AP. Every client counts the current number of concurrent transmissions by detecting their preamble. During channel contention, if a node checks that the transmission counter is smaller than the maximum number of allowed transmissions, all other nodes will continue to contend for transmission. If the transmission counter reaches a maximum value, all remaining nodes will defer channel access for a period longer than DIFS. Jin et al. in [195] present a MU-MIMO scheme that assumes synchronous transmission from multiple stations. Each station is assumed to have a unique orthogonal preamble. Hence, the AP knows which station transmits its data and also allows it to estimate the channel coefficients for each station. The authors in [196] also proposed a MIMO concurrent (MIMO/CON) uplink transmission scheme. The scheme uses compressive sensing to estimate the CSI of multiple

stations simultaneously without strict synchronization or coordination among users. MIMO/CON can boost channel utilization without explicit channel control by allowing the number of multiple concurrent transmission to exceed the number of receive antennas at the AP. This is advantageous as traditional MIMO schemes do not allow the number of transmissions greater than the number of receive antennas because they cause collisions. MIMO/CON solves this issue by using a novel scheme called delay packet decoding. This scheme can opportunistically decode collided packets at a later time by using partially retransmitted information. Hence, only partial retransmission of information is required to recover collided frames.

Jung et al. in [197] present an asynchronous uplink MAC scheme for MU-MIMO. The scheme allows concurrent transmissions from multiple nodes by employing an additional feedback channel from the AP. The proposed MAC utilizes the MU-MIMO channel more efficiently in scenarios where transmission duration are dynamically varying due to different packet sizes. The system includes an AP with multiple antennas and MPR capability whereas nodes have a single antenna. Each frame includes an orthogonal training sequence in the preamble in order to make it possible for the AP to estimate the channel coefficients. Once the AP obtains channel coefficients from training sequences, it can properly decode the mixed signal from simultaneous transmissions. The AP can decode $M$ simultaneous signals at a time. The value of $M$ depends upon MPR capability, number of antennas, antenna correlation and channel fading status. The AP computes $M$ at the start of each transmission interval. When the AP receives an RTS from any station, it broadcasts a CTS with vacant space information that tells all the nodes the capacity of the AP to decode concurrent transmissions. On receiving the CTS packet, the node that has sent the RTS packet starts data transmission. At the same time, other nodes who overheard the MPR vacancy will compete for the channel to transmit concurrently. Once a station finishes transmitting, the AP immediately sends an acknowledgment to all stations with the updated vacant space information.

Table 2.5 summarizes the above discussed works with respect to systems, aims,

problems and MAC types. The table shows that all of these papers aim to improve the performance of WLAN by incorporating MU-MIMO.

Table 2.5: A comparison of MU-MIMO papers

| **Paper** | **System** | **Aim** | **Problem** | **Centralized / Distributed** | TPC (Yes / No) | **MAC** | **Saturated / Unsaturated** |
|---|---|---|---|---|---|---|---|
| [149] | WLAN | To maximize the WLAN throughput by enhancing the design of IEEE 802.11 and incorporating MPR for simultaneous transmissions | To find the optimal waiting time at the receiver which is maximum tolerable time difference between arriving RTS messages | Distributed | No | CSMA | Saturated |
| [198] | WLAN | To balance uplink and downlink throughput in integrated uplink and downlink MU-MIMO | To decide the mode of each MU-MIMO cycle (uplink, downlink or integrated) based on the degree of freedom afforded by multiple antennas | Centralized | No | CSMA | Both cases |
| [199] | WLAN | To maximize throughput in Space Division Multiple Access (SDMA) | To find the optimal number of maximum transmitters for a given number of antennas | Distributed | No | CSMA | Saturated |
| [159] | WLAN | To fully utilize the capacity of wireless channel using MPR | Identification of the optimal stopping time of contention process | Distributed | No | CSMA | Unsaturated |
| [197] | WLAN | To efficiently utilize wireless channel in MU-MIMO networks in asynchronous scenario and varying transmission duration | To determine the transmission probability to transmit in a slot for nodes that have not transmitted a RTS packet | Distributed | No | CSMA | Saturated |
| [155] | WLAN | To maximize the throughput in a MPR based WLAN | To find the optimal transmission probability to maximize throughput | Distributed | No | CSMA | Saturated |
| [190] | WLAN | To enhance network throughput and reduce overheads in uplink MU-MIMO networks | Find the most spatial compatible nodes that can transmit with least inter-user interference | Centralized | Yes | TDMA | Unsaturated |
| [191] | WLAN | The paper aims to enable MU-MIMO transmissions in distributed manner | To group nodes in clusters such that all nodes in a cluster can transmit and receive together | Distributed | No | Cluster based CSMA | Both cases |
| [200] | WANET | To exploit the interference cancellation capacity of MIMO for throughput improvements | To find the optimal SINR threshold that can maximize the system throughput | Distributed | No | CSMA | Saturated |

## 2.5 Summary

In summary this chapter has discussed prior works that consider:

1. *MAC for single and multi-hop UAV networks.* These works propose different link access strategies for multi-to-one communication scenarios in UAVs. They aim to achieve one or more objectives; examples include maximizing overall throughput, minimizing the energy consumption of UAVs and ground stations, guaranteeing communication for all ground nodes.

2. *MPR MAC.* The objective of these works is to employ different MPR techniques such as SIC, CDMA and MU-MIMO to improve overall network performance.

3. *Placement optimization of UAVs.* The objective of these works is to optimize single or multiple UAVs placement or trajectory to improve overall link quality.

Existing works, however, leave the following gaps. First, there has only been a handful of works that consider SIC for UAV networks. Most of them consider contention based MAC that does not guarantee QoS requirement. Moreover, they assume the ground station has perfect CSI. In contrast, this thesis considers uncertain channel gains and proposes solutions that assume TDMA.

Very few MPR papers have used TDMA to guarantee transmission slots to multiple nodes. Moreover, most of these works consider fixed access points and not UAV. In addition, none of them allow nodes to learn the best time slot and data rate for a given frame size or schedule. Also, prior works do not consider adjusting the schedule length dynamically in order to improve throughput or to minimize collision and idle slots. By contrast, this thesis considers generating the joint problem of determining the shortest possible TDMA schedule and finding the best transmission slot and data rate for each UAV.

With regards to past works on placement optimization, none of them aims to minimize TDMA schedule length by optimizing UAV placement. Moreover, none

of them consider placement optimization of a SIC capable UAV base station in the presence of interference from other UAVs.

In the next chapter, this thesis will focus on filling these gaps. Specifically, this thesis will aim to maximize the overall throughput of multi-UAV networks by using SIC in the presence of imperfect CSI.

# Chapter 3

# Throughput Maximization Using Discrete Optimization

As shown in Chapter 2, past works using SIC have not focused on minimizing schedule length using TDMA. Most of the past works that consider multiple UAVs, assume a contention-based MAC, whereas this chapter considers a TDMA schedule. Moreover, in contrast to past works, this chapter considers dynamic channel conditions. Lastly, no one has considered using a discrete optimization approach to identify a TDMA schedule that yields the highest throughput.

To this end, this chapter aims to minimize the TDMA schedule length for use in multi-UAVs networks. To shorten the schedule length, the proposed approach equips the ground station with a SIC radio. A fundamental problem is ensuring the ground station is able to decode each transmission subject to some conditions being met; these conditions are elaborated in Section 3.1.

This chapter contains the following contributions. First, it addresses a novel problem in SIC-capable UAV networks: given a UAV network with a ground station equipped with a SIC-capable radio, determine the best TDMA transmission schedule that yields the highest expected number of transmission successes over random

channel gains. The work is significant as it allows multiple UAVs to transmit simultaneously to a ground station in a collision free manner using a TDMA transmission schedule that operates over random channel gains. Second, the chapter proposes a discrete optimization solution that allows a ground station to learn over time the best transmission schedule with a high expected number of successes. Third, it proposes a heuristic to generate a subset of transmission schedules. This then allows us to apply the discrete optimization solution in large scale UAV networks. Fourth, the proposed solutions are verified in small and large scale UAV networks. In addition, the chapter includes actual received signal strength values from a real-time implemented testbed with three UAVs.

The rest of this this chapter is organized as follows. Section 3.1 presents the system model. Section 3.2 discusses the solutions to the problems outlined in Section 3.1. The results are discussed in Section 3.3 and lastly conclusions are presented in Section 3.5.

## 3.1 System Model

The network consists of a set $U$ of UAVs. There are $|U|$ UAVs and a ground station. The time is divided into fixed time slots; each time slot given by $n$. Each UAV must have one transmission slot in the resulting schedule; in particular, this ensures fairness as each UAV has an equal transmission opportunity. It is assumed that each UAV has data to transfer to the ground station at all times. The ground station has full control of the orientation and position of each UAV, and it also has SIC capability [201]. Each UAV is aware of its location through GPS, and it is equipped with a radio for communication with the ground station. Each UAV has a half-duplex radio, whereby it can either transmit or receive to/from the ground station. The transmit power from UAV $U_i \in U$ to the ground station is given as $P_i$. The channel gain of links are independent and identically distributed (i.i.d). The channel gain from UAV $i$ is denoted as $g_i$ and it follows the Nakagami-m [56] distribution.

At time $n$, the random vector $\mathbf{g}^n = \{g_i^n \mid \forall i \in U\}$ and its probability distribution is defined as $\mathcal{X}$. The received power at the ground station for UAV $i$ at time $n$ is given as $P_r^i = P_i|g_i^n|^2$.

Transmissions from UAVs to the ground station are governed by a transmission schedule $\omega_z$. The collection of transmission schedules is given as $\Omega = \{\omega_1, \ldots, \omega_{|\Omega|}\}$. Each transmission schedule $\omega_z \in \Omega$ spans one or more time slots and affords each UAV one or more opportunities to transmit to the ground station. An example transmission schedule is shown in Figure 3.1. Figure shows that a transmission schedule is comprised of one or more transmission sets, denoted as $a_i$. Each transmission set $a_i \in \omega_z$ runs for a single time slot and all UAVs in a transmission set transmit simultaneously. In Figure 3.1, the transmission schedule uses transmission set $a_1 = \{U_1, U_2, U_3\}$ in time slot-1 followed by transmission set $a_2 = \{U_4, U_5\}$ in time slot-2. There can be up to $L$ transmitting UAVs in a transmission set. Note, $L$ denotes the SIC decoding factor and it cannot be too large since a large $L$ value will result in more inter-user interference. In particular, reference [202] shows that having SIC factor greater than three results in poor performance.

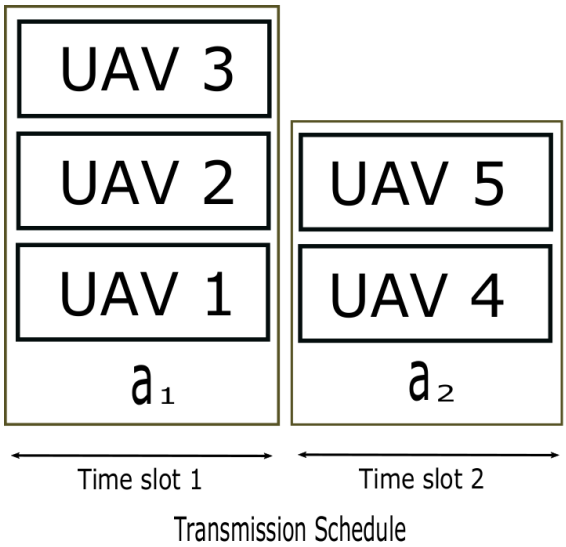


Figure 3.1: An example transmission schedule.

For a given transmission set, the ground station is capable of canceling the

interference from $L-1$ neighbors. The SINR threshold, denoted as $\beta$, is a threshold that must be satisfied for a given transmission to be successful. In practice, this threshold is dependent on the MCS used by UAVs. The transmission from node $i$ to the ground station, given noise power $N_o$, will be successful if it satisfies the following SINR constraint,

$$\frac{P_i|g_i|^2}{N_o + \sum_{q=1}^{L-1} P_q|g_q|^2} \geq \beta \tag{3.1}$$

Assume that there are $k$ transmitting nodes in $\omega_z$, and the received power from these nodes is ordered as follows: $P_r^1 \leq P_r^2 \leq \ldots P_r^k$. Then decoding is carried out in the following order: $k, k-1, \ldots, 1$. Specifically, the $k$-th transmission is successful if,

$$\frac{P_k|g_k|^2}{N_o + \sum_{q=1}^{k-1} P_q|g_q|^2} \geq \beta \tag{3.2}$$

Assuming the $k$-th transmission can be decoded, i.e., it satisfies (3.2), the ground station proceeds to decode the $(k-1)$-th transmission by subtracting the $k$-th signal from the composite signal. Then the second or $(k-1)$-th transmission will be successful if,

$$\frac{P_{(k-1)}|g_{(k-1)}|^2}{N_o + \sum_{q=1}^{k-2} P_q|g_q|^2} \geq \beta \tag{3.3}$$

The ground station repeats the above process for the $(k-2)$-th transmission until it decodes all $k$ transmissions. In the above decoding process, the difference in received power, i.e., product of $P_i$ and $g_i$ is critical to ensure $k$ is as large as possible [176].

For each transmission set $a_i$, let $\Gamma(a_i)$ return the number of transmissions that are decoded successfully by the ground station. Note that $\Gamma(a_i) \leq |a_i|$. Let the function $\Phi(\omega_z)$ return the *success rate* of transmission schedule $\omega_z$. Formally,

$$\Phi(\omega_z) = \frac{\sum_{a \in \omega_z} \Gamma(a)}{|\omega_z|} \tag{3.4}$$

Note, expression (3.4) can be converted to throughput via $\Phi(\omega_z) \times \frac{r}{\tau}$, where $r$ is

Table 3.1: List of Parameters

| Symbol | Definition |
|---|---|
| $P_i$ | Transmit power from node $i$ to ground station $s$ |
| $g_i$ | Channel gain from node $i$ to ground station $s$ |
| $L$ | SIC decoding factor or number of concurrent transmissions |
| $\beta$ | SINR threshold |
| $U$ | Set of UAVs |
| $n$ | Time slot index |
| $U_i$ | The $i$-th UAV |
| $a_i$ | The $i$-th transmission set |
| $\omega_z$ | The $z$-th transmission schedule |
| $\Omega$ | Collection of transmission schedules |
| $N_o$ | Ambient noise power |

the data rate corresponding to SINR threshold $\beta$ and $\tau$ is the duration of each time slot. It is also to note that instead of considering the data rate corresponding to $\beta$, the asymptotic capacity as calculated by $\log_2(1+\varphi)$ can also be used, where $\varphi$ corresponds to the left-hand-side of expression (3.1), (3.2) and (3.3).

The aim is to identify a transmission schedule in $\Omega$ that yields the highest throughput or success rate. Formally,

$$\omega^* = \arg\max_{\omega \in \Omega} \Phi(\omega) \tag{3.5}$$

In practice, it is not straightforward to identify $\omega^*$. This is because for a chosen transmission schedule, it may suffer varying number of decoding failures over time due to random channel gains. This means only a noisy estimate of $\Phi(\omega_z)$ is available, where the number of successful transmissions varies in the range $[0, |U|]$.

The goal is thus to identify a transmission schedule in $\Omega$ that has the best average performance. This problem is formulated as a transmission schedule selection problem. This can be posed as a discrete stochastic optimization problem [101] that is run at the ground station. Let $\phi(n, \omega_z)$ be an unbiased, noisy estimate of the

success rate of transmission schedule $\omega_z$ at time $n$. In other words, determine $\Phi(\omega_z)$ at time $n$ given random channel gain $\mathbf{g}$. This means the ground station will obtain a sequence of i.i.d random variables over time $n$, denoted as $\{\phi(n, \omega_z), n = 1, 2, \ldots\}$. Then discrete optimization problem is given as,

$$\omega^* = \arg\max_{\omega \in \Omega} \Phi(\omega) = \arg\max_{\omega \in \Omega} \mathbb{E}\{\phi(n, \omega)\} \tag{3.6}$$

The value of $\mathbb{E}\{\phi(n, \omega)\}$ for each transmission schedule $\omega \in \Omega$ is estimated empirically by the ground station. The key challenge to solving (3.6) is identifying the best transmission schedule in $\Omega$ given that the ground station only has a noisy estimate of the number of decoding successes for any transmission schedule.

As an aside, note that one straightforward method to solve (3.6) is to calculate the expected performance of each transmission schedule in $\Omega$. That is, for each $\omega \in \Omega$, i.i.d estimates of its performance can be obtained; i.e., to compute for each $\omega \in \Omega$, the quantity $\frac{1}{L}\sum_{l=1}^{L} \phi(l, \omega)$, where $L$ is the number of samples. By the law of large numbers, as $L \to \infty$, the expected performance of each transmission schedule is obtained. Then, $w^*$ is set to the transmission schedule with the highest expectation. This method, however, is inefficient. To this end, in the next section, comparatively more efficient algorithm to solve (3.6) is outlined.

## 3.2 Solutions

This section first outlines a discrete optimization based solution based on [203] that requires all possible transmissions schedules for a given UAV network. This solution can only be used to derive the optimal transmission schedule for small UAV networks. However, it cannot be used for large scale UAV networks because the set $\Omega$ grows exponentially with the number of UAVs. Consequently, the discrete optimization solution becomes computationally intractable. To this end, Section 3.2.2 presents a heuristic solution that generates a subset of the total transmission sets before using

the discrete optimization solution to identify the best transmission schedule.

### 3.2.1 Discrete Optimization Algorithm

This algorithm has the following key ideas. Let the selected transmission schedule at time $n$ be $\omega^{(n)}$. Initially, at time $n = 0$, the ground station selects a random transmission schedule, say $\omega_x$. Therefore, $\omega^{(0)} = \omega_x$. For each subsequent time slots, the ground station evaluates $\phi[n, \omega^{(n)}]$; i.e., it uses the transmission schedule $\omega^{(n)}$ to gauge its performance. It also picks another transmission schedule, say $\omega_z$ from $\Omega$ uniformly, where $\omega_z \neq \omega^{(n)}$. It then obtains an independent observation of $\phi[n, \omega_z]$. Based on these evaluations, the ground station determines whether $\omega^{(n)}$ is better than $\omega_z$. If so, it sets $\omega^{(n+1)} = \omega_x$. Otherwise, it sets $\omega^{(n+1)} = \omega_z$. After that the ground station updates the number of times or frequency it has chosen a given transmission schedule. This frequency can then be used to determine the most popular transmission schedule up till time $n$. As will be shown later, this will converge to the global optimal transmission schedule. It is worth noting that the sequence $\{\omega^{(n)}\}$ forms a Markov chain with states corresponding to the transmission schedules in $\Omega$. The optimal solution is the state or transmission schedule in which the algorithm visits the most frequently.

Algorithm 1 shows the details of the aforementioned steps. In the initialization stage, see lines 1-6, the time index $n$ is set to zero, and a random transmission schedule (line 3) from $\Omega$ is selected. Algorithm also initializes the best transmission schedule to be the one selected in line-3. Lines 6-7 initialize a vector or array $\pi[]$ with dimension $|\Omega|$. Each element, say $\pi[\omega]$, stores the number of times in which the algorithm has used transmission schedule $\omega$. Initially, $\omega^{(0)}$ has been used once (line 5) whilst the other transmission schedules in $\Omega - \omega^{(0)}$ have never been used (line 6). The purpose of lines 9-17 is to evaluate whether the current transmission schedule, i.e., $\omega^{(n)}$, is better than a *neighbor* transmission schedule $\tilde{\omega}^{(n)}$. Specifically, the algorithm selects a transmission schedule $\tilde{\omega}^{(n)}$ uniformly from the set $\Omega - \omega^{(n)}$. It then

obtains an independent estimate $\phi[n, \omega^{(n)}]$ and $\phi[n, \tilde{\omega}^{(n)}]$. Given these estimates, the algorithm decides the transmission schedule to use in time $n+1$; lines 12. In line 14 and 17, the algorithm also increases the usage count of the transmission schedule chosen in time $n+1$. Lastly, in lines 19-22, the algorithm determines the best transmission schedule thus far; i.e., the transmission schedule that has been visited or used the most often.

**Algorithm 1** Discrete Stochastic Approximation Algorithm

1: **Initialization**
2: $n \leftarrow 0$
3: Set $\omega^{(n)} = \text{Rand}(\Omega)$
4: Set $\hat{\omega} = \omega^{(n)}$
5: Set $\pi[\omega^{(n)}] = 1$
6: Set $\pi[\omega] = 0$, for all $\omega \in \Omega - \omega^{(n)}$
7: **Main Body**
8: **for** $n = 0, 1, \ldots,$ **do**
9: ▷ *Sample and evaluate*
10: Set $\tilde{\omega}^{(n)} = \text{Rand}(\Omega - \omega^{(n)})$
11: Evaluate $\phi[n, \omega^{(n)}]$ and $\phi[n, \tilde{\omega}^{(n)}]$
12: **if** $\phi[n, \tilde{\omega}^{(n)}] > \phi[n, \omega^{(n)}]$ **then**
13: $\omega^{(n+1)} = \tilde{\omega}^{(n)}$
14: $\pi[\tilde{\omega}^{(n)}]$++
15: **else**
16: $\omega^{(n+1)} = \omega^{(n)}$
17: $\pi[\omega^{(n)}]$++
18: **end if**
19: ▷ *Track the best transmission schedule*
20: **if** $\pi[\omega^{(n+1)}] > \pi[\hat{\omega}]$ **then**
21: $\hat{\omega} = \omega^{(n+1)}$
22: **else**
23: $\hat{\omega} = \hat{\omega}$
24: **end if**
25: **end for**

Next part presents and discusses the sufficient conditions that will be used to prove convergence to the optimal state. Recall that the sequence $\{\omega^n\}$ is a Markov chain. In fact, it forms an homogeneous irreducible and aperiodic Markov chain. This sequence converges to the optimal state $\omega^*$; i.e., it will spend or visit this transmission schedule more frequently than any other states in $\Omega$. This fact is stated formally in the next proposition.

**Proposition 3.7.** *As per [101], for given transmission schedules $\omega^*$, $\omega$ and $\tilde{\omega}$, where $\omega^* \neq \omega$ and $\omega^* \neq \tilde{\omega}$, Algorithm 1 converges to the optimal transmission schedule(s) if it satisfies the following conditions:*

$$P\{\phi(n,\omega^*) > \phi[n,\omega]\} > P\{\phi(n,\omega) > \phi[n,\omega^*]\} \tag{3.8}$$

$$P\{\phi(n,\omega^*) > \phi[n,\tilde{\omega}]\} > P\{\phi(n,\omega) > \phi[n,\tilde{\omega}]\} \tag{3.9}$$

In words, at time $n$, inequality (3.8) represents the fact that the optimal state $\omega^*$ is always more favorable (or likely), due to a higher $\phi(n,\omega^*)$ value, than any other states in $\Omega$. Inequality (3.9) says that that when Algorithm-1 is in a non-optimal state, e.g., $\tilde{\omega}$, it is more likely to transition into the optimal state $\omega^*$ than any other state $\omega \in \Omega$. Next step shows that Algorithm-1 satisfies inequalities (3.8) and (3.9), and thus allow us to draw the following conclusion.

**Proposition 3.10.** *Algorithm 1 finds the transmission schedule $\omega^*$ that maximizes problem (3.6).*

*Proof.* It is assumed the random values of $\phi(n,\omega)$ follow a Gaussian distribution $\mathcal{N}(\mu,\sigma^2)$. This is reasonable as the ground station is able to obtain independent samples of $\phi(n,\omega)$ and compute the sample mean. Hence, as per the Central Limit Theorem, the distribution of the sample mean approaches a Gaussian distribution. Also note that the variance of $\phi(n,\omega)$ is finite; it varies from $[0,|U|]$. Denote the mean and variance of $\phi(n,\omega)$ as $\mu_\omega$ and $\sigma^2_\omega$, respectively. Consider three transmission schedules: $\omega^*$, $\omega$ and $\tilde{\omega}$, where $\max\{\mu_{\omega^*},\mu_\omega,\mu_{\tilde{\omega}}\} = \mu_{\omega^*}$

As $\phi(n,\omega^*) > \phi(n,\omega)$ then, $\mu_{\omega*} > \mu_\omega$, meaning condition (3.8) can be revised to

$$P\{(\phi(n,\omega^*) - \phi[n,\omega] > 0\}) > P\{(\phi(n,\omega) - \phi[n,\omega^*]) > 0\}. \tag{3.11}$$

This can be rewritten as,

$$P\{\big(\mathcal{N}(\mu_{\omega^*}, \sigma^2_{\omega^*}) - \mathcal{N}(\mu_\omega, \sigma^2_\omega)\big) > 0\} > P\{\big(\mathcal{N}(\mu_\omega, \sigma^2_\omega) - \mathcal{N}(\mu_{\omega^*}, \sigma^2_{\omega^*}\big) > 0\} \quad (3.12)$$

$$P\{\mathcal{N}(\mu_{\omega^*} - \mu_\omega, \sigma^2_{\omega^*} + \sigma^2_\omega) > 0\} > P\{\big(\mathcal{N}(\mu_\omega - \mu_{\omega^*}, \sigma^2_\omega + \sigma^2_{\omega^*}\big) > 0\} \quad (3.13)$$

The condition expressed by inequality (3.13) is equivalent to,

$$\frac{\mu_{\omega^*} - \mu_\omega}{\sqrt{\sigma^2_{\omega^*} + \sigma^2_\omega}} > \frac{\mu_\omega - \mu_{\omega^*}}{\sqrt{\sigma^2_\omega + \sigma^2_{\omega^*}}} \quad (3.14)$$

Observe that the variance is the same. Hence, $\mu_{\omega^*} - \mu_\omega > \mu_\omega - \mu_{\omega^*}$, which is true as $\mu_{\omega^*} > \mu_\omega$. This proves sufficient condition (3.8).

As for condition (3.9),

$$P\{(\phi(n, \omega^*) - \phi[n, \tilde{\omega}]) > 0\} > P\{(\phi(n, \omega) - \phi[n, \tilde{\omega}]) > 0\}, \quad (3.15)$$

and can be rewritten as,

$$P\{\big(\mathcal{N}(\mu_{\omega^*}, \sigma^2_{\omega^*}) - \mathcal{N}(\mu_{\tilde{\omega}}, \sigma^2_{\tilde{\omega}})\big) > 0\} > P\{\mathcal{N}(\mu_\omega, \sigma^2_\omega) - \mathcal{N}(\mu_{\tilde{\omega}}, \sigma^2_{\tilde{\omega}}) > 0\} \quad (3.16)$$

$$P\{\mathcal{N}(\mu_{\omega^*} - \mu_{\tilde{\omega}}, \sigma^2_{\omega^*} + \sigma^2_{\tilde{\omega}}) > 0\} > P\{\mathcal{N}(\mu_\omega - \mu_{\tilde{\omega}}, \sigma^2_\omega + \sigma^2_{\tilde{\omega}}) > 0\} \quad (3.17)$$

Then, (3.17) can also be rewritten as

$$\frac{\mu_{\omega^*} - \mu_{\tilde{\omega}}}{\sqrt{\sigma^2_{\omega^*} + \sigma^2_{\tilde{\omega}}}} > \frac{\mu_{\omega} - \mu_{\tilde{\omega}}}{\sqrt{\sigma^2_{\omega} + \sigma^2_{\tilde{\omega}}}} \tag{3.18}$$

As the variance is same for all $\phi(n, \omega)$, i.e., $[0, |U|]$, thus $\mu_{\omega^*} - \mu_{\tilde{\omega}} > \mu_{\omega} - \mu_{\tilde{\omega}}$. Hence, Algorithm-1 satisfies sufficient conditions (3.8) and (3.9). This completes the proof. □

### 3.2.2 Dynamic Transmission Sets

The discrete optimization algorithm explained in Section 3.2.1 requires a collection of transmission schedules $\Omega$ as input. When there are a large number of UAVs, the total number of transmission sets in $\Omega$ grows exponentially with the number of UAVs. Hence, it becomes computationally infeasible to check all the transmission sets in $\Omega$ for large UAV networks. To this end, this section proposes a heuristic that only generates a subset of the maximum possible transmission schedules. After that Algorithm-1 is applied on these reduced number of transmission schedules in order to determine the best one; note that the computed transmission schedule in this case may not be optimal as all transmission schedules are not available at hand.

The basic idea of the proposed algorithm is as follows. For each schedule, in each slot, $L$ number of random UAVs are included. Note that the value of $L$ cannot be larger than four. Otherwise, inter-user interference will be too large [176]. This basic idea is illustrated in Algorithm 2. It accepts as input the set of UAVs and the maximum number of transmission schedules to be generated $\Gamma$.

In line 4, it first selects a random $L$ value. This will determine the number of UAVs that can transmit simultaneously in each slot. In line 7, the function **RandShuffle**() is used to return a random ordered set $U'$. For example, if $U = \{1, 2, 3, 4\}$, then **RandShuffle**() may return $U' = \{U_3, U_1, U_2, U_4\}$. In line-9, it constructs a set $a_i$ of size $L$. Specifically, it calls the function **PickUAVs()**, which picks UAVs in the following order from the set $U'$: $\varphi, \varphi + 1, \ldots, \varphi + L - 1$. For

example, if $U' = \{U_3, U_1, U_2, U_4\}$, $L = 2$ and $\varphi = 1$, then $a_i = \{U_3, U_1\}$. This set is then added into the transmission schedule $\omega_j$. The while loop from lines 8-13 continues until all UAVs are in a transmission set. Once a transmission schedule is generated, function **TxScheduleExist()** is used to determine whether $\omega_j$ exists in $\Omega$. If it is a new transmission schedule, it is added to $\Omega$. In total, there will be $\Gamma$ transmission schedules; i.e., $|\Omega| = \Gamma$. Note, in practice, a counter can also be included that records the number of times Algorithm 2 has tried to compute $\Gamma$ transmission schedules. If the counter reaches a predefined threshold, then it exits. Lastly, the analysis of run time property of Algorithm-2 is presented.

**Algorithm 2** Dynamic Transmission Algorithm

**Input:** $U$ **and** $\Gamma$
**Output:** $\Omega$

1: $\Omega = \emptyset$
2: $j = 1$
3: **while** $|\Omega| \neq \Gamma$ **do**
4: Set $L =$**Rand**(1,5)
5: Set $i = \varphi = 1$
6: Set $\omega_j = a_i = \emptyset$
7: $U' =$ **RandShuffle**(U)
8: **while** $\sum_i |a_i| \leq |U|$ **do**
9: $a_i =$ **PickUAVs**($\varphi$, $\varphi + L$, $U'$)
10: $\omega_j \cup a_i$
11: $\varphi = \varphi + L$
12: i = i + 1
13: **end while**
14: **if** **TxScheduleExist**($\omega_j, \Omega$) == false **then**
15: $\Omega \cup \omega_j$
16: j = j + 1
17: **end if**
18: **end while**
19: return $\Omega$

**Proposition 3.19.** *Algorithm-2 has a run time complexity of* $\mathcal{O}(\Gamma^2|U|^2)$.

*Proof.* The while loop from lines 3-18 runs for at most $\mathcal{O}(|\Gamma|)$ times. In the worst case, line-4 returns $L = 1$. That means lines 8-13 will run $\mathcal{O}(|U|)$ times, where each transmission schedule only has one transmitting UAV. Line 14 needs to check whether the schedule $\omega_j$ is a member of $\Omega$. Specifically, it needs to check for each

transmission schedule $\omega_k \in \Omega$, whether the condition $\omega_j = \omega_k$ is true. The max size of each transmission schedule is $\mathcal{O}(|U|)$; i.e., each UAV transmits by itself. Hence, to compare two transmission schedule it takes $\mathcal{O}(|U|^2)$. As $|\Omega| = \Gamma$, then the function **TxScheduleExist(.)** takes $\mathcal{O}(\Gamma|U|^2)$. Therefore, the run time complexity of $\mathcal{O}(\Gamma^2|U|^2)$. This completes the proof. □

## 3.3 Results

## 3.4 Evaluation

The experiments are conducted in Matlab. The first set of results considers a small network consisting of four UAVs. After that, a network with thirty UAVs is considered, Algorithm-2 is used as generating all possible transmission schedules is intractable. In the evaluations, except for those in Section 3.4.3, all UAVs are static. However, their channel gain is random. In Section 3.4.3, experiments conducted using the received signal strengths from an actual testbed with three mobile UAVs are presented. It is worth noting that UAVs always have data to transmit in their assigned time slot. All UAVs and the ground station are equipped with a 2.4 GHz radio and transmit at a fixed power of 1 Watt.

### 3.4.1 Small UAV Networks

This section first considers the case where all the transmission sets are known. This part considers four UAVs, which equate to a total of eight transmission schedules; see Table 3.2. Each transmission schedule allows all UAVs to transmit at least once. The UAVs are placed at a distance of 100, 200, 150 and 300 meters from the ground station. The channel gain is simulated using Nakagami distribution with $\mu = 5$ and $\omega = 2$. The system runs each transmission set for 100 time slots and record the total number of successful transmissions. This process is repeated for 10 runs and average of the results is obtained; this is known as a single iteration. Average result

Table 3.2: Transmission Sets. The SIC factor $L$ indicates the number of concurrent transmitters

| Transmission Set (k) | Combination of UAVs | SIC Factor L |
|---|---|---|
| 1 | $\{U_1, U_2\}$, $\{U_3, U_4\}$ | 2 |
| 2 | $\{U_1, U_3\}$, $\{U_2, U_4\}$ | 2 |
| 3 | $\{U_1, U_4\}$, $\{U_2, U_3\}$ | 2 |
| 4 | $\{U_1, U_2, U_3\}$, $\{U_4\}$ | 3 |
| 5 | $\{U_1, U_2, U_4\}$, $\{U_3\}$ | 3 |
| 6 | $\{U_1, U_3, U_4\}$, $\{U_2\}$ | 3 |
| 7 | $\{U_2, U_3, U_4\}$, $\{U_1\}$ | 3 |
| 8 | $\{U_1, U_2, U_3, U_4\}$ | 4 |

of 100 iterations is plotted.

#### 3.4.1.1 Probability Mass Function

This section studies the impact of different SINR thresholds ($\beta$), where $\beta$ is set to either 2, 4, 6 or 8 dB. The Probability Mass Function (PMF) is generated for each $\beta$ value. The symbol $P(k)$ in Figure 3.2 shows the probability of each transmission set. From Figure 3.2, we see that the optimal transmission schedule can be different for each $\beta$ value. This is reasonable because a given $\beta$ value requires a certain SINR threshold; e.g., if $\beta$ is high, then there must be fewer links in each time slot to guarantee there is sufficient gap between received power to ensure the SINR of transmissions is at least $\beta$. Otherwise, there is too much inter-user interference, which results in a high failure rate. For example, when $\beta = 2$, the optimal set is the sixth set where $L = 3$; i.e., up to $L = 3$ transmissions can co-exist in a time slot. However, for higher values of $\beta$, a transmission set with $L = 2$ becomes the optimal transmission schedule, meaning there needs to be fewer transmissions in each time slot.

The results for the shape parameter $\mu$ of the Nakagami-m distribution are discussed next. The shape parameter $\mu$ controls the depth of fading [56], where lower $\mu$ values correspond to higher fading; this represents the case where UAVs are highly

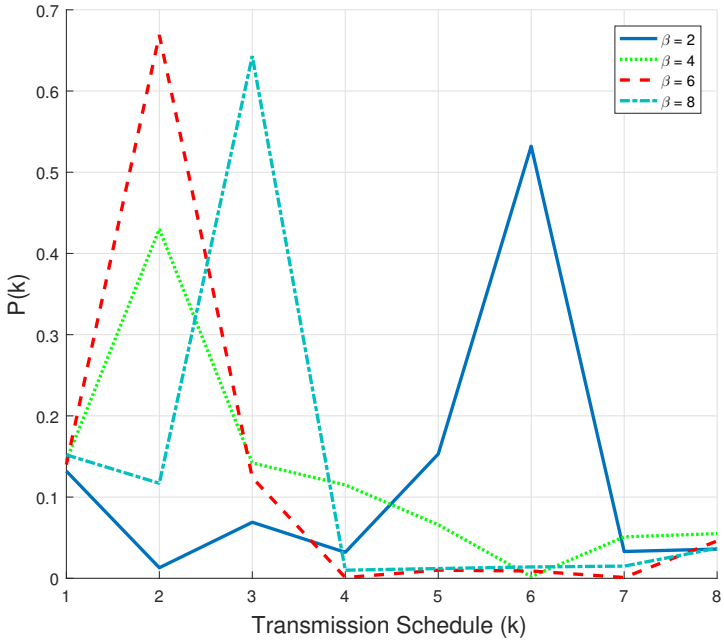


Figure 3.2: Probability vectors for different SINR threshold ($\beta$) values.

mobile. This means as the SINR changes more rapidly, there needs to be fewer number of transmitting UAVs in each time slot in order to account for the wide ranging received power. This is confirmed in Figure 3.3, where lower values of $\mu$ result in the use of transmission schedules with a smaller SIC factor $L$. For example, when $\mu \in \{0.1, 1.5\}$, the optimal transmission schedules are three and two, respectively. These transmission schedules have fewer concurrent transmissions, which are required given the higher fading experienced by UAVs. For higher values of $\mu$, namely $\mu \in \{3, 5\}$, transmission schedules with $L = 3$ perform better; namely transmission schedules five and six are optimal for these cases. This is because with better channel conditions, more UAVs can be accommodated in each transmission schedule.

#### 3.4.1.2 Impact of SINR Threshold

Based on the results in Section 3.4.1.1, next part compares the number of successful transmissions for different $\beta$ values. Figure 3.4 shows that the performance degrades with increasing SINR thresholds. Figure 3.4 shows that the number of successful

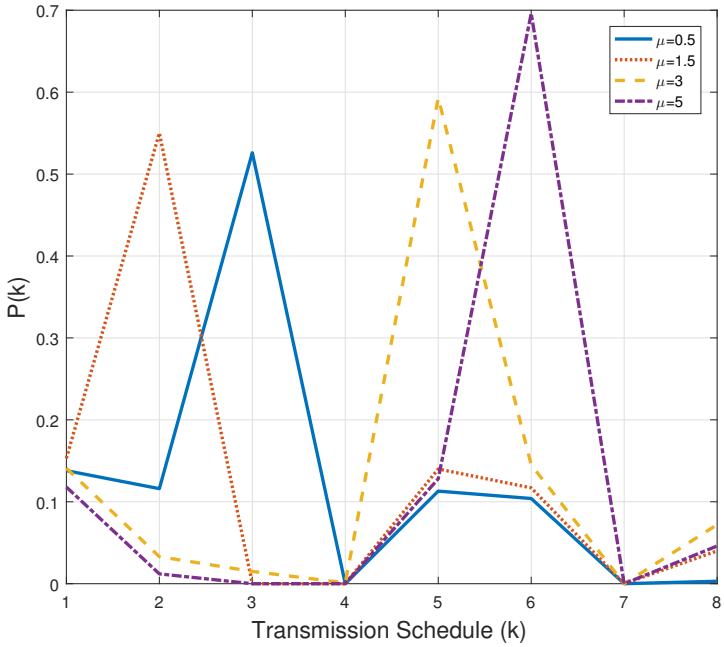


Figure 3.3: Probability vectors for different $\mu$ values.

transmissions is highest when $\beta$ is either one or two; i.e., more than 70%. When $\beta$ is increased to four, the percentage of successful transmissions drops to less than 50%. The performance further drops below 20% when $\beta$ is increased to six. This is because a high threshold corresponds to a high data rate requirement. That is, the received power must be high to ensure sufficient SINR threshold; equivalently, each transmission must experience minimal interference.

#### 3.4.1.3 Epsilon-Greedy Algorithm

This part compares the performance of the optimal transmission schedule against the $\epsilon$-greedy algorithm. Note that $\epsilon$-greedy is widely used in reinforcement learning approaches to balance between exploration and exploitation of actions; see [204] for details. The $\epsilon$-greedy approach is tested with two different values: $\epsilon = 0.2$ and then again with $\epsilon = 0.4$. When $\epsilon = 0.4$, it has a 40% chance of selecting a transmission that does not have the maximum performance. This means it uses the transmission schedule with the highest number of successes 60% of the time. Similarly, when $\epsilon = 0.2$, it explores other transmission schedules 20% of the time,

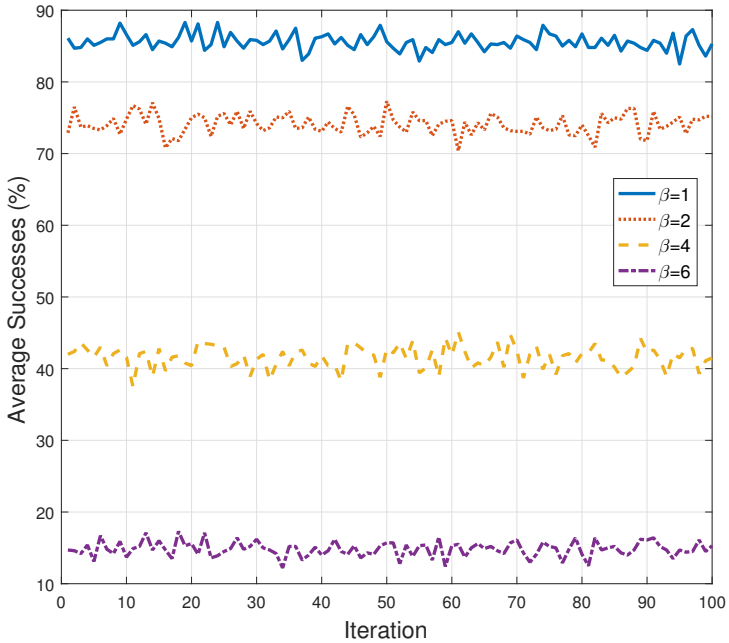


Figure 3.4: Performance comparison with different $\beta$ values.

and in the remaining time, it uses the best performing transmission schedule thus far.

Figure 3.5 and 3.6 show that the percentage of successful transmissions is higher when $\epsilon = 0.2$ as compared to $\epsilon = 0.4$. The plots show that the optimal schedule has a success rate of 75% on average whereas $\epsilon$-greedy with $\epsilon = 0.2$ has a success rate of near 55%. In contrast $\epsilon$-greedy with $\epsilon = 0.4$ has a success rate of less than 50% on average. This is because $\epsilon$-greedy with $\epsilon = 0.2$ explores for only 20% of the time and uses the transmission schedule with the highest success at till that point 80% of the times. On the other hand, $\epsilon = 0.4$ explores all other transmissions sets 40% of the time while using the best transmission schedule up till that point 60% of the time. Figure 3.5 and 3.6 show that $\epsilon$-greedy can fluctuate significantly and sometimes it can perform closer to the optimal schedule. This can be explained by the fact that it frequently explores other transmission schedules, meaning it may find the best transmission schedule in some time slots whilst at other times, it may use a transmission schedule with a high failure rate.

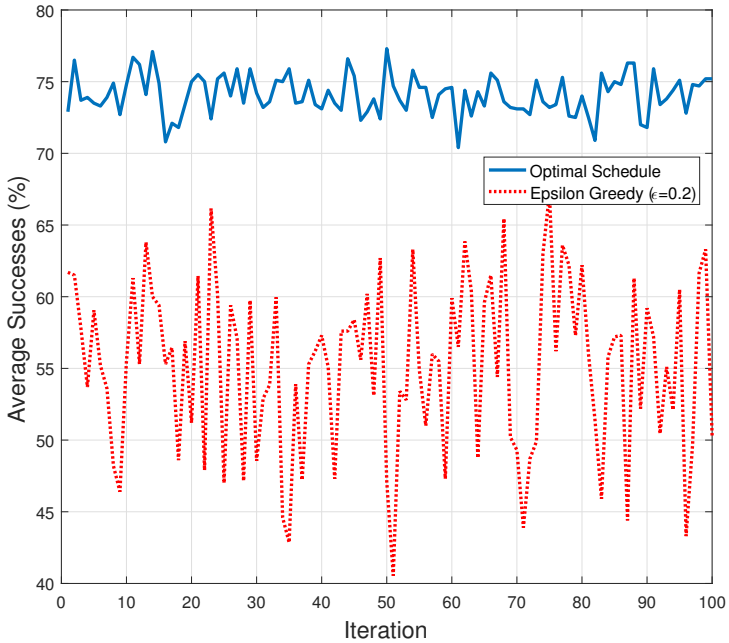


Figure 3.5: $\epsilon$-Greedy versus the optimal transmission schedule ($\epsilon = 0.2$).

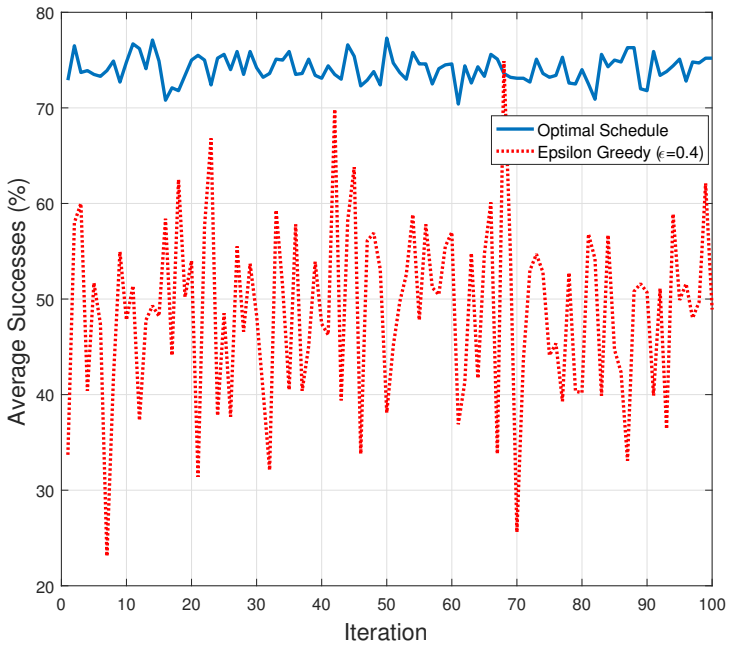


Figure 3.6: $\epsilon$-greedy versus the optimal transmission schedule ($\epsilon = 0.4$).

### 3.4.2 Large UAV Networks

In the next experiment, a large UAV network is considered. Algorithm-2 is used to generate transmission sets for scenarios with 30 UAVs. The UAVs are placed randomly in the air with a distance ranging from 50 to 500 meters.

#### 3.4.2.1 Comparison of SINR Threshold values

Figure 3.7 compares the performance Algorithm-2 for different $\beta$ values. Its performance is better for lower values of $\beta$ as transmissions easily meet the lower SINR threshold. On the other hand, with higher $\beta$ values, then interference caused by simultaneously transmissions means it is unlikely that a transmission's SINR meets the high $\beta$ value. Figure 3.7 also shows that performance declines as the number of UAVs increases. This is due to the decreasing spacing between UAVs which results in lower differences in received power levels at the ground station. A higher difference in received power level is important for the operation of SIC.

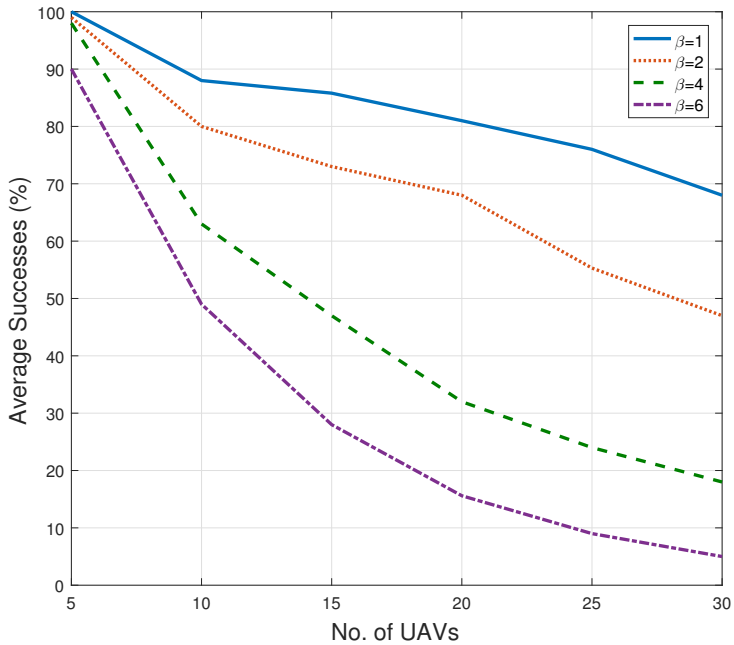


Figure 3.7: Performance comparison with different $\beta$ values.

#### 3.4.2.2 Dynamic versus Epsilon-Greedy

This subsection studies the performance of Algorithm-2 against the $\epsilon$-greedy algorithm. For the case of large number of UAVs, the $\epsilon$-greedy protocol is executed with $\epsilon = 0.2$ and $\epsilon = 0.4$. Figure 3.8 and 3.9 show that the performance of $\epsilon$-greedy algorithm fluctuate more than Algorithm-2. This is because of its exploration process where it uniformly selects another transmission schedule 20% or 40% of the time. As a result, the ground station may pick a transmission schedule with a high number of successes or one that fails frequently

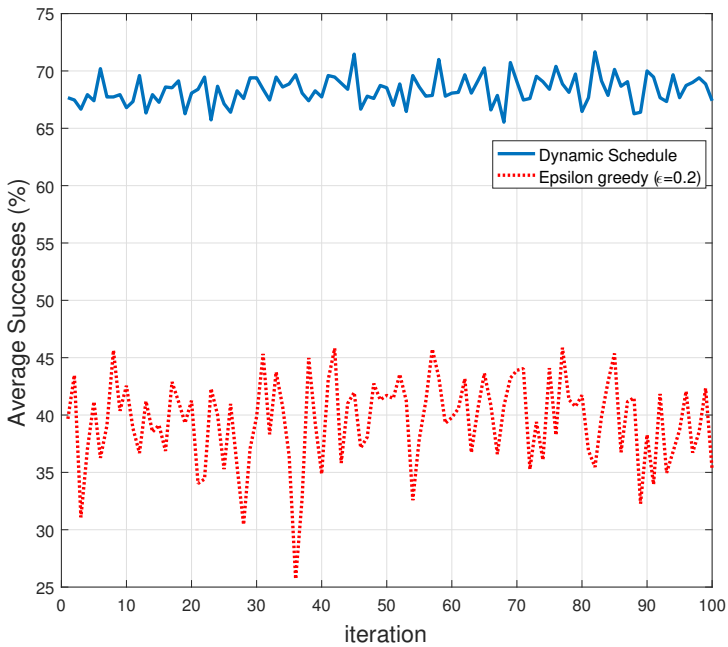


Figure 3.8: $\epsilon$-greedy versus the optimal transmission schedule ($\epsilon = 0.2$).

### 3.4.3 Experiments on a UAV Testbed

This subsection includes the results achieved by conducting trace-based simulation using the received power from three UAVs shown in Figure 3.10. Specifically, received strength values were collected from three quad-copter UAVs. All UAVs are equipped with a 433 MHz Long Range (LoRa) radio. The transmission sets for this experiment are shown in Table 3.3. The experiment considers two cases: *static*

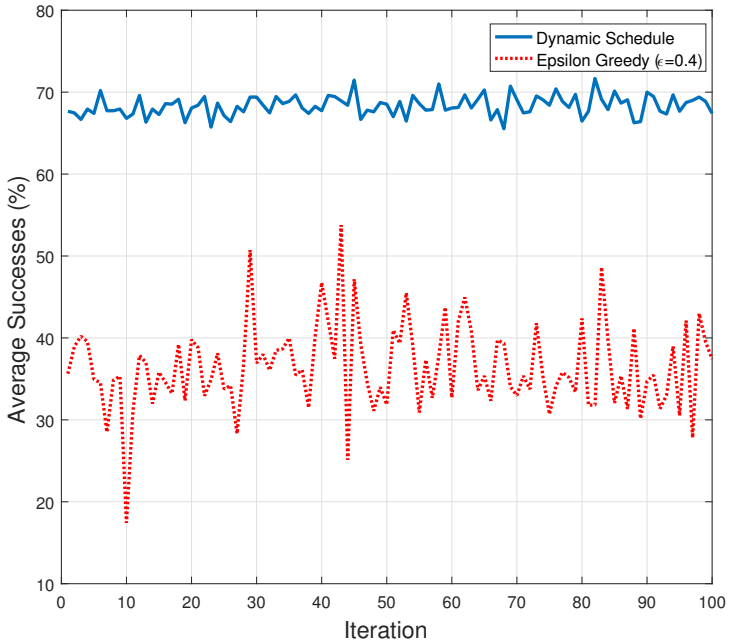


Figure 3.9: $\epsilon$-greedy versus the optimal transmission schedule ($\epsilon = 0.4$).

and *mobile* UAVs. In both cases, RSSI values are collected from each UAV for five minutes and the UAVs are located at a height of 30 meters. For the mobile case, the three UAVs circle the ground station at a speed of 3 m/s. The trace-based simulations were conducted for 300 time slots. The SINR threshold was set to 0 dB for this experiment.

Referring to Figure 3.11, we see that transmissions are successful nearly half of the times for transmission schedules with $L = 2$. For the transmission set with $L = 3$, the number of successful transmissions is quite low, where we see only 70 successes out of 300 attempts for the static case. This number is even lower for the mobile case with only 10 successes because the received power levels are very close to each other. This results in more decoding errors. Hence, the results indicate that the UAVs should be operated at different distances from the ground station. The aforementioned results agree with those in Section 3.4.1.1. That is, if UAVs are mobile, then a transmission schedule with fewer number of transmitters per slot is required. This is reasonable as a wider gap in received power or lower interference is required to ensure a transmission meets its required SINR threshold.

Table 3.3: Transmission Sets for the testbed scenario

| Transmission Set | Combination of UAVs | SIC Factor L |
|---|---|---|
| 1 | $\{U_1, U_2\}$, $\{U_3\}$ | 2 |
| 2 | $\{U_2, U_3\}$, $\{U_1\}$ | 2 |
| 3 | $\{U_1, U_3\}$, $\{U_2\}$ | 2 |
| 4 | $\{U_1, U_2, U_3\}$ | 3 |

Figure 3.10: Three quadcopter UAVs experiments

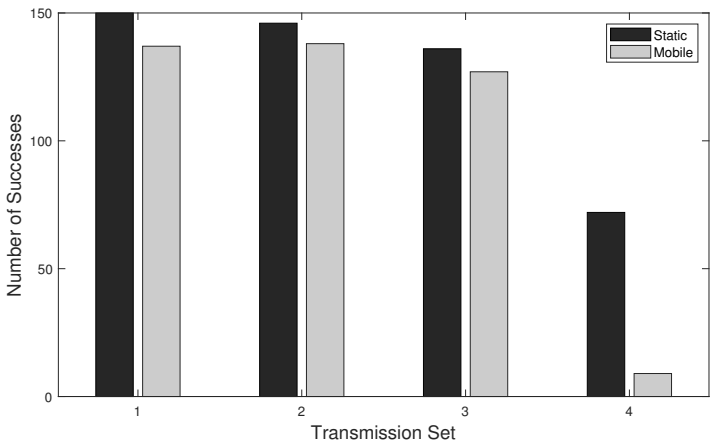


Figure 3.11: Number of successful transmissions for static and mobile UAVs scenarios.

## 3.5 Conclusion

A multi-UAVs network requires a robust TDMA schedule that performs well across all possible channel gain realizations. To this end, this chapter proposes two solutions that allow an operator to identify the best transmission schedule that has the highest average number of transmission successes. The first solution requires all possible transmission schedules and yield the optimal transmission schedule. The second solution uses the first solution but with a reduced number of transmission schedules generated using a heuristic. The results show that both solutions allow a ground station to learn the best transmission schedule for the given channel condition. In particular, if the channel condition is poor due to highly mobile UAVs, it selects a transmission schedule with fewer number of UAVs in each time slot. On the other hand, if the channel condition is favourable or UAVs are relatively static, then the ground station employs a transmission schedule with a high number of transmitting UAVs in each time slot.

A limitation of the proposed MAC is that it is a centralized solution. Therefore, a ground station is responsible for generating transmission schedules. As discussed in Section 1.2, a distributed MAC is preferable over centralized MAC due to less overheads. In particular, collecting information about all nodes at a ground station can add extra overheads. To this end, the next chapter proposes a distributed link access mechanism that allows UAVs to learn their transmission policy. Another limitation in the proposed MAC is that it does not consider multiple data rates. UAVs may experience transmission failures due to random channel conditions. In such a case, it is preferable for UAVs to switch to a lower order MCS. Therefore, the next chapter also deals with this problem and proposes a MAC that allows UAVs to select a MCS for a given channel condition.

Chapter 4

# A Learning MAC for Multi-UAVs Networks

As discussed in Chapter 2, previous works do not consider equipping UAVs with learning capabilities. None of them equip UAVs with capability to learn the best time slot and data rate for a given frame size or schedule. Also, prior works do not consider adjusting the schedule length dynamically in order to improve throughput or to minimize collision and idle slots when a receiver has SIC capability By contrast, this chapter focuses on the joint problem of determining the shortest possible TDMA schedule and finding the best transmission slot and data rate for each UAV.

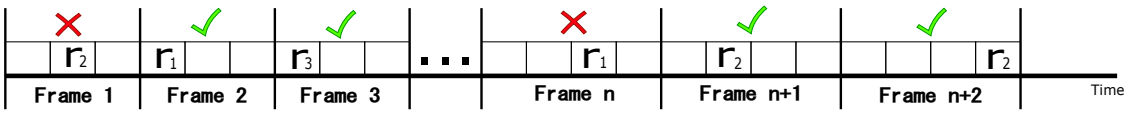


Figure 4.1: A UAV's learning process.

The proposed scheme is known as L-MAC scheme and it is used by UAVs and a ground station to learn the transmission schedule that yields the highest throughput. Figure 4.1 gives an overview of L-MAC running at a UAV, where $r_i$ indicates a data rate, where $i \in \{1, 2, 3\}$. Assume the data rate $r_i$ is higher than $r_j$ if $j < i$. Figure 4.1 also shows that in the first frame, the UAV transmits in the second time slot with a

data rate of $r_2$, which let's assume fails due to collision or interference. In the next frame, the UAV transmits in the first time slot, which is successful. The transmission is also successful in slot-1 of frame-3 but with a higher data rate. Hence, the best transmission policy for the UAV is to transmit in slot-1 of each frame with data rate $r_3$. When the learning process is over for a frame size, the ground station may adjust the frame size after noticing a high number of collisions and idle slots; in Figure 4.1, starting from frame $n$, the ground station changes the frame size to four slots. This causes UAVs to restart their learning process for the new frame size.

In summary, contributions for this chapter are as follows:

- The chapter addresses the following problem: given a multi-rate UAVs network with a ground station that has SIC capability, determine the shortest possible schedule and transmission policy of each UAV. The work proposes a novel distributed solution called L-MAC, whereby UAVs use a Softmax based function to learn the best time slot for a given frame or schedule size. They also use the same function to determine the best data rate for the selected time slot. Once all UAVs have learned the best time slot and data rate, the frame size is repeated until the ground station finds that it causes too many collisions and idle slots. It then sets a new frame size.

- The considered aim and problem are novel. It is to emphasize that prior works have not considered deriving a TDMA schedule dynamically for a receiver equipped with a SIC radio, and no works have considered a learning approach to determine the best time slot and MCS in conjunction with a dynamic frame length adjustment algorithm. This work is in contrast to those that use CSMA/CA where a UAV does not have a designated transmission slot. In this case, once the best slot and data rate are found, a UAV continues to use them for the given frame size. In other words, L-MAC enables UAVs to transmit in a deterministic time slot and data rate. Moreover, by learning the shortest possible schedule, UAVs are able to transmit frequently; i.e., their

link capacity to the ground station is high. Lastly, the derived schedule can serve as a capacity upper-bound for any random channel access protocols.

The remaining sections of this chapter are organized as follows. Section 4.1 discusses the system model. Then in Section 4.2, the problem statement is defined formally. Section 4.3 presents the details of L-MAC. The results are discussed in Section 4.4. The conclusions are presented in Section 4.5.

## 4.1 System Model

Each UAV $u_i$, where $i = 1, 2, \ldots, |U|$ supports multiple data rates. UAVs need to support multiple data rates due to highly varying channel conditions. Therefore, UAVs can switch to a higher or lower order MCS index based on channel conditions. Specifically, UAVs have a set $\mathcal{M}$ containing MCS indexes. Each MCS index corresponds to a predefined SINR threshold $\beta_z$, where $z \in \mathcal{M}$. In particular, the SINR at the ground station must exceed $\beta_z$ in order to attain a data rate of $r_z$. It is assumed that each UAV has data to transfer to the ground station at all times. The channel gain from UAV $i$ to the ground station is denoted as $g_i$. Lastly, UAVs do not cooperate with each other.

Transmissions from UAVs to the ground station are carried out in terms of frames. Each frame is denoted as $\mathcal{F}_n$ which contains $|\mathcal{F}_n|$ time slots. Each time slot is given as $t_j$, where $j = \{1, 2, \ldots, |\mathcal{F}_n|\}$. UAVs are responsible for selecting a time slot and an MCS in each frame. Each UAV selects a time slot and a MCS based on a probability; this is explained in Section 4.3. Each UAV can only transmit once in each frame. Figure 4.2 shows an example frame structure. We see that each time slot $t_j \in \mathcal{F}_n$ can include multiple UAVs. Specifically, in Figure 4.2, the first frame comprises of two time slots with the following UAVs: $t_1 = \{u_1, u_2, u_3\}$ followed by $t_2 = \{u_4, u_5\}$.

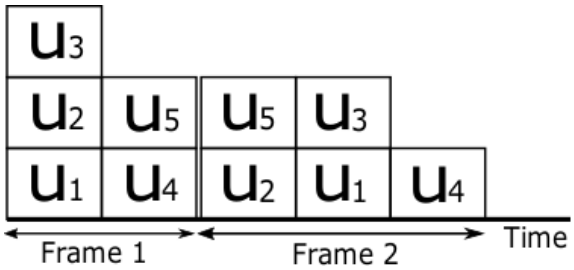


Figure 4.2: An example frame structure

Table 4.1: List of Parameters

| **Symbol** | **Definition** |
|---|---|
| $P_i$ | Transmit power from node $i$ to ground station |
| $g_i$ | Channel gain from node $i$ to ground station |
| $L$ | SIC decoding factor - Number of concurrent transmissions |
| $U$ | Set of UAVs |
| $u_i$ | $i$-th UAV |
| $t_j$ | Time slot index |
| $\sigma^2$ | Ambient noise power |
| $\mathcal{M}$ | Set of modulation indexes |
| $r_z$ | Corresponding data rate for MCS index z |
| $\beta_z$ | Corresponding SINR threshold for MCS index $z$ |
| $\mathcal{F}_n$ | The $n$-th frame |
| $\sigma_i$ | Mixed strategy for $u_i$ |
| $\bar{\sigma}_i$ | PMF over the time slots in $\mathcal{F}_n$ for $u_i$ |
| $\tilde{\sigma_{ij}}$ | PMF over the MCS $\mathcal{M}$ for time slot $t_j$ |
| $\bar{\sigma}_i(t_j)$ | Probability of using time slot $t_j$ when $u_i$ uses strategy $\sigma_i$ |
| $\tilde{\sigma_{ij}}(z)$ | Probability of using MCS $z$ in time slot $t_j$ for $u_i$ |
| $V_i(t_j, z)$ | Reward for using MCS $z$ in time slot $t_j$ for UAV $i$ |
| $\tau$ | Temperature parameter of the Softmax function |

## 4.2 Problem Statement

The objective is to maximize the overall throughput of a UAV network. This objective can be divided into two parts: (i) identify the optimal frame size that yields the maximum sum rate, and (ii) for each UAV and each frame size, it needs to identify

the best time slot and MCS. The main issue is interference caused by multiple UAVs transmitting in the same slot. In this respect, if the frame size is short, there will be more UAVs that share a slot and UAVs may need to use a lower order MCS to ensure SIC decoding is successful, or UAVs may experience more collisions or decoding failures. In both cases, the total sum-rate will be low or zero. By contrast, if the frame size is long, then there will be idle slots and the frequency of transmissions will be low; both of which lower throughput.

Let's start by modeling part (ii). For a given frame size $|\mathcal{F}_n|$, each UAV $u_i$ needs to take two actions: (a) $\bar{a}_i$, which corresponds to the slot selected by $u_i$ in $\mathcal{F}_n$, and (b) $\tilde{a}_i$ is the MCS that UAV $u_i$ uses in slot $\bar{a}_i$. Denote $A_i = \mathcal{F}_n \times \mathcal{M}$, where $\times$ is the Cartesian product. Define a joint action as $\mathbf{s} = (s_1, s_2, \ldots, s_{|U|})$, where $s_i \in A_i$ and $\mathbf{s} \in \mathcal{A} = \times_{i \in U} A_i$. In words, each joint action $\mathbf{s}$ consists of tuples $(\bar{a}_i, \tilde{a}_i)$, which represent the time slot and MCS selected by UAV $i$.

For a given joint action $\mathbf{s}$, let its reward when used in frame $\mathcal{F}_n$ be denoted as $u(\mathbf{s})$; formally, $u : \mathcal{A} \to \mathbb{R}_{\geq 0}$. In order to define $u(\mathbf{s})$ precisely, a few notations will be needed. Let $I(\bar{a}_i, t_j)$ be an indicator function that returns a value of one if UAV $u_i$ selected time slot $t_j$ in frame $\mathcal{F}_n$. Also, $N(t_j, \mathbf{s})$ denotes the set of UAVs that selected to transmit in time slot $t_j$; i.e., $N(t_j, \mathbf{s}) = \{u_k \mid I(\bar{a}_k, t_j) = 1, \forall k \in U\}$. Let $\mathcal{P}(u_i, t_j, \mathbf{s})$ return a list of UAVs with received power that is less than the received power of UAV $u_i$ in time slot $t_j$ given strategy $\mathbf{s}$. Formally, $\mathcal{P}(u_i, t_j, \mathbf{s}) = \{u_j | P_j |g_j|^2 < P_i |g_i|^2, \forall j \in N(t_j, \mathbf{s}), i \neq j\}$. The reward $u_i(\mathbf{s})$ received by UAV $u_i$ for a joint action $\mathbf{s}$ is therefore,

$$u_i(\mathbf{s}) = \begin{cases} r_{\tilde{a}_i}, & \frac{P_i |g_i|^2}{\sigma^2 + \sum_{q \in \mathcal{P}(u_i, t_j, \mathbf{s})} P_q |g_q|^2} \geq \beta_{\tilde{a}_i} \\ 0, & \text{Otherwise.} \end{cases} \tag{4.1}$$

Lastly, the *total* reward of all UAVs is therefore,

$$u(\mathbf{s}) = \sum_{i \in U} u_i(\mathbf{s}) \tag{4.2}$$

We are now ready to define part (ii) formally: identify a joint action $\mathbf{s}^*$ that yields the maximum reward. That is,

$$\mathbf{s}^* = \arg\max_{\mathbf{s}\in\mathcal{A}} u(\mathbf{s}) \tag{4.3}$$

Part (i) is solved by the ground station, where it seeks to identify a frame size that yields the maximum throughput. For a given optimal strategy $\mathbf{s}^*$, the sum rate for frame $\mathcal{F}_n$ is

$$\mathcal{R}(\mathbf{s}^*, \mathcal{F}_n) = \sum_{j\in\mathcal{F}_n} \sum_{i\in U} u_i(\mathbf{s}^*) \tag{4.4}$$

Let $\phi$ denote the frame length; i.e., $\phi = |\mathcal{F}_n|$ and the throughput ($\mathcal{T}_\phi$) at the ground station when using frame length $\phi$ as

$$\mathcal{T}_\phi = \frac{\mathcal{R}(\mathbf{s}^*, \mathcal{F}_n)}{\phi} \tag{4.5}$$

The ground station thus seeks to determine a frame length $\phi$ that maximizes the overall throughput $\mathcal{T}^*$; formally,

$$\mathcal{T}^* = \max_{\phi\in\mathbb{N}_{>0}} \mathcal{T}_\phi \tag{4.6}$$

## 4.3 A Learning MAC

This part proposes a distributed MAC for the aforementioned problem. The MAC scheme comprises of two parts. The first part runs at each UAV whilst the second is run by the ground station. Each UAV employs a mixed strategy to learn the best slot and the corresponding MCS that yields the highest reward or sum-rate for a given frame size; see Section 4.3.1. On the other hand, the ground station employs an iterative strategy to determine the optimal frame size. Specifically, it adjusts the frame size according to the number of failures and idle slots.

Figure 4.3 provides an overview of the proposed MAC scheme. The ground

station starts by sending a frame size to all UAVs. These UAVs then learn the best slot and data rate for the said slot for the given frame size. After all UAVs have learned the best slot and data rate, they inform the ground station. After that, the ground station then determines whether the present frame size has good performance. Specifically, it adjusts the frame size according to the number of observed idle slots and slots with collisions. If the frame size changes, the ground station informs UAVs of the new frame size. The UAVs then restart the learning process in order to learn the best slot and data rate for the new frame size.

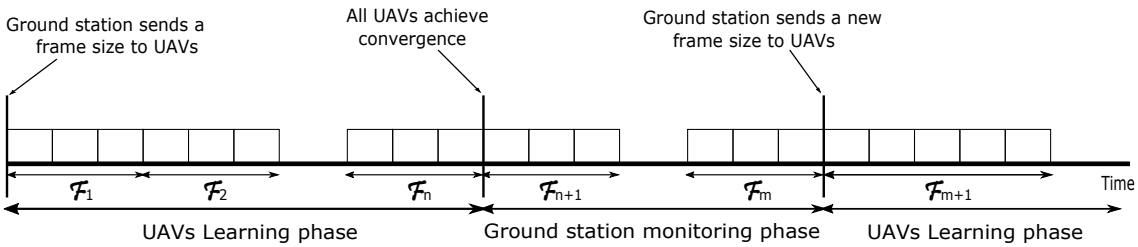


Figure 4.3: An overview of L-MAC.

### 4.3.1 UAV Strategy

For a given frame size, each UAV independently calculates a probability for selecting a time slot as well as a probability for using a MCS in the selected time slot. As discussed below, the best time slot and corresponding MCS that yields the most successes will naturally have the highest probability. Let $\sigma_i = (\bar{\sigma}_i, \tilde{\sigma_{ij}})$ denote the *mixed* strategy of UAV $u_i$; in particular, $\bar{\sigma}_i$ denotes the PMF over the time slots in $\mathcal{F}_n$, and $\tilde{\sigma_{ij}}$ is the PMF over the set of MCSs $\mathcal{M}$ for time slot $t_j$. Then, $\bar{\sigma}_i(t_j)$ can be written as the probability that UAV $i$ assigns to time slot $t_j$ when it uses strategy $\sigma_i$. Similarly, $\tilde{\sigma_{ij}}(z)$, where $z \in \mathcal{M}$, denotes the probability assigned to MCS $z$ in time slot $t_j$. Note that for each time slot $t_j$, $\sum_{z \in \mathcal{M}} \tilde{\sigma_{ij}}(z) = 1$. Also, $\sum_{j \in \mathcal{F}_n} \bar{\sigma}_i(t_j) = 1$.

L-MAC uses the Softmax function [205] to determine the PMF $\bar{\sigma}_i$ and $\tilde{\sigma_{ij}}$. Specifically, depending on the outcome of each transmission, the chances of using that time slot or a MCS are increased or decreased. Assume that a UAV has selected time slot $t_j$, then the reward of using MCS $z$ is given as $u_i(z)$. Then, the probability $\tilde{\sigma_{ij}}(z)$

of using MCS $z$ in time slot $t_j$ using the Softmax function will be,

$$\tilde{\sigma_{ij}}(z) = \frac{e^{u_i(z)/\tau}}{\sum_{z' \in \mathcal{M}} e^{u_i(z')/\tau}} \tag{4.7}$$

where $\tau$ is called the temperature parameter. If the temperature is high, then the probability of using any MCS index in $\mathcal{M}$ is equal. On the other hand, if the temperature is low, the MCS index with the highest reward will be used most often.

Similarly, Softmax function is used in order to determine the best time slot within frame $\mathcal{F}_n$. Assume that a UAV $u_i$ transmits in time slot $t_j$, then it obtains the reward $u_i(t_j)$. Here, the reward $u_i(t_j)$ depends on whether UAV $u_i$ successfully transmits in slot $t_j$ or not. Then, the probability of selecting slot $t_j$ using the Softmax function is given as,

$$\bar{\sigma}_i(t_j) = \frac{e^{u_i(t_j)/\tau}}{\sum_{t \in \mathcal{F}_n} e^{u_i(t)/\tau}} \tag{4.8}$$

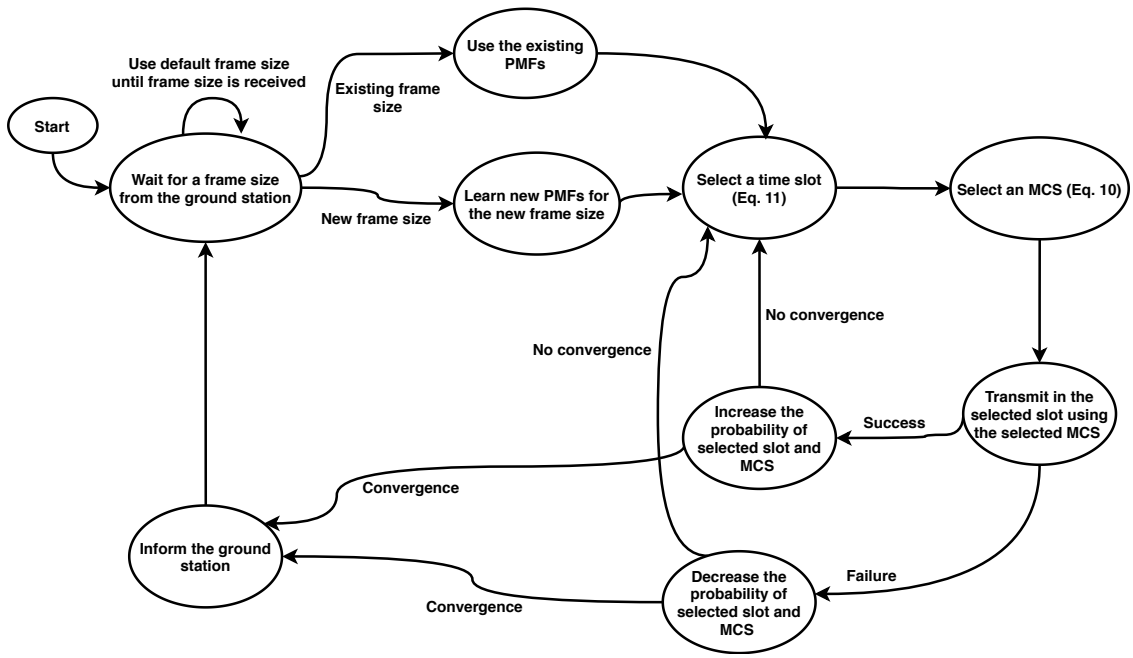


Figure 4.4: UAV strategy.

Figure 4.4 shows the strategy taken by a UAV. Initially, a UAV waits for the frame size from the ground station. During this time, the UAV uses a default frame size for transmission. Once the UAV receives a frame size from the ground station, it checks whether the transmitted frame size is new or an existing frame size. If

it is an old frame size, the UAV will continue to use the corresponding PMFs for that frame size. On the other hand, if the frame size is new, the UAV will learn the PMFs for that particular frame size. It does this in the following manner. It initializes the PMF $\tilde{\sigma_{ij}}$ and $\bar{\sigma}_i$ to the uniform distribution. After each transmission, the corresponding PMF is updated as per (4.7) and (4.8). This process is repeated until the variance of the average throughput is within a given a threshold. Lastly, a UAV informs the ground station that it has chosen the best data rate and slot for the given frame.

### 4.3.2 Ground Station Strategy

The ground station is responsible for adjusting the frame length. It does this after all UAVs have learned the PMFs for a given frame size. The ground station strategy is depicted using a state diagram in Figure 4.5. Initially, the ground station transmits an arbitrary frame size to all UAVs. This prompts UAVs to learn the PMF for the best time slot, and within each slot, the PMF of MCSs. When all UAVs report that they have converged, the ground station starts the monitoring phase, where it monitors the number of idle and collision slots. This process is explained in Algorithm 3. The input to the algorithm is current frame size $|\mathcal{F}_n|$. From line 2-16, the main loop is executed, which runs until a new frame size is achieved. At line 3, the algorithm uses the function **getCurrentTimeSlot()** to get the current time slot number. From line 4-14, a while loop is executed which runs through each time slot in current frame to check for any idle and collision slots. The algorithm uses the function **GetSlotStatus()** to check the status of a time slot. The status can be collisions, idle or successful. At line 15, the ground station updates the frame size based on the status of a time slot. Here, the weight 0.1 is used to reduce the frequency in which the frame size changes. Lastly, line 17 is reached if the frame size changes.

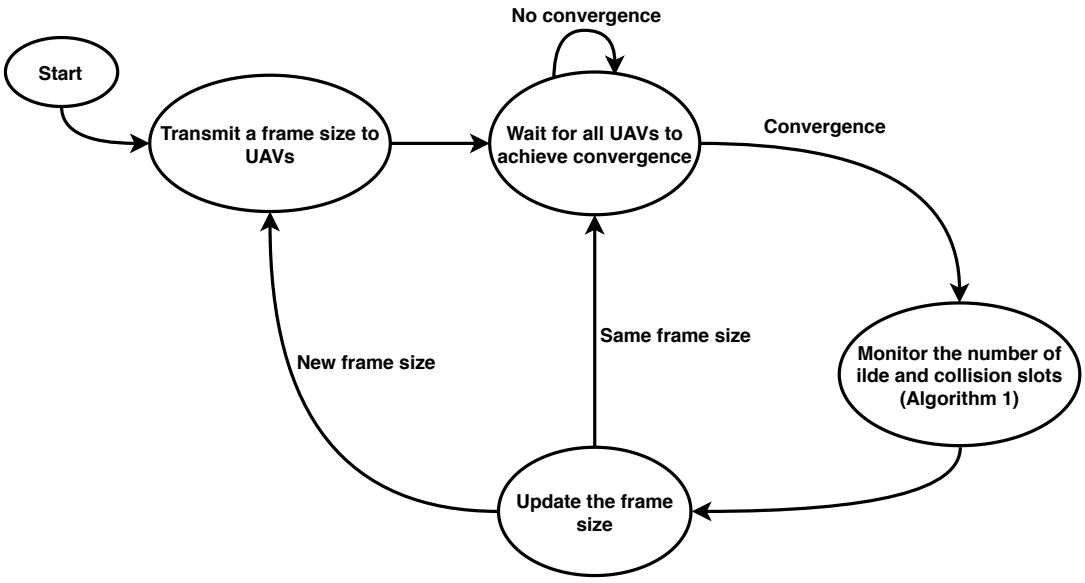


Figure 4.5: Ground station strategy

**Algorithm 3** The ground station's monitoring process.

**Input:** $|\mathcal{F}_n|$
**Output:** $|\mathcal{F}_{n+1}|$

Set $\Delta_I = \Delta_C = \Delta_S = 0$
**while** $|\mathcal{F}_n|$ does not change **do**
    tStart $= t =$ getCurrentTimeSlot()
    **while** $t \leq=$ tStart $+ |\mathcal{F}_n|$ **do**
        $t =$getCurrentTimeSlot
        Status = GetSlotStatus($t$)
        **switch** Status **do**
            **case** Collision:
                $\Delta_C$++
            **case** Idle:
                $\Delta_I$++
            **case** Success:
                $\Delta_S$++
    **end while**
    $|\mathcal{F}_{n+1}| = \lceil |\mathcal{F}_n| - (0.1 \times \Delta_I) - (0.1 \times \Delta_S) + (0.1 \times \Delta_C) \rceil$
**end while**
return $|\mathcal{F}_{n+1}|$

## 4.4 Results

The experiments are conducted in Matlab. The system consists of up to twenty UAVs that are placed linearly at distances ranging from 20 to 400 meters. All UAVs and the ground station are equipped with a 2.4 GHz radio and transmit at a fixed transmission power of 1 Watt. First, L-MAC is trained over 100,000 frames. After that, the obtained PMF is used for both data slots and MCS over 1000 frames, and the throughput obtained by L-MAC versus other competing MAC protocols is compared, which are explained below. For the experiments in Section 4.4.1-4.4.2, three MCSs are used. Their corresponding SINR threshold $\beta$ is given in Table 4.2. A dynamic $\tau$ value is used for all experiments. Specifically, the value of $\tau$ is decreased according to the total number of frames. For example, if the total number of frames is $N = 100$, then the scaling factor will be $1.05(110 - 5/N)$. In all experiments with a fixed frame size, each frame comprises of five time slots. L-MAC is compared against three different protocols:

**Aloha with SIC (ASIC)**: Each UAV randomly selects a slot in each frame and an MCS. These simultaneous transmissions are decoded at the ground station using SIC.

**Aloha without SIC (AWSIC)**: This method corresponds to the standard Aloha protocol whereby the ground station does not support SIC. Therefore, if multiple UAVs select the same time slot, they experience a collision.

**TDMA MAC**: This protocol assumes the ground station knows the channel gain of each UAV and that the channel gain remains constant for the duration of each frame. Given the channel gain to each UAV, this protocol then schedules a UAV into a time slot as long as it can decode the signal from all UAVs that are scheduled to transmit in that slot. A set of UAVs are considered *compatible* if the ground station is able to decode their signal in each slot using SIC. When using this protocol, the ground station first schedules the UAV with the highest received power in the first slot. Then, the protocol selects the UAV with the next highest

Table 4.2: Simulation Parameters

| **Parameter** | **Value** |
|---|---|
| SINR threshold $\beta$ | [0,1,2] dB |
| Number of Frames | 100,000 |
| Channel model | Nakagami-m |
| $\mu$ | 0.5 |
| Transmit power | 1 Watt |
| Temperature parameter $\tau$ | 110 to 5 |

received power. If they are compatible, the two UAVs are scheduled to transmit together. The third UAV with the next highest received power is then included into the same time slot. The protocol then checks whether all these three UAVs are compatible. This process continues until a UAV is incompatible with other transmitting UAVs in the same time slot. The last added UAV is then removed. The aforementioned process is then repeated for the next time slot. It ends when either all UAVs have been scheduled or there are no more time slots. If there are UAVs without a scheduled slot, they are marked as failed.

### 4.4.1 Throughput

Figure 4.6 and 4.7 show that, as expected, TDMA outperforms all other protocols because it schedules only compatible UAVs in each time slot. This means UAVs do not experience collisions. Therefore, its performance is better as compared to other protocols. In Figure 4.6, TDMA operates with $\beta = 1$ dB; therefore, its maximum achievable throughput is 500 kbps [206]. In this case, L-MAC outperforms TDMA when the number of UAVs is less than ten because the throughput of TDMA is capped at 500 kbps while L-MAC achieves a throughput higher than 500 kbps. Specifically, L-MAC achieves 691 kbps for four UAVs and 582 kbps for eight UAVs. The reason is because five slots are sufficient to accommodate up to ten UAVs. When the number of UAVs increases further, the throughput reduces. For example, when there are twenty UAVs, the throughput of TDMA drops to 254 kbps and the

throughput of L-MAC drops to 71 kbps. This is because each time slot may contain more than three UAVs; this results in very high inter-user interference. Similarly, Figure 4.7 with $\beta = 2$ also shows that TDMA outperforms other protocols because it schedules only compatible UAVs together. Figure 4.7 also shows that when there are four UAVs, L-MAC achieves a throughput of 700 kbps. In comparison ASIC achieves a throughput of near 550 kbps and 270 kbps for AWSIC for the same number of UAVs.

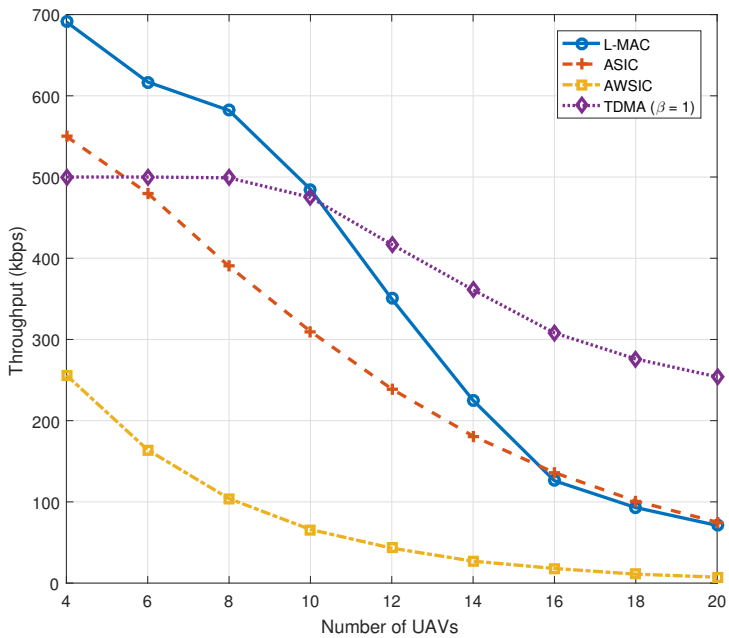


Figure 4.6: A comparison of L-MAC, ASIC, AWSIC and TDMA ($\beta = 1$)

ASIC has a lower throughput as compared to TDMA and L-MAC because it chooses slots and MCSs randomly while L-MAC learns which slots and MCS yield the highest throughput. For example, when there are ten UAVs, L-MAC achieves a throughput of approximately 500 kbps whereas for the same number of UAVs, ASIC only achieves 300 kbps. The performance of ASIC and L-MAC is similar when the number of UAVs exceeds fifteen. For example, when there are sixteen UAVs, both ASIC and L-MAC achieve a throughput of around 130 kbps. The throughput further drops to 70 kbps when the number of UAVs is twenty. This is because the number of slots in each frame is very small as compared to number of

UAVs, which results in a very high number of decoding failures. UAVs are not able to learn which slots to choose since nearly all slots lead to failures. Hence, L-MAC cannot outperform Aloha when the number of UAVs is greater than fifteen. As expected, AWSIC performs poorly as compared to all other protocols. For example, in case of four UAVs, AWSIC achieves a throughput of 256 kbps whereas L-MAC achieves a throughput of 691 kbps for the same number of UAVs. This is because when UAVs use AWSIC, a transmission fails when more than one UAV transmits in the same time slot.

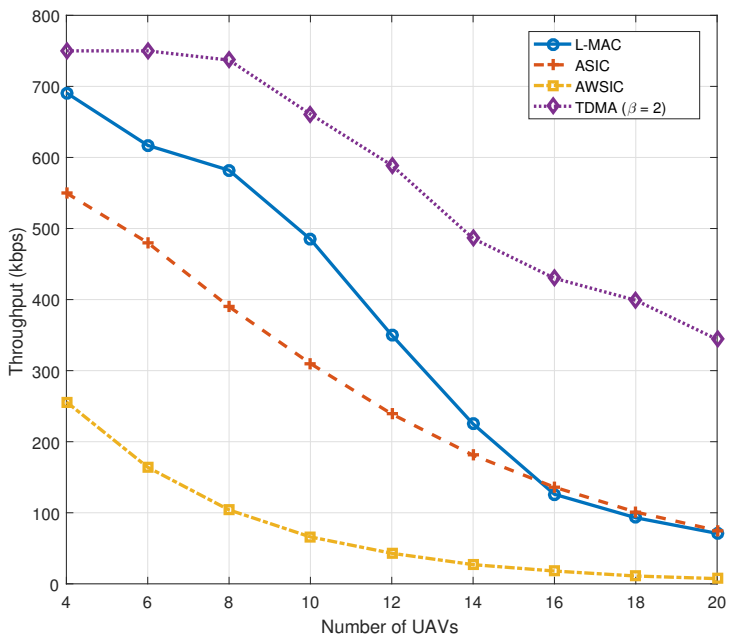


Figure 4.7: A comparison of L-MAC, ASIC, AWSIC and TDMA ($\beta = 2$)

### 4.4.2 Effect of Temperature parameter

In this experiment, the number of UAVs is fixed to ten and the impact of using different $\tau$ values is studied. The total number of frames is 100,000. Average throughput of every 1000 frames is obtained. The experiment compares the throughput performance of dynamic $\tau$ with fixed values of $\tau$. From Figure 4.8, we see that the maximum throughput of 630 kbps is achieved when a dynamic $\tau$ is used. On the other hand, throughput is only 300 kbps when $\tau = 100$. For smaller values of $\tau$

such as $\tau = 10$, the throughput remains near 470 kbps. This is because for higher $\tau$ values, rewards are lower because the ground station will give chances to even those slots that do not yield good results. Conversely, throughput is higher smaller $\tau$ values are used such as $\tau = 10$. This is because at these $\tau$ values, the reward is very high for each successful transmission. Therefore, the probability of trying other time slots is very small in case of a successful transmission. We can see that initially when the number of frames is less than 10,000, the throughput is less than 470 kbps for $\tau = 10$. This is because initially, each slot has the same probability of being chosen. Therefore, there are more chances of transmission failures. The throughput improves after 10,000 frames and remains constant around 470 kbps because the $\tau$ is very small, meaning UAVs no longer explore other slots and MCSs. On contrary, we can see that the throughput for $\tau = 100$ does not remain constant and keeps fluctuating around 380 to 410 kbps. This large $\tau$ causes UAVs to continuously try different slots and MCSs.

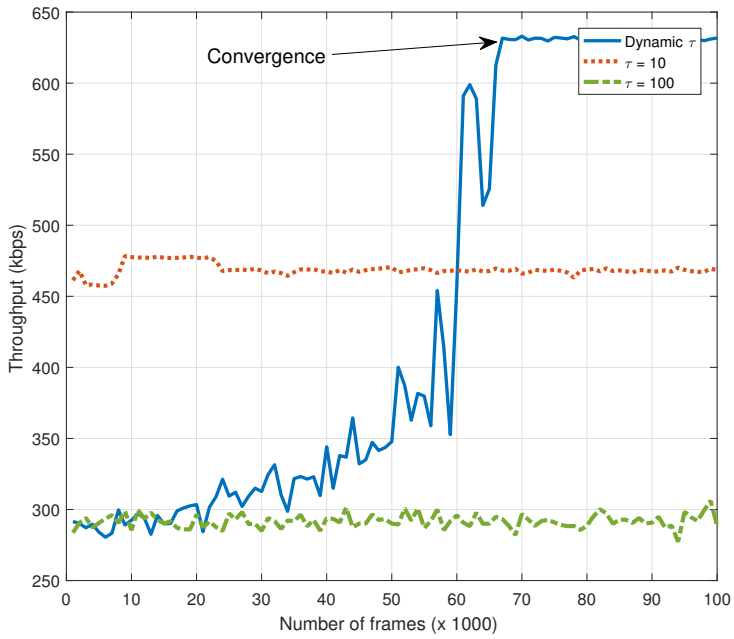


Figure 4.8: Performance with different $\tau$ values

Figure 4.8 shows that with fixed $\tau$ values, there is no major improvement in throughput. Therefore, a dynamic $\tau$ must be used where a high $\tau$ is used initially

i.e., $\tau = 110$ and reduce it in each frame so that exploration reduces over time and becomes minimal. In this way, L-MAC is able to learn better performing slots and also explore other slots. When L-MAC has learnt the best slots and MCSs, it stops exploring and uses the same slots and MCSs for future frames. To this end, convergence for L-MAC is defined as the point where it has learnt the best slot and MCS to use for the current frame. In other words, L-MAC achieves convergence when the difference in average throughput between adjacent frames is less than a predefined value of $\epsilon$.

From Figure 4.8, we see that the throughput of L-MAC with dynamic $\tau$ fluctuates widely when the number of frames is less than 65,000. For example, the throughput before 50,000 frames remains less than 350 kbps. After 50,000 frames, it increases to 450 kbps and then reduces back to 350 kbps. This is because L-MAC is in the learning phase, where it explores all slots and MCSs, leading to highly varying throughput. L-MAC converges when the number of frames passes 65,000. At this point, the ground station has learnt the best slots and $\tau$ has a smaller value. After 65,000 frames, the ground station continues using these best slots. Therefore, the throughput remains constant at 630 kbps which is 34% higher than $\tau = 10$.

### 4.4.3 Increasing Number of MCSs

This experiment studies the effect of using higher SINR threshold ($\beta$) values on throughput. Specifically, following $\beta$ values (in dB): $\{0, 1, 2, 4, 6, 8, 10, 12, 16, 20\}$ are considered. There are ten UAVs. TDMA is not used in this experiment because it is designed to work with a fixed MCS. Figure 4.9 shows that throughput significantly improves for all protocols when new MCSs are introduced. The chances of successful transmissions are reduced with the introduction of higher threshold $\beta$ values. However, the reward for each success is greater for a higher threshold or $\beta$ value because it offers greater data rates. Therefore, using higher $\beta$ values improves throughput. For example, L-MAC obtains a throughput of 485 kbps with three

MCSs. When there are five MCSs, its throughput is 762 kbps. The throughput is 2.5 Mbps when there are ten MCSs. Similarly, the throughput of ASIC improves from 267 kbps to 3.4 Mbps.

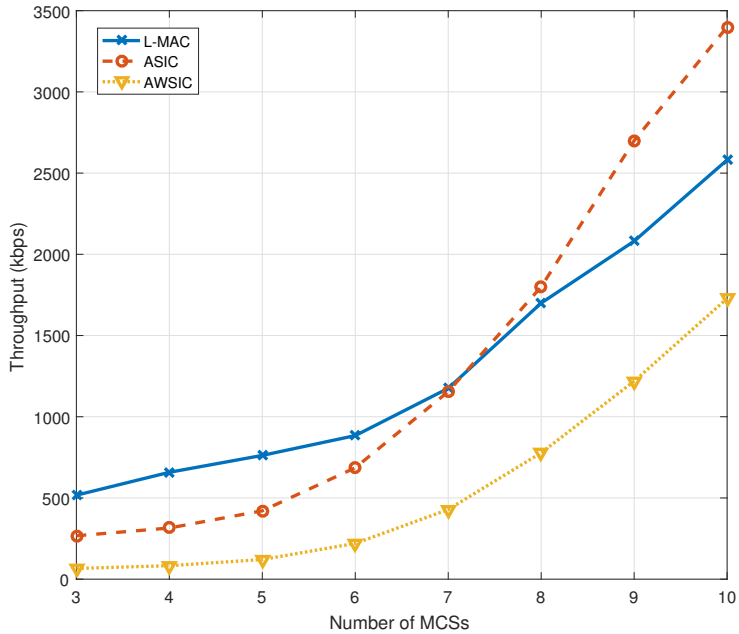


Figure 4.9: Comparison with different number of MCSs

Figure 4.9 compares the throughput of different protocols. L-MAC outperforms ASIC when the number of MCSs is less than seven. For example, when there are five MCSs, the throughput of L-MAC is 762 kbps whereas for ASIC it is only 421 kbps. This is because L-MAC learns and intelligently selects which slots and MCS to choose for higher success rates. In comparison, ASIC has no such capability as it always selects a random slot and MCS. On the other hand, for higher MCS values, i.e., greater than 10 dB, ASIC performs better. For example, when there are ten MCSs, L-MAC achieves 2.5 Mbps. For the same number of MCSs, ASIC achieves a throughput of 3.4 Mbps. This is because very high $\beta$ values such as 16 and 20 dB result in more decoding failures. Consequently, L-MAC will reduce the probability of selecting these high $\beta$ values. In particular, L-MAC prefers lower $\beta$ values that produce more successful transmissions but a lower throughput. On the other hand, ASIC will select all MCSs with equal probability. As expected, AWSIC

performs poorly as compared to L-MAC and ASIC. Specifically, AWSIC achieves a throughput of only 66 kbps when there are three MCSs; as a comparison, L-MAC obtained a throughput of 517 kbps. When there are ten MCSs, AWSIC obtains 1.7 Mbps whereas L-MAC obtains 2.5 Mbps. AWSIC obtains poorer results because it has no SIC capability and there is a collision when more than one UAV transmits in the same slot.

### 4.4.4 Shape Parameter

This part studies the shape parameter $\mu$ of the Nakagami-m distribution. The number of UAVs is fixed to ten and the impact of changing $\mu$ values is studied. Recall that the shape parameter $\mu$ controls the fading depth [207], where lower $\mu$ values correspond to higher fading. Figure 4.10 shows that throughput improves as the value of $\mu$ increases. Specifically, the throughput for L-MAC improves by 7% (335 to 360 kbps) when $\mu$ is increased from 0.5 to 5. Similarly, the throughput for TDMA improves by 3% (465 to 480 kbps). This is because increasing $\mu$ decreases fading depth, and thus UAVs experience fewer decoding failures.

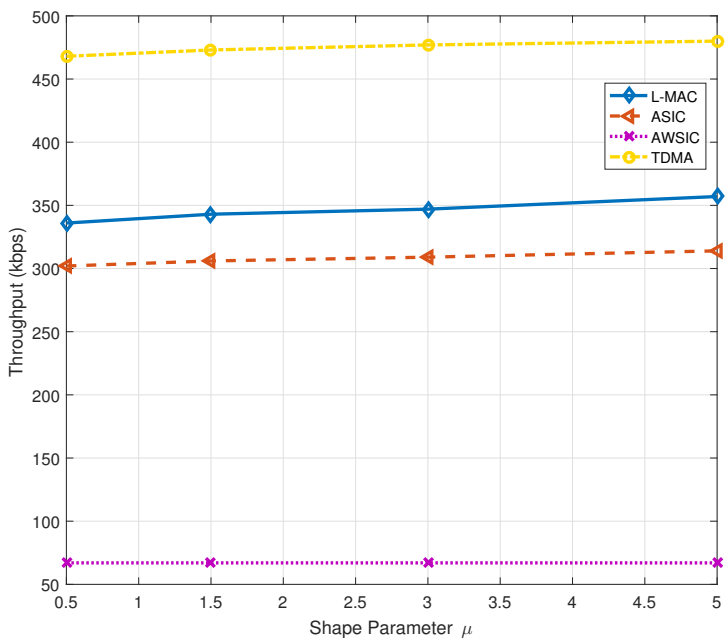


Figure 4.10: Performance with different $\mu$ values

### 4.4.5 Dynamic Frame Sizes

This part of the evaluation studies the performance of L-MAC when the ground station changes the frame size according to the process explained in Section 4.3.2. Figure 4.11 shows the frame lengths used by the ground station when four, ten and twenty UAVs are considered. For twenty UAVs, we can see that the ground station uses 12-15 time slots for nearly 90% of the frames. This is because for twenty UAVs, having fewer than twelve time slots means each slot has to accommodate more than two UAVs. Consequently, there is higher inter-user interference and more decoding failures. Similarly, having too many slots will result in idle slots, in which case the ground station reduces the number of slots. Due to these reasons, the frame length for ten UAVs remains near 6-8 time slots per frame. Similarly, is the case of four UAVs, the frame length remains 3-4 slots per frame. Looking at the frame lengths for four, ten and twenty UAVs, we can observe that the frame length always remains around 60% to 75% of the number of UAVs.

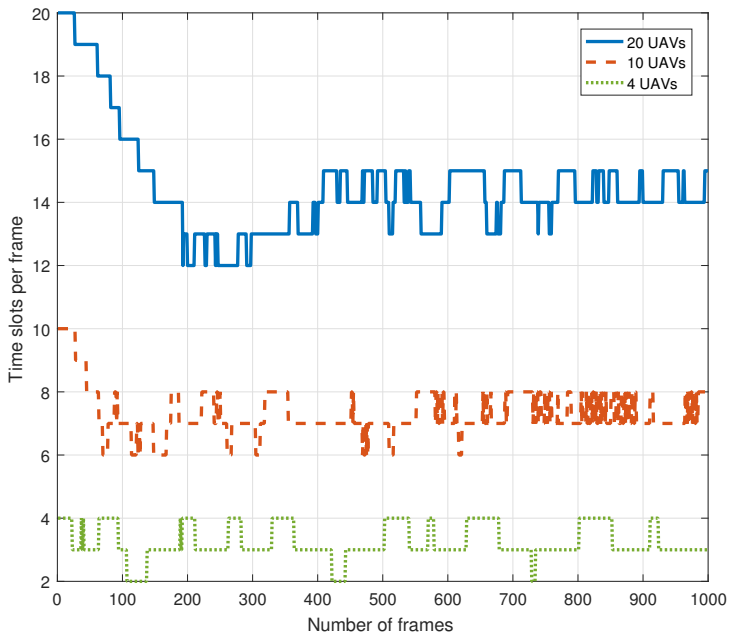


Figure 4.11: Time slots per frame.

Figure 4.12 shows a comparison of throughput when L-MAC uses either a fixed or dynamic frame length. We can see that the throughput for dynamic frame L-MAC

remains around 600 kbps and does not drop when the number of UAVs increases. This is because L-MAC with a dynamic frame is able to adjust its frame length when the number of decoding failures increases when there are more UAVs.

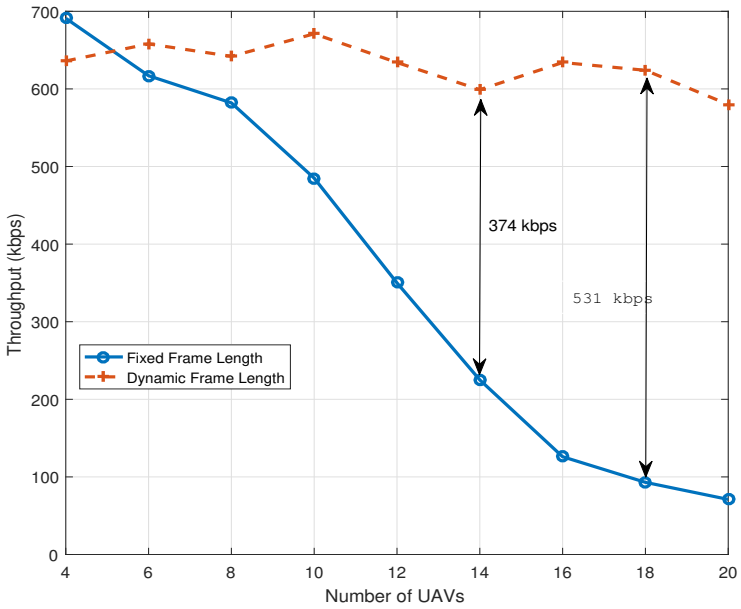


Figure 4.12: Throughput comparison between fixed and dynamic frame length L-MAC

Figure 4.12 also shows that when there are four UAVs, with a fixed frame size, L-MAC outperforms the case when the frame size is dynamic. Specifically, in the fixed frame size case, L-MAC achieves a throughput of 693 kbps when there are four UAVs. On the other hand, if the frame is sized dynamically, L-MAC manages only 636 kbps. This is because when the frame size is fixed, L-MAC has five slots per frame for four UAVs, which means some of the time slots will always be idle. On the other hand, dynamic frame L-MAC will reduce the number of time slots from five to four or three. Having fewer time slots increases the chances of decoding failures. Consequently, the throughout is also reduced from 693 to 613 kbps. We can also see that both L-MAC protocols achieve nearly the same throughput when the number of UAVs is six to eight. Specifically, both achieve a throughput of nearly 600 kbps. This is because a frame length of five time slots is sufficient to accommodate six to eight UAVs. However, as the number of UAVs further increases from eight to twenty,

the fixed frame size of five slots proves to be insufficient for such large number of UAVs. Consequently, throughput reduces with increasing number of UAVs. For example, L-MAC achieves a throughput of 485 kbps for ten UAVs, which reduces to 71 kbps for twenty UAVs. On the other hand, using a dynamic frame results in a throughput of 671 kbps for ten UAVs and 580 kbps when there are twenty UAVs.

## 4.5 Conclusion

This chapter has proposed a MAC scheme that allows a number of UAVs to learn when to transmit in a distributed manner. Additionally, UAVs collaborate with a ground station, which is responsible for adjusting the frame size. The proposed approach is tested under different network parameters and also compared against other related schemes. Simulation results show that the proposed MAC scheme outperforms other schemes in different network conditions such as varying temperature parameter $\tau$, shape parameter $\mu$, number of UAVs and frame sizes.

As discussed in Section 1.2, changing a UAV's antenna orientation changes its channel gain. This can be advantageous in SIC capable networks since one or multiple UAVs can switch their antenna orientation to improve SIC decoding. However, the current version of L-MAC does not consider antenna orientation. Therefore, the next chapter extends L-MAC to incorporate antenna orientation of UAVs.

Chapter 5

# An orientation aware MAC for multi-UAV Networks

This chapter proposes an orientation aware L-MAC. The proposed scheme aims to utilize the capability of UAVs to switch their antenna orientations. In particular, a number of works, such as [73], have shown that the orientation of a UAV has an impact on the channel condition or gain at a ground station. This is particularly advantageous when the ground station has a SIC radio. UAVs are able to re-orient themselves to improve SIC decoding success. Consider the example scenario with two UAVs in Figure 5.1. We can see in Figure 5.1(a) that the two UAVs have the same antenna orientation. Suppose that at this orientation, the received power is not sufficient to cause a difference that allows SIC decoding to be successful. Hence, the transmission from these two UAVs fails. Now consider Figure 5.1(b), where a UAV changes its orientation, which causes a different receive power at the ground station. In this case, this new orientation allows the ground station to successfully decode all transmissions. To this end, this chapter allows UAVs to learn the most suitable antenna orientation.

A number of works have focused on UAVs placement or optimizing antenna

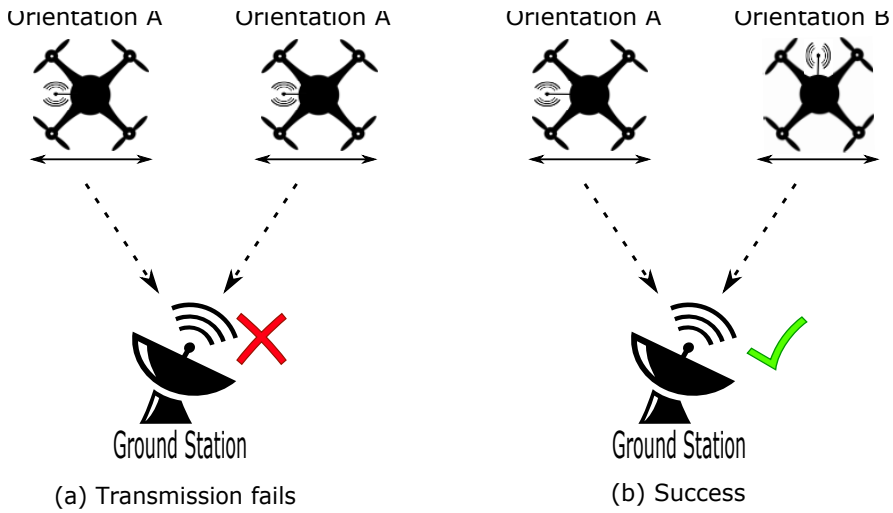


Figure 5.1: An example transmission scenario.

heading angles such as [123]. They have a similar aim as ours, i.e., throughput maximization. However, they do not aim to derive a transmission schedule, and their UAVs do not have any learning ability.

In this chapter, there are two actions to be optimized: (i) transmission time, and (ii) orientation. To this end, this chapter introduces an orientation aware MAC scheme for UAVs. Specifically, it addresses the following optimization problem: given a UAVs network with a ground station that has SIC capability, determine the shortest possible transmission schedule for UAVs. Each UAV is tasked with learning the best transmission policy i.e., to determine the best time slot and antenna orientation. A challenging issue is the random channel gains caused by UAVs mobility. To this end, a novel stochastic optimization problem is formulated in Section 5.2. Next section then proposes a distributed MAC called L-MAC that uses the well-known Softmax based function to determine the said actions; see Section 5.3. Advantageously, L-MAC does not require the ground station to collect channel state information from each UAV, and thus making it suitable for use in large-scale UAVs networks. Results show that L-MAC achieves up to 68% higher throughput as compared to the Aloha protocol. The conclusions are presented in Section 5.5.

## 5.1 Network Model

The network comprises of $|U|$ fixed/mobile UAVs and a ground station, denoted as $s$, where $U = \{1, 2, \ldots, |U|\}$ is the set of UAVs. Each UAV $i \in U$ is equipped with a radio for communication with ground station $s$ and transmits with power $P$. In addition, UAVs always have traffic to transmit. The UAVs network operates in terms of frames. Each frame contains $z$ time slots; each time slot is represented as $t$, where $t \in \{1, 2, \ldots, z\}$. In each time slot $t$, if UAV $i$ is scheduled to transmit, it selects an orientation $k \in O$ to transmit data to ground station $s$, where $O$ is a set of orientations. For example, a possibility can be $|O| = 4$, where $O = \{\text{'North'}, \text{'South'}, \text{'East'}, \text{'West'}\}$. Let $G_{ik}^t$ denote the channel coefficient of UAV $i$ when it transmits in orientation $k$ at time $t$. Moreover, $G_{ik}^t$ is drawn from a Nakagami-m [56] distribution, which includes the path loss. Also, $\Gamma^t \subseteq U$ denotes the set of UAVs that have chosen to transmit in time slot $t$.

## 5.2 The Problem

The problem consists of two parts: (i) the ground station needs to determine the best frame size $z$, and (ii) for each frame, each UAV $i$ needs to select a transmission slot. In both parts, the aim is to maximize the sum-rate. In part (i), for a given frame size $m$, each UAV $i$ has two decisions or actions: (a) $a_i^t$, which is set to one ($a_i^t = 1$) if it selects to transmit in slot $t \in \{1, 2, \ldots, m\}$, and (b) $a_{ik}^t$, which is set to one if it chooses to use orientation $k$ when transmitting in slot $t$; i.e., $a_{ik}^t = 1$ and $a_i^t = 1$. Define the vector or transmission schedule $\mathbf{a}_m = [(a_i^t, a_{ik}^t)]$, with $t \in \{1, 2, \ldots, m\}$, $i \in U$ and $k \in O$, meaning vector $\mathbf{a}_m$ has dimension $m \times |U| \times |O|$. Let $\mathcal{A}_m$ denote a collection of all possible transmission schedules $\mathbf{a}_m$; i.e., the set $\mathcal{A}_m$ contains all possible combinations of transmission slots and orientations of all UAVs. Also, each UAV only transmits once in each frame; formally, $\sum_{t=1}^{m} a_i^t = 1$. In addition, if $a_i^t = 1$, then at most one orientation can be chosen: $\sum_{k \in O} a_{ik}^t = 1$.

For a time slot $t$, the reward for UAV $i$ is defined as,

$$r_i^t(\mathbf{a}_m) = \begin{cases} r_\beta, & \frac{a_i^t \sum_{k \in O} \mathcal{P}_{ik}^t a_{ik}^t}{\sigma^2 + \sum_{p \in \varphi_i^t(\mathbf{p}^t)} p} \geq \beta \\ 0, & \text{Otherwise.} \end{cases} \tag{5.1}$$

Note, if UAV $i$ does not transmit ($a_i^t = 0$), then its SINR will be less than $\beta$, and thus $r_i^t(\mathbf{a}_m) = 0$. Also, $\mathbf{p}^t = \{\mathcal{P}_{jk}^t \mid \mathcal{P}_{jk}^t a_{jk}^t > 0, \forall j \in U, \forall k \in O\}$. Using (5.1), the *total* reward or sum rate is therefore,

$$R(\mathbf{a}_m) = \sum_{t=1}^{m} \sum_{i \in U} r_i^t(\mathbf{a}_m) \tag{5.2}$$

Part (ii) of the problem can formally be defined now. Formally, for a given frame of length $m$, the aim is to identify an action $\mathbf{a}_m^*$ that yields the maximum average reward,

$$\mathbf{a}_m^* = \arg\max_{\mathbf{a} \in \mathcal{A}_m} \mathbb{E}\left[R(\mathbf{a})\right] \tag{5.3}$$

The expectation is taken with respect to the joint probability distribution of channel gains to UAVs.

Let's consider the part (i) of the problem now. The ground station aims to determine a frame size $m$ that yields the maximum average throughput.

In particular, it seeks to optimize the following quantity,

$$\mathcal{T} = \max_{m \in \mathbb{U}_{>0}} \mathbb{E}\left[R(\mathbf{a}_m^*)\right] \tag{5.4}$$

where $\mathbf{a}_m^*$ is the optimal joint action for frame size $m$.

To conclude this section, note that if all channel gains are fixed or known, then the problem of determining the shortest link schedule/frame is a known NP-hard problem [208]. Intuitively, this is supported by the fact that the size of $\mathcal{A}_m$ increases exponentially with the number of UAVs and orientations. In particular, the problem can be reduced to that in [208] by treating each orientation of a UAV as a link.

Hence, for the perfect channel gain case, the proposed problem is at least as hard as that in [208]. Lastly, obtaining channel gain information is not practical if there are a large number of UAVs. This requires the ground station to probe each UAV, which becomes prohibitively expensive increasing number of UAVs. Moreover, the ground station will have to probe devices in every time slot of each frame and assume the channel to/from each UAV does not vary for the duration one slot, which is unlikely to be the case if UAVs are mobile. These limitations motivate the proposed distributed MAC protocol.

## 5.3 An Orientation Learning MAC

The proposed distributed MAC enables each UAV to learn the best time slot in a given schedule and also orientation that yields the highest transmission success. It associates a probability to each time slot and orientation, where a high probability indicates a high reward. Figure 5.2 shows the steps taken by a UAV to learn the transmission probability of each slot and corresponding antenna orientation for a schedule length $m$ that is transmitted by the ground station.

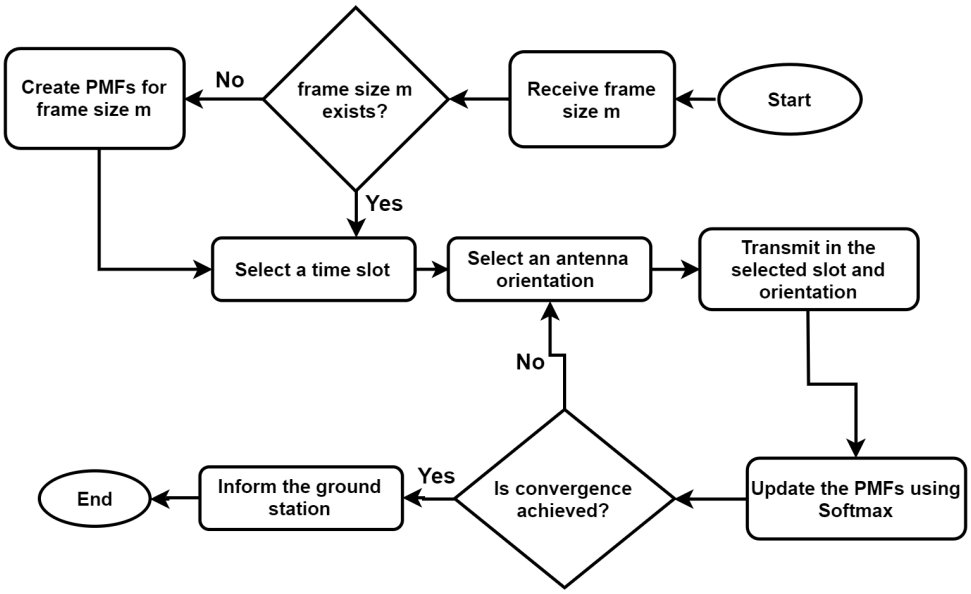


Figure 5.2: A UAV's learning process.

For a given frame length $m$, let $\alpha_i^m$ denote the PMF over time slots $t \in \{1, 2, \ldots, m\}$,

and $\alpha_{it}^m$ is the PMF over the set $K$ of antenna orientations for the selected time slot $t$. Let $\alpha_i^m(t)$ represent the probability that UAV $i$ transmits in time slot $t$, and $\alpha_{it}^m(k)$ is the probability that UAV $i$ will use the $k$-th antenna orientation in slot $t$.

Next steps explain how UAV $i$ constructs the PMF $\alpha_i^m(t)$ and $\alpha_{it}^m(k)$. Initially, all UAVs set both PMFs to be the uniform distribution. Thus each UAV selects a transmission slot and an orientation uniformly. Assume UAV $i$ selects time slot $t$, and orientation $k$. Let the reward corresponding to orientation $k$ be denoted $u_{it}(k)$, which equals the transmission rate $r_\beta$ if the ground station indicates UAV $i$'s transmission is successful. Otherwise, it is zero. Then UAV $i$ calculates the probability $\alpha_{it}^m(k)$ using the following Softmax function,

$$\alpha_{it}^m(k) = \frac{e^{u_{it}(k)/\tau}}{\sum_{k' \in K} e^{u_{it}(k')/\tau}} \tag{5.5}$$

where $\tau$ is called the *temperature parameter*, which controls the probability that a UAV exploits the best action or orientation thus far or explore other orientations in $O$. The PMF $\alpha_i^m$ is calculated in a similar way. Let $u_i(t)$ be the reward, e.g., data rate, for transmitting in time slot $t$. Then,

$$\alpha_i^m(t) = \frac{e^{u_i(t)/\tau}}{\sum_{t=1}^{m} e^{u_i(t)/\tau}} \tag{5.6}$$

The above process of learning the best slots and orientations is repeated until convergence, whereby the difference in throughput between adjacent schedules is less than a predefined value of $\epsilon$. Upon reaching convergence, UAVs select a time slot and an antenna orientation based on PMFs $\bar{\alpha_i}$ and $\hat{\alpha_{ij}}$ respectively.

The ground station is responsible for informing UAVs and adjusting the schedule length based on the number of observed transmission successes, failures and idle slots. After informing UAVs of a given schedule length $m$, it waits for UAVs to achieve convergence. After that, it monitors the performance in terms of the number of success, collision and idle slots for the schedule with length $m$; see Figure 5.3.

As an example, if there are two collisions, i.e., $c = 2$, then the value 0.2 will be added to the schedule length. If the schedule length changes after rounding up, the ground station informs all UAVs. Note that if UAVs have existing PMFs for a schedule length $m$, then they simply use these PMFs to select a transmission slot and orientation; i.e., they do not need to learn new PMFs. In Figure 5.3, the value 0.1 controls the sensitivity in which the schedule length increases/decreases. For example, assume it observed two collisions then $c = 2$, therefore 0.2 will be added to the current schedule length. Once the ground station has a new schedule length, it is transmitted to the UAVs and the process repeats.

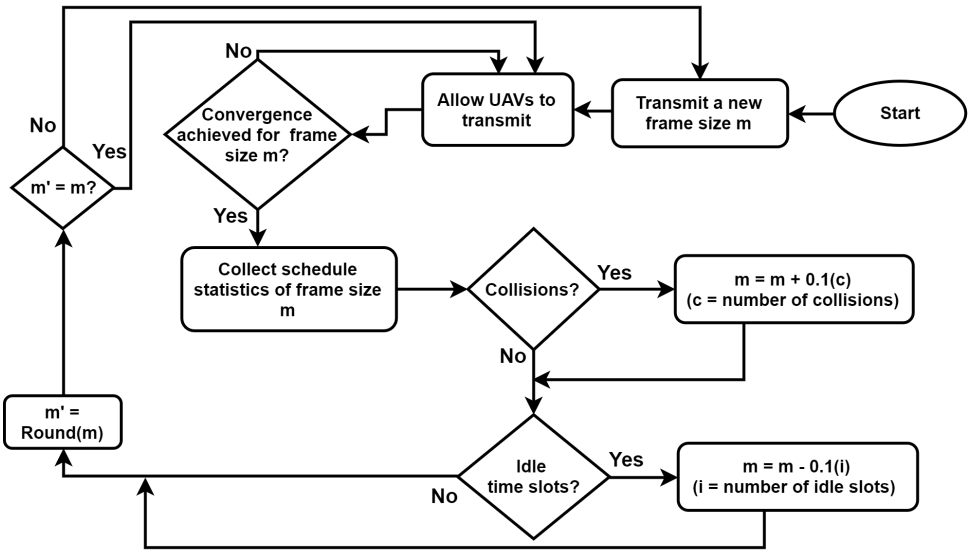


Figure 5.3: A ground station's schedule length adjustment process.

## 5.4 Evaluation

The experiments are conducted in Matlab. The system considers up to twenty UAVs. The distance from the ground station to UAVs ranges from 20 to 400 meters. The proposed L-MAC is first trained over a period of 100,000 frames. After that, the data rate of UAVs over 1000 frames are recorded. The SINR threshold is set to $\beta = 1$ (dB); this corresponds to a rate of 500 kbps. Each plot is an average of ten simulation runs. The temperature $\tau$ decreases linearly after each frame, where

Table 5.1: Simulation Parameters

| **Parameter** | **Value** |
|---|---|
| Number of UAVs | 4 to 20 |
| Time slots per frame | 5 |
| Number of Frames | 100,000 |
| Transmit power | 1 Watt |
| SINR threshold | [1,2] dB |
| Channel model | Nakagami-m |
| Antenna orientations K | 0°, 90°, 270°, 360° |
| Temperature parameter $\tau$ | 110 to 5 |

it starts from $\tau = 110$ from the first frame and reaches a value of $\tau = 5$ in the last frame; this affords the ground station and UAVs sufficient time to explore their action space before converging onto the best action. The set of antenna orientations is $K = \{0°, 90°, 180°, 270°\}$. Note that as the problem is new, there are no other MACs to compare against fairly. As a benchmark, the Aloha protocol is customized to operate over a ground station with (i) a SIC radio, labeled as *Aloha with SIC (ASIC)*, and (ii) no SIC radio, labeled as *Aloha without SIC (AWSIC)*. The list of simulation parameters is presented in Table 5.1.

### 5.4.1 Throughput

From Figure 5.4, we see that L-MAC outperforms ASIC and AWSIC. This is because UAVs using L-MAC learn which time slot and antenna orientation will lead to higher chance of successful transmissions. On the other hand, UAVs that employ ASIC and AWSIC select a time slot randomly. Consequently, they perform poorly as compared to L-MAC. For example, in case of ten UAVs, the average data rate is approximately 430 kbps for L-MAC. However, ASIC and AWSIC with a frame size of ten achieves 360 kbps and 280 kbps, respectively, for the same number of UAVs.

Referring to Figure 5.4), we also see that the average data rate for ASIC and AWSIC decreases as the number of UAVs increases. This is because these protocols have a fixed number of time slots per frame i.e., five and ten. For small number

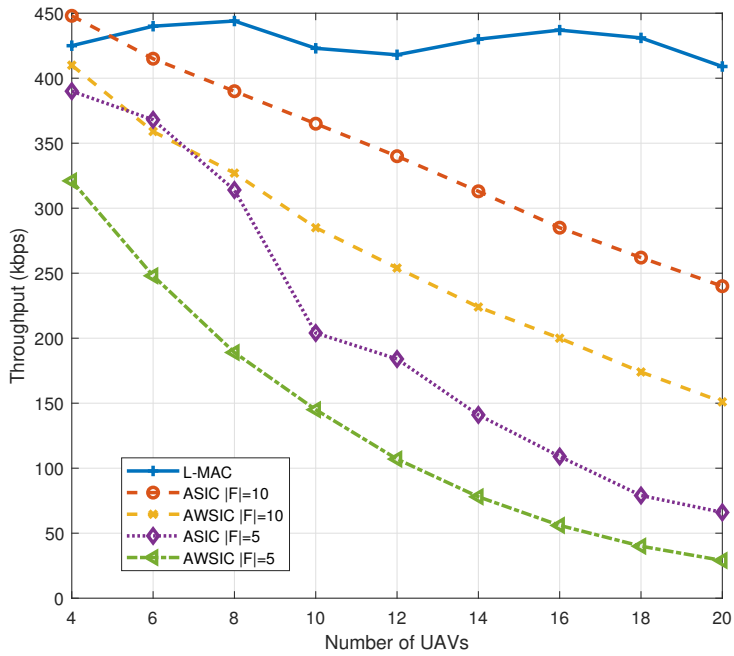


Figure 5.4: L-MAC, ASIC vs. AWSIC at $\beta = 1$

of UAVs, these frame sizes are appropriate. However, with more UAVs, collisions increases, which results in a lower data rate. For example ASIC with a frame length of ten achieves a data rate of 450 kbps for four UAVs, which drops to 240 kbps for twenty UAVs. On the other hand, L-MAC manages to maintain a data rate of around 425 kbps as it is able to adjust the frame length based on the number of transmission failures.

### 5.4.2 Convergence of L-MAC

Figure 5.5 shows the convergence rate of L-MAC for ten UAVs when $\tau$ is either fixed or dynamic. The average data rate is over 1000 frames. We see that when $\tau$ is large, i.e., 100, the average data rate is low; i.e., 285 kbps. This is because Softmax is less likely to explore, and thus it may converge onto the local optima solution. If $\tau$ is dynamic, the average data rate fluctuates initially as UAVs explore and learn the reward of each time slot and corresponding orientation. Finally, they converge onto the best time slot and orientation; initially, the average data rate is approximately

285 kbps before settling to 325 kbps at the 98-th frame.

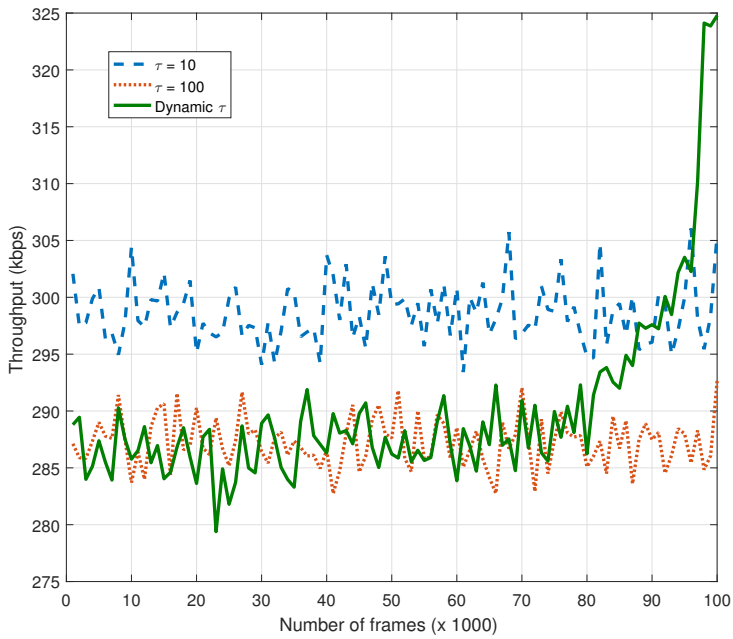


Figure 5.5: Convergence rate of L-MAC

### 5.4.3 Effect of Increasing Antenna Orientations

Lastly, this subsection investigates how the available number of antenna orientations affect the average data rate. For this simulation, $K = \{0°, 45°, 90°, 135°, 180°, 225°, 270°, 315°\}$. We see from Figure 5.6 that if UAVs more orientations, then the average data rate is higher. That is because of higher diversity in channel gains. Figure 5.6 shows that the data rate for a single orientation is 383 kbps, which increases to 397 kbps for two orientations and 420 kbps when there are eight orientations. The shape parameter $\mu$ of the Nakagami-m distribution is also modified, where $\mu$ controls the fading depth [56]; a lower $\mu$ value corresponds to a higher fading depth. From Figure 5.6, we see that the average data rate increases by 2% the value of $\mu$ is increased from 0.5 to 2 and by 5% when $\mu = 5$.

Specifically, when $\mu = 0.5$, a throughput of 409 kbps is obtained. At $\mu = 2.5$, the throughput increases to 416 kbps, and when $\mu = 5$, the throughput is 426 kbps. Advantageously, L-MAC is able to learn the best orientation for all channel

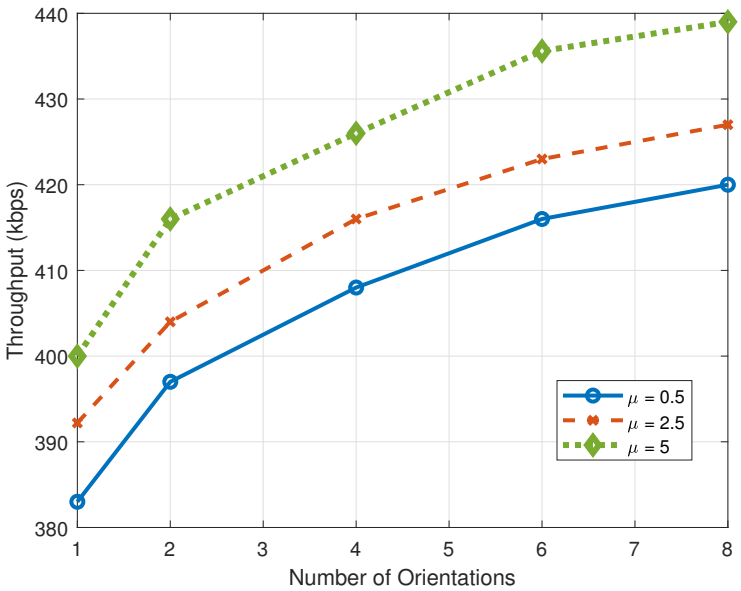


Figure 5.6: Number of orientations

conditions or $\mu$ values.

## 5.5 Conclusion

This chapter has proposed a distributed MAC that enables UAVs to learn the best transmission slot and corresponding orientation for a given schedule length. The results show that L-MAC has at least double the average data rate of the Aloha protocol. Simulation results show that a dynamic learning rate is necessary, and a higher number of orientation yields better average data rate.

Beside orientation, another approach to change the received power at a receiver is to optimize the placement of nodes. In other words, the position of a SIC capable receiver can be optimized in order to maximize the number of concurrent transmissions from ground nodes. However, L-MAC considers a SIC receiver is at a fixed location. To this end, the next chapter considers a mobile SIC receiver. In particular, the next chapter aims to optimize UAVs placement.

# Chapter 6

# UAV Placement Optimization using Gibbs Sampling

As discussed in Chapter 1, UAVs are likely to function as mobile base stations. In this respect, a MAC protocol plays a critical role in ensuring ground stations or sensor nodes transmit frequently to a UAV. In particular, a short TDMA schedule allows ground devices to transmit periodically in a dedicated slot without contention, and ensure a high link capacity.

Figure 6.1 shows an example cell with six possible UAV positions and two ground devices $A$ and $B$. When the UAV is placed at position '5', the received power from both ground devices is nearly the same. In this case, SIC decoding may not perform well and both ground devices transmit individually. As SIC decoding is unlikely to be successful, the resulting TDMA schedule contains two time slots. However, at position '1', there is a significant difference in received power, which allows the SIC decoder at the UAV to decode both transmissions successfully. Both sensor $A$ and $B$ can thus transmit in the same slot, which results in a shorter TDMA schedule length.

Henceforth, this chapter considers a problem that aims to find the optimal UAV

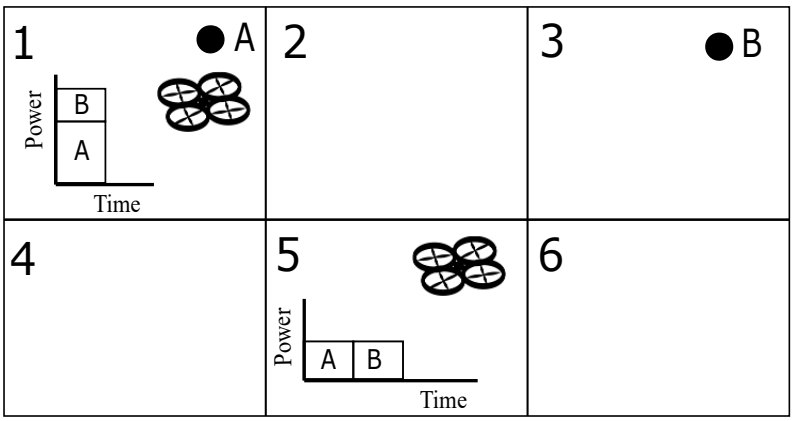


Figure 6.1: An example cell depicting two possible UAV positions.

position in each cell that offers the maximum received power diversity. Specifically, it contains the following contributions. First, it addresses a novel problem of minimizing the schedule length by optimizing the location of one or more UAVs. Second, for the first time, it shows how Gibbs sampling can be used to address such a problem. Advantageously, the proposed solution allows a UAV to learn the optimal position in a cell in a distributed manner. Third, it considers a scenario with multiple UAVs. This is significant because each UAV may experience interference from neighbouring cells. Again, the proposed solution uses Gibbs sampling to find the optimal position in presence of interference from neighbouring cells. The simulation results show that the schedule length is up to 17% shorter at the optimal location as compared to other locations.

The next section discusses the system model. Section 6.2 presents the problem mathematically. Section 6.3 presents the Gibbs sampling approach. The results are discussed in Section 6.4 and lastly, conclusions are presented in Section 6.5.

## 6.1 System Model

Time is divided into fixed duration slots. Each slot is denoted as $t_j$, where $j$ is the slot index. Let $F_m$ be the $m$-th frame, and $|F_m|$ represents the number of slots in the $m$-th frame. Each ground device is assigned a time slot in every frame. A fixed geographical area is considered that is divided into $M$ cells. Each cell is further

divided into $Z$ grid positions. The set of grid positions in the $j$-th cell is denoted as $\Gamma^j = \{\gamma_1^j, \gamma_2^j, \ldots, \gamma_Z^j\}$. Figure 6.2 depicts an example cell with $Z = 9$. The set of ground devices denoted as $S$ and the UAV in the $j$-th cell is denoted as $u_j$. Each sensor is assumed to be equipped with a half-duplex radio for communication. The coordinate or location of sensor $s_i$ is denoted as $(x_i, y_i)$, where $i = 1, 2, \ldots, |S|$. Assume that the ground devices are saturated, meaning they always have data to transfer. The UAV in the $j$-th cell can select any grid position in $\Gamma^j$. The altitude of each UAV is fixed at $h$ meters. The transmit power from sensor $s_i \in S$ to the UAV is given as $p_t^i$. Also, it is assumed that each sensor node manages to harvest energy at the start of each TDMA schedule to transmit with power $p_t^i$. Let $g_i^k$ denote the channel gain from sensor $s_i$ to the UAV that is located at the $k$-th position. Let $p_r^i = g_i^k p_t^i$ denote the received power at the UAV for sensor $s_i$ at location $k$. Note that the UAV has imperfect channel gain information; hence, the value of $g_i^k$ is unknown.

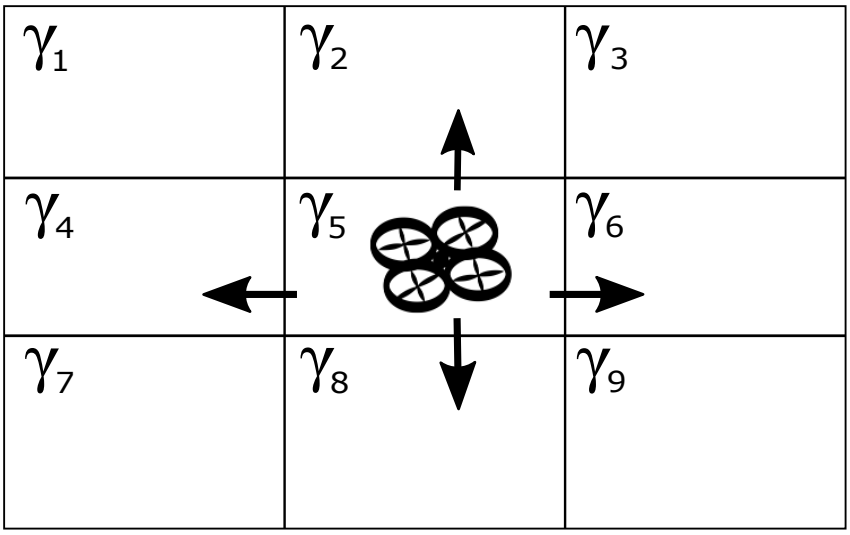


Figure 6.2: An example cell with nine grid positions.

## 6.2 The Problem

The objective is to minimize $|F_m|$, in terms of slots, while ensuring each sensor is assigned a time slot. The problem at hand is to determine the most suitable

position for the UAV that yields the shortest schedule. Note that each of the $Z$ positions yields a different received power for each sensor, which may improve SIC decoding success [201]. If a position allows multiple transmissions to be decoded, then it helps reduce the frame length. Let the function $\Phi(\gamma_k)$ represent the schedule length obtained for location $\gamma_k$. The problem at hand is to identify the optimal UAV location $\gamma^*$ that yields the shortest schedule length. Formally,

$$\gamma^* = \min_{\gamma \in \Gamma} \mathbb{E}\left[\Phi(\gamma)\right]. \tag{6.1}$$

The expectation is taken with respect to the joint probability distribution $\{g_i^k\}$ for all $k \in \Gamma$ and $i \in S$.

The next aim is to maximizes the throughput. In particular, the objective to identify a location $\gamma \in \Gamma$ that maximized the overall throughput $\mathcal{T}^*$; formally,

$$\mathcal{T}^* = \max_{\gamma \in \Gamma} \mathcal{T}_\gamma \tag{6.2}$$

## 6.3 A Gibbs Sampling Solution

### 6.3.1 Background

To address problem (6.1), the proposed solution employs Gibbs sampling [209]. Gibbs sampling is a Markov Chain Monte Carlo (MCMC) method that can be used to obtain a sequence of observations from a probability distribution. Consider a probability distribution with $K$ possible states. Let $\bar{\sigma}$ represent the probability distribution of these states, and the states at the $n$-th iteration are $\{b_1^n, b_2^n, \ldots, b_K^n\}$. The main idea is to sample from the probability distribution to determine the most likely state in each iteration. Gibbs sampling then evaluates the reward of a sampled state and proceeds to update the probability distribution using the obtained reward.

A Gibbs-sampler, see Algorithm 4, operates as follows. Line 1 initializes the probability distribution $\bar{\sigma}$. A function **Sample()** is used to select a state from the

probability distribution. Another function **Calc()** is used to update the probability distribution after each sample. In line 4, the Gibbs sampler samples $b_1^n$ based on the current value of all other states $b_2^{n-1}, b_3^{n-1}, \ldots, b_K^{n-1}$. In the next step, it samples $b_2^n$ based on $b_1^n, b_3^{n-1}, b_4^{n-1}, \ldots, b_K^{n-1}$. In the same way, it samples through all $K$ states in each iteration. Let $\mathcal{U}(b_k^n)$ denote the reward for selecting the $k$-th state in the $n$-th iteration. After sampling each state, the Gibbs sampler updates the probability distribution $\bar{\sigma}$ based on the reward $\mathcal{U}(b_k^n)$. The goal is to find state(s) that maximize the reward function. To find such state(s), each state is weighted or is assigned a high probability if it has a high reward. The probability of selecting state $b_k^n$ in the $n$-th iteration, denoted as $\bar{\sigma}(b_k^n)$ is,

$$\bar{\sigma}(b_k^n) = \frac{e^{\mathcal{U}(b_k^n)/\tau}}{\sum_{b \in B} e^{\mathcal{U}(b)/\tau}}. \tag{6.3}$$

where $\tau > 0$ is the temperature parameter. A high $\tau$ value means the Gibbs sampler will more likely test or explore all other states, whereas a low $\tau$ value means it will quickly converge onto a possibly sub-optimal probability distribution.

**Algorithm 4** A generic Gibbs sampler

**Input: J (Total number of iterations)**

1: Initialize probability vector $\bar{\sigma}$
2: n = 1
3: **while** $n < J$ **do**
4: Sample $(b_1^n \mid b_2^{n-1}, b_3^{n-1}, \ldots, b_K^{n-1}), Calc(\bar{\sigma}, b_1^n)$
5: Sample $(b_2^n \mid b_1^n, b_3^{n-1}, \ldots, b_K^{n-1}), Calc(\bar{\sigma}, b_2^n)$
6: $\vdots$
7: Sample $(b_K^n \mid b_1^n, b_2^n, \ldots, b_{K-1}^n), Calc(\bar{\sigma}, b_K^n)$
8: n = n + 1
9: **end while**

The aforementioned probability distribution corresponds to all locations in $\Gamma$; each state corresponds to a location in $\Gamma$. The probability of selecting a location $\gamma_k$ is given as $\bar{\sigma}(\gamma_k)$. The reward function $\mathcal{U}(\gamma_k)$ of the $k$-th location is defined as,

$$\mathcal{U}(\gamma_k) = 1/\Phi(\gamma_k). \tag{6.4}$$

In words, the reward is inversely proportional to the schedule length, meaning a location with a shorter schedule will have a higher reward. Equivalently, a location with a shorter schedule will have a higher probability of being selected.

### 6.3.2 Single Cell

The Gibbs-based placement process is depicted in Figure 6.3. Initially, the UAV selects a location randomly and a schedule is constructed for the selected location. A schedule is constructed for each location according to Algorithm 5. The basic idea is to greedily add sensor node into a slot $t_m$. Line 4 sorts all ground devices in non-decreasing order of their received power level. At line 6, function **GetSensor()** retrieves the $k$-th sensor from the set $S$. Algorithm then checks whether this sensor is compatible with those in slot $t_m$; i.e., whether their respective transmission satisfies the required SINR threshold. If so, sensor $s_k$ is included into slot $t_m$. After checking all sensor nodes, those that have been scheduled are removed from the set $S$. The constructed time slot $t_m$ is then added into the set $F$. Once the schedule is constructed for a given location, the UAV calculates (6.4), which is then used to update the probability mass function (Eq. 6.3) and the UAV moves to a new location as per Algorithm 4.

### 6.3.3 Multiple Cells

In this part, there are $M$ cells, with one UAV base station in each cell. Therefore, each UAV may experience interference from other UAVs. Optimizing a UAV placement in the presence of interference is challenging because the optimal location for one cell may cause interference to a neighbouring cell's UAV. The first objective is to optimize each UAV's location in its cell. Once the optimal location is identified for each UAV, the next aim is to use the optimal positions and identify the optimal schedule length for each UAV.

The proposed approach works in the following way. Let $\phi_i \in \Phi$ be the initial

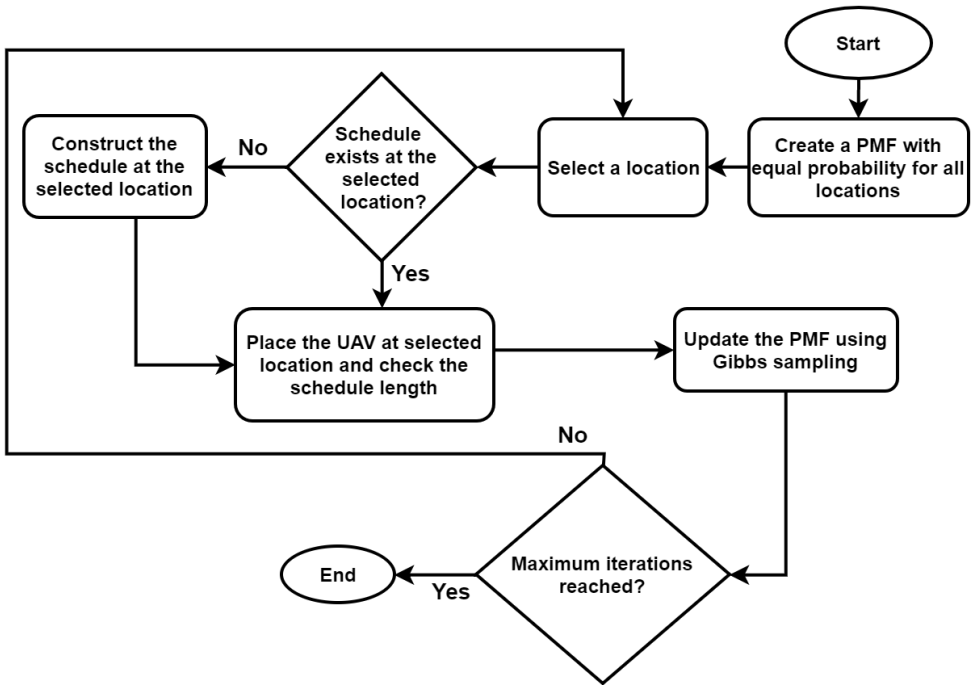


Figure 6.3: A UAV's learning process in single cell scenario.

**Algorithm 5** Link schedule construction

**Input:** $S$

**Output:** $F$

```
m = 1, F = ∅
while |S| > 0 do
    k = 1, t_m = ∅
    S = Sort(S)
    while k ≤ |S| do
        s_k = GetSensor(S, k)
        if CheckCompatible(t_m, s_k) = true then
            t_m = t_m ∪ s_k
        end if
        k = k + 1
    end while
    S = S \ t_m
    F = F ∪ t_m
    m = m + 1
end while
return F
```

schedule length for all cells. Ground devices transmit by selecting a random time slot in the given schedule of length $\phi_i$. Then, The Gibbs sampler optimizes the UAV location in each cell by exploring different locations on the cell grid. After placing the UAV at each location, it records the obtained throughput, known as the reward.

Let the reward for using the $k$-th location in the $j$-th cell $\gamma_k^j$ be denoted as $\mathcal{U}(\gamma_k^j) = \mathcal{T}(\gamma_k^j)$. Note that the reward for each location also takes into consideration the interference from neighbouring cells. Therefore, a location that experiences higher interference from neighbouring cells, will have a smaller throughput and thus reward. Equivalently, a location with a higher throughput will have a higher probability of being selected by a UAV. Then, the probability of selecting the $k$-th location $\gamma_k^j$ in the $j$-th cell, given as $\bar{\sigma}(\gamma_k^j)$, is,

$$\bar{\sigma}_j(\gamma_k^j) = \frac{e^{\mathcal{U}(\gamma_k^j)/\tau}}{\sum_{\gamma^j \in \Gamma^j} e^{\mathcal{U}(\gamma^j)/\tau}}. \tag{6.5}$$

The UAV in the $j$-th cell uses the PMF $\bar{\sigma}_j$ to select a location in each iteration of the Gibbs sampler. The process of learning the optimal UAV location in each cell is further explained using a flowchart in Figure 6.4. Figure 6.4 shows that the schedule length is initially fixed and the UAV in each cell selects a location based on the PMF $\bar{\sigma}$. The process continues until the Gibbs sampler identifies the optimal location in all cells. This process repeats until the overall throughput does not change over a number of iterations. At that point, the Gibbs sampler is assumed to have achieved convergence for location.

The next task is to identify the optimal schedule length in the set of all schedules $\Phi$. Again, Gibbs sampling is used to find the optimal schedule length. The objective in this case is to identify the optimal schedule length for each UAV that results in the maximum throughput. The Gibbs sampler identifies the optimal schedule length by exploring different schedule length in $\Phi$. Suppose the Gibbs sampler selects the $k$-th schedule $\phi_k$. Then, the reward for selecting this schedule length will be $\mathcal{U}(\phi_k) = \mathcal{T}(\phi_k)$. Then, the probability of selecting the $k$-th schedule in the $j$-th cell,

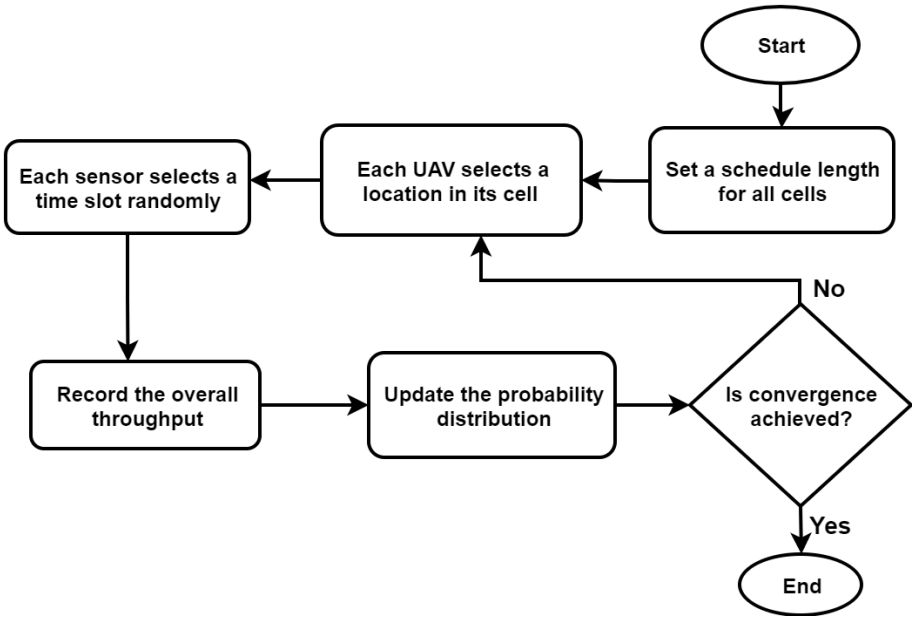


Figure 6.4: The learning process for the optimal UAV position.

given as $\tilde{\sigma}_j(\phi_k)$ is given as,

$$\tilde{\sigma}_j(\phi_k^j) = \frac{e^{\mathcal{U}(\phi_k)/\tau}}{\sum_{\phi_k \in \Phi} e^{\mathcal{U}(\phi_k)/\tau}}. \tag{6.6}$$

The process of learning the optimal schedule length is further depicted in Figure 6.5 using a flowchart. We can see in Figure 6.5 that all UAVs are placed at the optimal positions at the start. Then, the PMF $\tilde{\sigma}$ is used to select a schedule. After that, each ground device transmits in the selected schedule. Then, the Gibbs sampler updates the PMF $\tilde{\sigma}$ based on the recorded reward for the selected schedule length. This process repeats until the convergence is achieved for the schedule length.

## 6.4 Evaluation

The experiments are conducted in Matlab. The system consists of multiple ground devices and one UAV in each cell. The UAV is placed at a height of 200 meters from the ground. The UAV and ground devices are equipped with a 2.4 GHz radio and transmit at a fixed power of 1 Watt. For simplicity, assume each cell to be

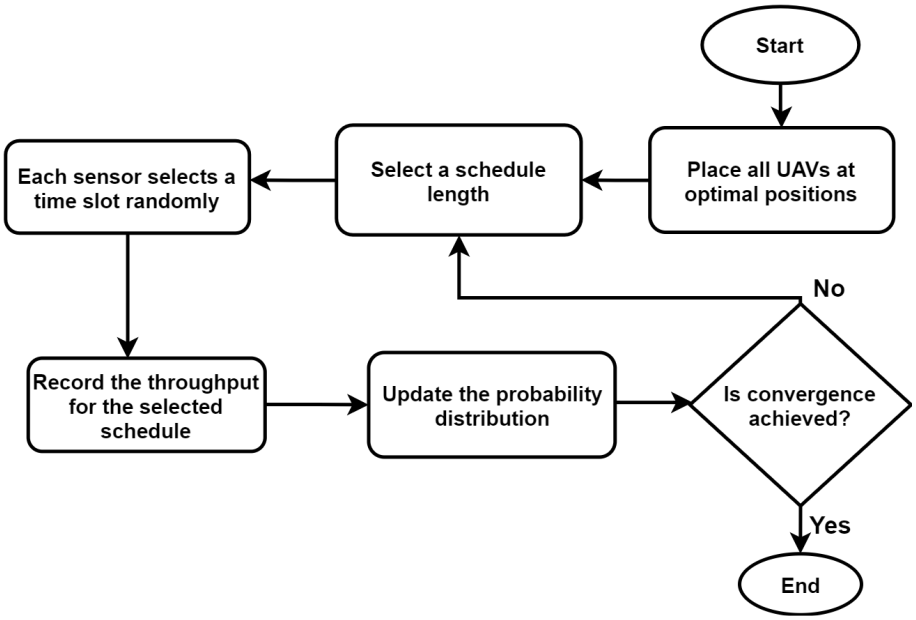


Figure 6.5: The learning process for the optimal schedule length.

Table 6.1: Simulation Parameters.

| Parameter | Value |
|---|---|
| Frequency | 2.4 GHz |
| UAV height | 200 meters |
| Channel model | Nakagami-m |
| Area of cell | 500 $m^2$ |
| Transmit power | 1 Watt |
| Temperature parameter $\tau$ | 110 to 5 |

square-shaped where the area of each cell is 500 $m^2$, unless specified. The results presented in Section 6.4.1 consider a single cell whereby there is no interference from neighboring cells. After that, Section 6.4.2 considers multi-cells, meaning ground stations will experience interference from transmissions in neighboring cells. Table 6.1 summarizes the simulation parameters.

### 6.4.1 Single Cell

Figure 6.6 shows an example cell with optimal location. We can see the optimal UAV position is between the corner and center of a cell. This is because at the optimal location, a UAV is able to obtain the highest diversity in received power

from all nodes. On the other hand, when the UAV is placed at the center of a cell, its distance to the nodes is smaller, resulting in less difference in received power levels. Therefore, we observe better performance when the UAV is placed at the optimal location.

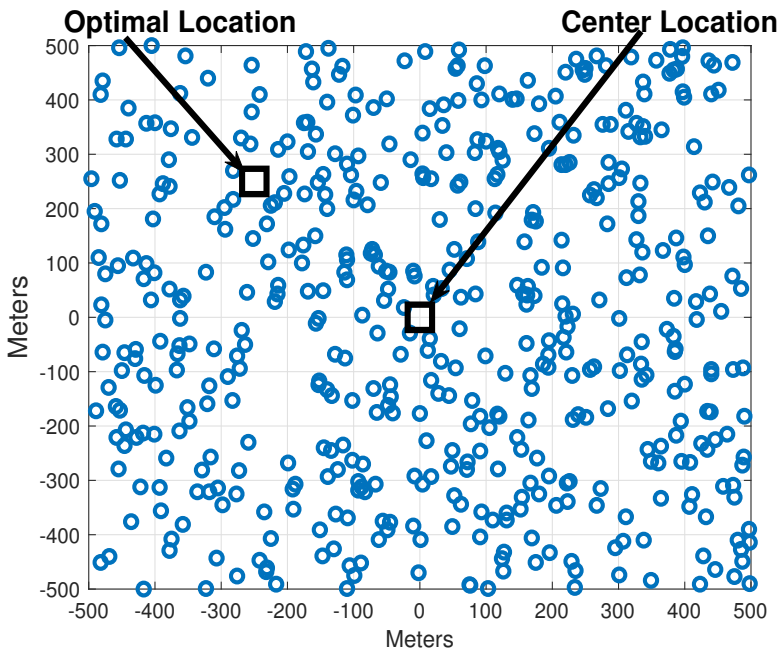


Figure 6.6: An example cell with 250 ground devices depicting the optimal UAV position

Figure 6.7 and 6.8 show the obtained schedule length for the optimal and center UAV locations. We can see in Figure 6.7 that the schedule length is significantly shorter when the UAV is placed at the optimal location as compared to the center location. Specifically, the frame length is 195 slots for the optimal location when the area is 200 $m^2$. In comparison, the frame length is 235 slots when the UAV is placed at the center. From Figure 6.7, we also observe that the schedule length decreases as the area of cell increases. The schedule length is bigger for a smaller cell such as 200 $m^2$ because the distance between the nearest and farthest nodes is very small. Consequently, SIC cannot perform well due to a lower difference in received power levels. The difference in received power levels increases as the area increases. Therefore, the schedule length decreases. For example, the schedule length for the optimal location is 195 time slots per frame when the area is 200 $m^2$, which decreases

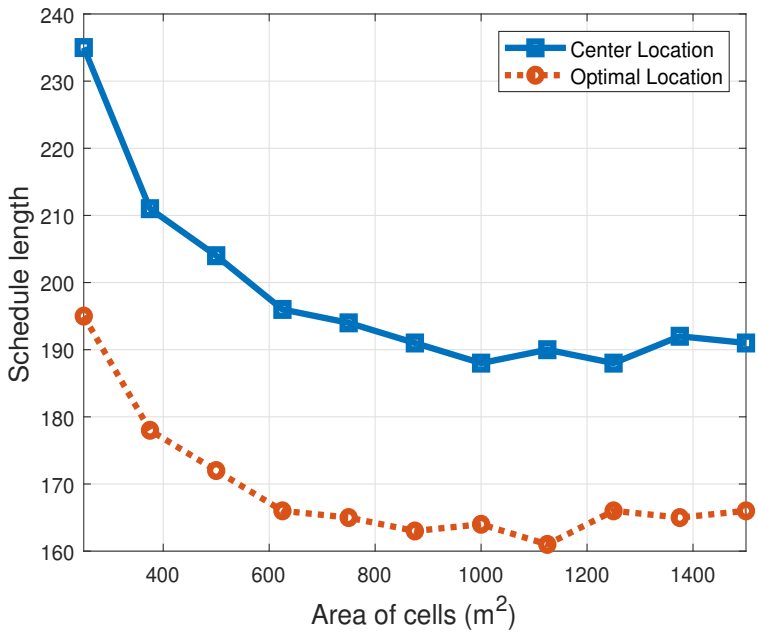


Figure 6.7: Performance with increasing cell area.

to 167 time slots when the area is increased to 1500 $m^2$. This is due to the increase in distance between the ground devices and the UAV, which results in a higher difference in received power levels. The schedule length for the center location also drops from 235 to 200 time slots per frame. We also observe from Figure 6.7 that the schedule length decreases significantly when the area increases up to 800 $m^2$. However, it remains nearly the same when the area is increased further. This is because, when the cell area is too big, e.g., greater than 1000 $m^2$, the obtained SINR becomes very small. Consequently, the chances of failed transmissions increase due to a lower SINR. As a result, the schedule length does not reduce further.

Figure 6.8 shows the impact of increasing number of ground devices on schedule length. We can see that as expected, the schedule length increases when the number of ground devices increases. This is because having more ground devices means more time slots are needed to accommodate them. Therefore, the schedule length increases as the number of ground devices increases. In particular, the schedule length for the optimal UAV location increases from 32 to 345 time slots per frame when the number of ground devices increases from 50 to 500. The schedule length

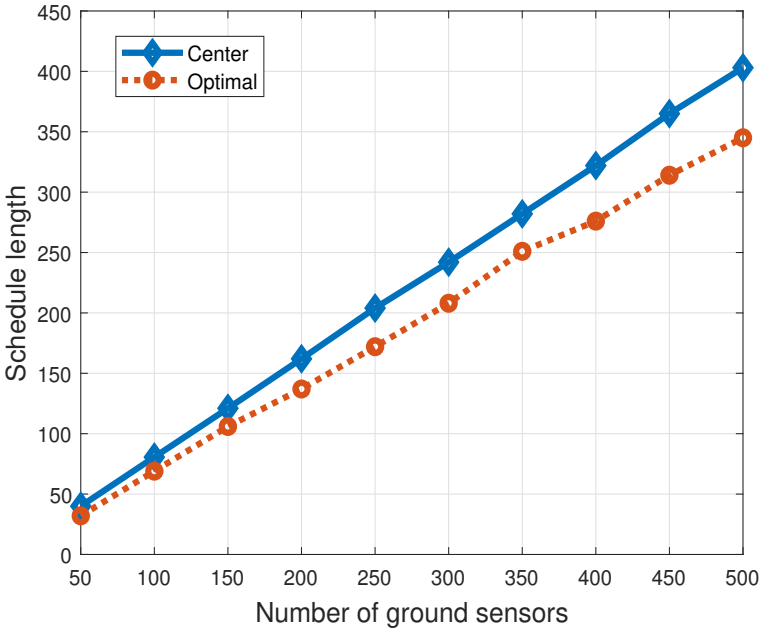


Figure 6.8: Performance with increasing number of ground devices.

is nearly 15% higher when the UAV is placed at the center of a cell.

### 6.4.2 Multiple Cells

This subsection discusses the results obtained for multiple cells, thereby, taking into account the interference from neighbouring cells.

#### 6.4.2.1 Optimizing Location

In this experiment, the number of cells is increased from one to four. The number of ground devices in each cell is 250 and the schedule length is fixed to 125 time slots per frame.

From Figure 6.9, we see that the success rate reduces as the number of cells increases. In particular, the success rate for the optimal location reduces from 47% to 23% when the number of cells increases from one to four. Similarly, the success rate for the center location decreases from 45% to 20%. This is because increasing the number of cells increases the interference. In the case of four cells, each transmission in any cell can experience up to three interfering transmissions from other cells.

Therefore, the success rate decreases as the number of cells increases.

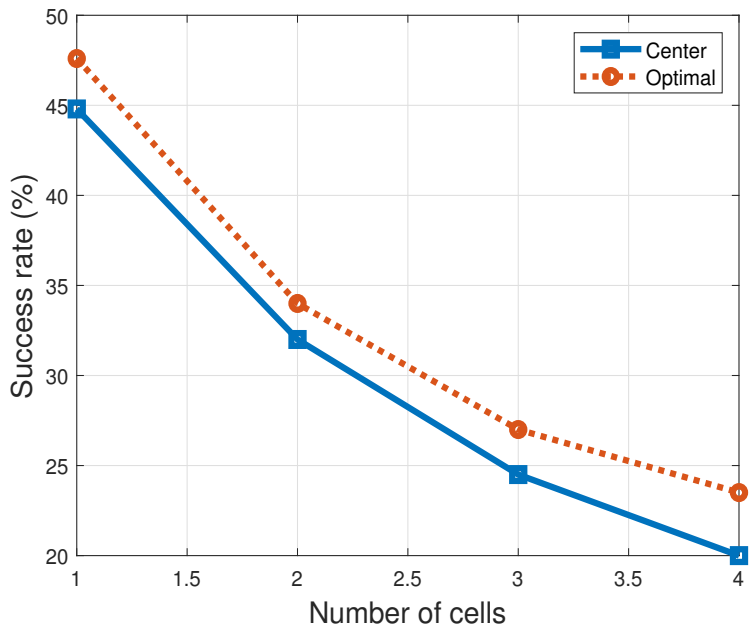


Figure 6.9: Performance with increasing number of cells.

The next experiment increases the area of each cell from one square km to eight square km and studies the impact on success rate. Figure 6.10 shows that the success rate increases with an increase in cell area. Specifically, we observe that the success rate for the optimal location increases from 19% to 27% when the area size increases from 1000 to 8000 $m^2$. Similarly, the success rate when an UAV is placed at the center of each cell increases from 17% to 23%. The lowest success rate is obtained for the shortest cell area because the interference is highest when the area is small. As the area is increased, interference reduces. In addition, SIC also works better as area increases due to a higher difference in received power levels. Consequently, the success rate increases with increasing cell area.

This part studies the impact of schedule length on success rate. The area of each cell is fixed to 5000 $m^2$ and the number of ground devices to 250. Figure 6.11 shows that as expected, the success rate increases as the schedule length increases. In particular, the success rate for optimal location increases from 16% to 35% whereas, for center location, it increases from 14 to 32%. This is because when there are

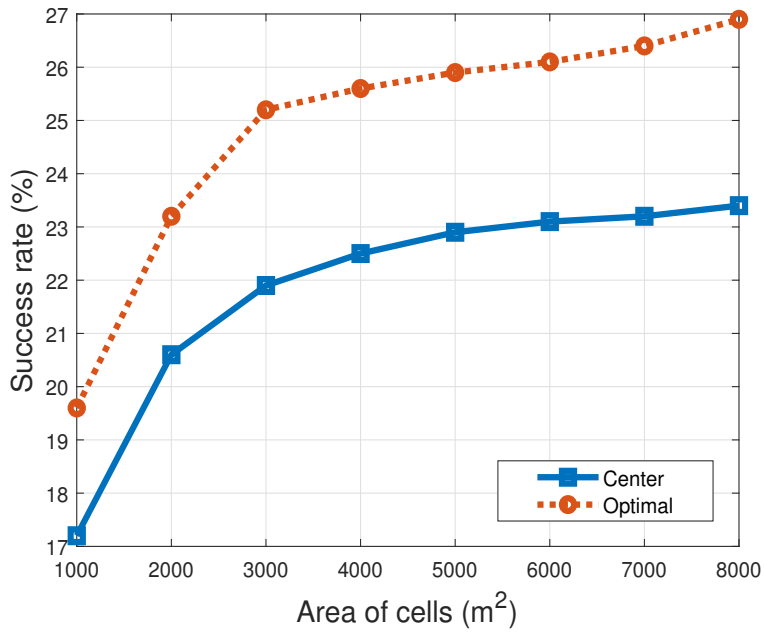


Figure 6.10: Performance with increasing cell size.

fewer time slots per frame, more ground devices will transmit together in each slot. Correspondingly, when the number of time slots is higher, there are fewer ground devices that select the same time slots, resulting in a better success rate.

Figure 6.12 shows the number of ground devices per time slot for different schedule lengths. We can see that as expected when there are a higher number of ground devices, each time slot accommodates more ground devices. For example, in the case of 400 ground devices, if the schedule length is 100, four ground devices will occupy each time slot. If the total number of ground devices is decreased to 250, only 2.5 ground devices occupy each time. We can also observe that the number of ground devices per slot decreases as the schedule length increases. For example in the case of 250 ground devices, each time slot accommodates 2.5 ground devices if the schedule length is 100 slots. If the schedule length is increased to to 450, each slot will accommodate only 0.66 ground devices.

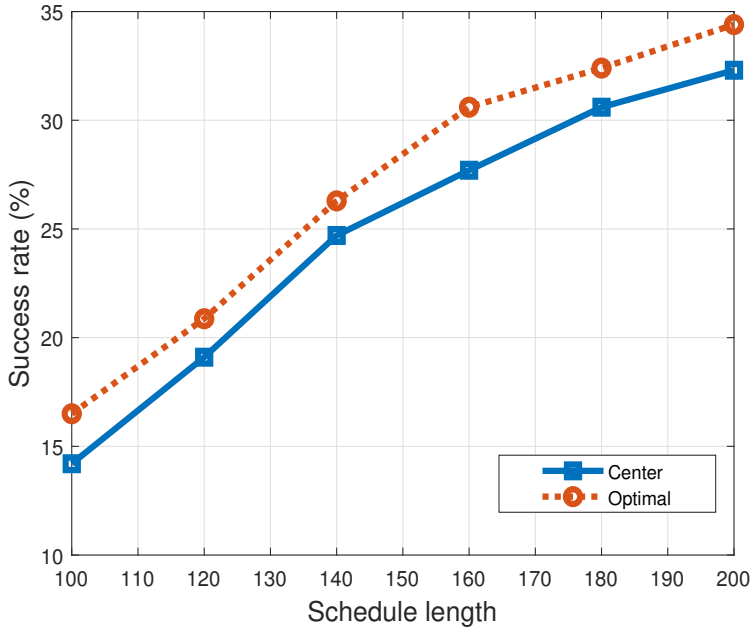


Figure 6.11: Performance with increasing schedule length.

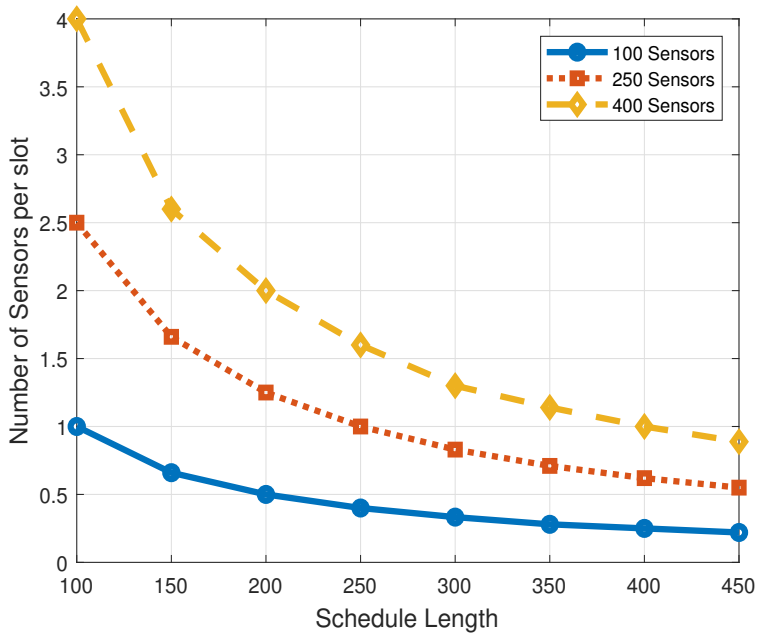


Figure 6.12: Number of ground devices occupying each time slot.

#### 6.4.2.2 Optimal Schedule Length

In this subsection, each UAV's location is fixed to the optimal position as per Section 6.4.2.1. The objective here is to find the optimal schedule length. Figure 6.13 shows that the optimal schedule length remains around 110 time slots per frame when there are 250 ground devices. When the schedule length is smaller than 100, each time slot is occupied by 2.5 ground devices on average, which results in higher transmission failures. On the other hand, for a bigger frame length such as 200, it takes more time for the ground devices to transmit, which reduces their throughout. Figure 6.13 shows the throughput comparison between fixed and optimal schedule length. We can see that the obtained throughput for optimal schedule length remains around 0.26 Mbps when the area of cell is 7000 $m^2$. For the same area, a throughput of 0.24 Mbps is obtained when $L = 125$ and 0.23 Mbps when $L = 100$.

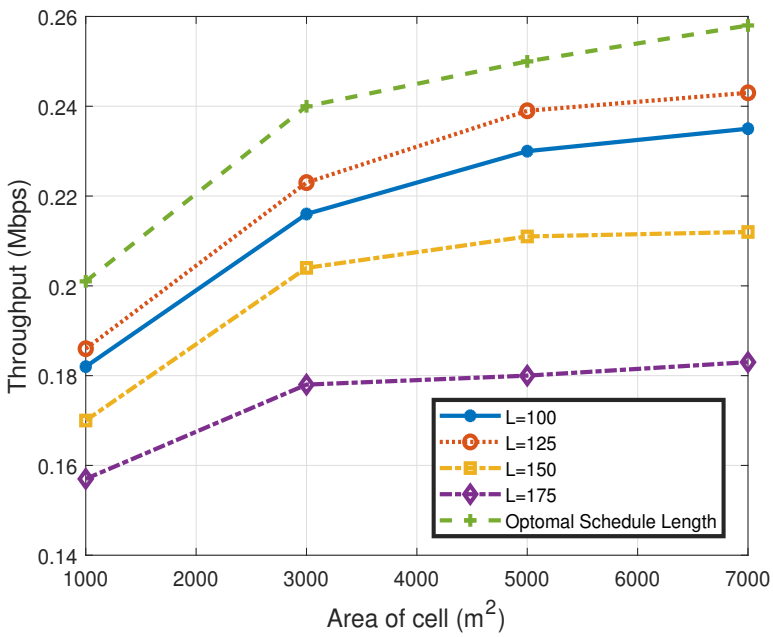


Figure 6.13: Throughput comparison between fixed and optimal schedule length.

## 6.5 Conclusion

The optimal placement of a mobile base station is important in UAV aided WSNs. This is because a UAV base station needs to offer frequent transmission opportunities to all ground nodes. To this end, this chapter proposes a method to identify the optimal schedule length through placement optimization of a SIC capable UAV. Advantageously, the chapter also considers a challenging scenario with multiple cells, thereby, considering interference from neighbouring cells. The chapter identifies the optimal position of each UAV by using Gibbs sampling based approach. The results show that the proposed method significantly reduces the schedule length and thereby, allows the ground devices to transmit frequently.

Chapter 7

# Conclusion

This thesis studies link scheduling approaches for multi-UAV networks. In particular, it studies centralized and distributed TDMA MACs. Critically, it studies whether UAVs and ground stations can be equipped with learning approaches to select a TDMA schedule as well as optimize parameters such transmission slot, data rate, schedule length, and orientation and/or placement of UAVs. These approaches can be useful for multi-UAV networks working in a variety of applications such as cellular base stations, reconnaissance, farming and border surveillance.

Henceforth, this thesis addresses a number of problems. The first problem is to identify the best TDMA schedule that works best over random channel gains. This is a challenging problem because the total number of possible schedules can be very large and the ground station has imperfect channel state information. Another issue of concern is information required to compute a schedule. As discussed in Chapter 1, a distributed MAC is preferred for UAVs. This is because it allows UAVs to make decisions based only on local information. Lastly, this thesis considers optimizing the placement or location of UAVs. This problem is significant because placing a UAV at the optimal position can result in a shorter TDMA schedule length and also helps minimize interference caused to or by neighboring cells.

To address the first problem, Chapter 3 proposes a discrete optimization based

algorithm to identify the best schedule. The chapter also proposes a solution to generate a subset of transmission schedules when the number of UAVs is high. The second problem is addressed in Chapter 4, which outlines a distributed MAC called L-MAC. The proposed L-MAC allows UAVs to learn the most suitable time slots in a transmission schedule. UAVs use the Softmax function to learn which time slot in a TDMA schedule is more suitable for transmission. The next problem addressed in this thesis is to determine the optimal schedule length. The proposed MAC, called L-MAC, requires a ground station to monitor the number of collisions and idle slots. If there is a high number of collisions, the ground station increases the schedule length. Otherwise, in case of idle time slots, it decreases the schedule length. Chapter 6 presents a problem that aims to optimize the placement of UAVs. The hypothesis is that changing the location of a UAV would change the received power from ground devices, and thereby help increase the number of SIC decoding successes. In addition, this chapter also considers interference from neighboring cells, and outlines a learning approach based on Gibbs sampling to determine the optimal location of UAVs.

This thesis confirms that using SIC and TDMA based link access protocols significantly improve UAV network performance. For example, Chapter 3 shows that up to four UAVs can be scheduled in a single time slot. This means the resulting schedule will be significantly shorter as compared to a schedule with a single transmitter in each time slot. This thesis also showed that learning techniques can be used to configure network parameters. In this way, UAVs are able to learn the most suitable schedule length, transmission slots, data rate, orientation, or/and placement.

There are numerous future directions. One of which is to add transmit power control to L-MAC. This would then allow UAVs to adapt their transmit power to meet SIC requirements. Another possible direction is to extend the work to multi-hop UAV networks. This will enable greater network coverage. However, any developed solutions will have to address the hidden terminal problem and aim to maximize spatial reuse. Lastly, developing energy efficient MAC protocols is an

important direction as UAVs are energy constrained.

# Bibliography


[1] T. Michael, J. Robert, and B. John, "The predator ACTD; a case study for transition planning to the formal acquisition process," tech. rep., Defence Technical Information Center, 1997.

[2] G. Grenzdörffer, A. Engel, and B. Teichert, "The photogrammetric potential of low-cost UAVs in forestry and agriculture," *The International Archives of the Photogrammetry, Remote Sensing and Spatial Information Sciences*, vol. 31, no. B3, pp. 1207–1214, 2008.

[3] M. Corcoran, "Drone journalism: Newsgathering applications of unmanned aerial vehicles (UAVs) in covering conflict, civil unrest and disaster," 2014.

[4] X. Zhenyu, X. Pengfei, and X. Xiang-Gen, "Enabling UAV cellular with millimeter-wave communication: potentials and approaches," *IEEE Communications Magazine*, vol. 54, pp. 66–73, May 2016.

[5] M. Abdelkader, M. Shaqura, C. Claudel, and W. Gueaieb, "A UAV based system for real time flash flood monitoring in desert environments using lagrangian microsensors," in *International Conference on Unmanned Aircraft Systems (ICUAS)*, (Atlanta, Georgia), pp. 25–34, May 2013.

[6] L. Koh and S. Wich, "Dawn of drone ecology: low-cost autonomous aerial ve-

hicles for conservation," *Tropical Conservation Science*, vol. 5, no. 2, pp. 121–132, 2012.

[7] S. Gupte, P. Mohandas, and J. M. Conrad, "A survey of quadrotor unmanned aerial vehicles," in *Proceedings of IEEE Southeastcon*, (Florida, US), pp. 1–6, Mar. 2012.

[8] Z. Li, Y. Yan, Y. Jing, and S. Zhao, "The design and testing of a LiDAR platform for a UAV for heritage mapping," *The International Archives of Photogrammetry, Remote Sensing and Spatial Information Sciences*, vol. 40, no. 1, p. 17, 2015.

[9] M. Hirose, Y. Xiao, Z. Zuo, V. R. Kamat, D. Zekkos, and J. Lynch, "Implementation of UAV localization methods for a mobile post-earthquake monitoring system," in *IEEE Workshop on Environmental, Energy, and Structural Monitoring Systems (EESMS)*, (Trento, Italy), pp. 66–71, July 2015.

[10] U. Factory, *UAV Factory, "Penguin B Datasheet"*, 2009.

[11] H. Eisenbeiss, "The potential of unmanned aerial vehicles for mapping," 2011.

[12] R. P. Weinert, *A History of Army Aviation - 1950-1962*. Office of the Command Historian United State Army Training and Doctrine Command, 1991.

[13] D. Konstantinos, V. Kimon, and P. Les, *Aviation History and Unmanned Flight*, pp. 11–42. Springer, 2012.

[14] S. M. Shavarani, M. G. Nejad, F. Rismanchian, and G. Izbirak, "Application of hierarchical facility location problem for optimization of a drone delivery system: a case study of amazon prime air in the city of san francisco," *The International Journal of Advanced Manufacturing Technology*, vol. 95, no. 9-12, pp. 3141–3153, 2018.

[15] R. V. Petrescu, R. Aversa, B. Akash, F. Berto, A. Apicella, and F. I. Petrescu, "Unmanned helicopters," *Journal of Aircraft and Spacecraft Technology*, vol. 1, no. 4, pp. 241–248, 2017.

[16] M. Moon, "Dubai tests a passenger drone for its flying taxi service," *Engadget*, 2017.

[17] V. Bas, N. Huub, B. Geert, and C. Bart, *Drone Technology: Types, Payloads, Applications, Frequency Spectrum Issues and Future Developments*, pp. 21–45. The Hague, 2016.

[18] F. S. Leira, T. A. Johansen, and T. I. Fossen, "Automatic detection, classification and tracking of objects in the ocean surface from UAVs using a thermal camera," in *IEEE Aerospace Conference*, (Montana, USA), pp. 1–10, Mar. 2015.

[19] G. A. M. d. Santos, Z. Barnes, E. Lo, B. Ritoper, L. Nishizaki, X. Tejeda, A. Ke, H. Lin, C. Schurgers, A. Lin, and R. Kastner, "Small unmanned aerial vehicle system for wildlife radio collar tracking," in *IEEE International Conference on Mobile Ad Hoc and Sensor Systems*, (Pennsylvania, US), pp. 761–766, Oct. 2014.

[20] P. Andreas, "Redrawing the line: borders and security in the twenty-first century," *International security*, vol. 28, no. 2, pp. 78–111, 2003.

[21] D. Bein, W. Bein, A. Karki, and B. B. Madan, "Optimizing border patrol operations using unmanned aerial vehicles," in *International Conference on Information Technology - New Generations*, (Las Vegas, USA), pp. 479–484, Apr. 2015.

[22] S. Z. Gürbz, U. Kaynak, B. Özkan, O. C. Kocaman, F. Kyc, and B. Tekeli, "Design study of a short-range airborne UAV radar for human monitoring," in

*Asilomar Conference on Signals, Systems and Computers*, (California, USA), pp. 568–572, Nov. 2014.

[23] P. Tokekar, J. V. Hook, D. Mulla, and V. Isler, "Sensor planning for a symbiotic UAV and UGV system for precision agriculture," *IEEE Transactions on Robotics*, vol. 32, pp. 1498–1511, Dec. 2016.

[24] A. Dhekne, M. Gowda, and R. R. Choudhury, "Extending cell tower coverage through drones," in *International Workshop on Mobile Computing Systems and Applications*, (New York, US), pp. 7–12, Feb. 2017.

[25] W. Guo, C. Devine, and S. Wang, "Performance analysis of micro unmanned airborne communication relays for cellular networks," in *International Symposium on Communication Systems, Networks & Digital Signal Processing (CSNDSP)*, (Manchester, UK), pp. 658–663, July 2014.

[26] T. Y. Chi, Y. Ming, S. Y. Kuo, C. C. Liao, and Tseng, "Civil UAV path planning algorithm for considering connection with cellular data network," in *International Conference on Computer and Information Technology (CIT)*, (Sichuan, China), pp. 327–331, Oct. 2012.

[27] M. Mozaffari, W. Saad, M. Bennis, and M. Debbah, "Efficient deployment of multiple unmanned aerial vehicles for optimal wireless coverage," *IEEE Communications Letters*, vol. 20, pp. 1647–1650, Aug. 2016.

[28] T. Villa, F. Gonzalez, B. Miljievic, Z. Ristovski, and L. Morawska, "An overview of small unmanned aerial vehicles for air quality measurements: Present applications and future prospective," *Sensors*, vol. 16, p. 1072, July 2016.

[29] M. Jarzabek-Rychard and M. Karpina, "Quality analysis on 3D building models reconstructed from UAV imagery," *ISPRS - International Archives of the*

*Photogrammetry, Remote Sensing and Spatial Information Sciences*, vol. XLI-B1, pp. 1121–1126, 2016.

[30] F. Nex and F. Remondino, "UAV for 3D mapping applications: a review," *Applied Geomatics*, vol. 6, no. 1, pp. 1–15, 2014.

[31] K. L. B. Cook, "The silent force multiplier: the history and role of UAVs in warfare," in *IEEE Aerospace Conference*, (Montana, USA), pp. 1–7, Mar. 2007.

[32] S. Szabó, P. Enyedi, M. Horváth, Z. Kovács, P. Burai, T. Csoknyai, and G. Szabó, "Automated registration of potential locations for solar energy production with light detection and ranging (LiDAR) and small format photogrammetry," *Journal of Cleaner Production*, vol. 112, pp. 3820–3829, 2016.

[33] R. Carolyn, G. Paul, and S. R. Timothy, "Multi-rotor unmanned aerial vehicles (UVAs) and high-resolution compact digital cameras: a promising new method for monitoring changes to surface karst resources," *Acta Carsologica*, vol. 43, no. 2-3, 2014.

[34] V. Pandit and A. Poojari, "A study on amazon prime air for feasibility and profitability – graphical data analysis," *IOSR Journal of Business and Management (IOSR-JBM)*, vol. 16, pp. 6–11, Nov. 2014.

[35] W. Matt, "Journalism with flying robots," *XRDS: Crossroads, The ACM Magazine for Students*, vol. 20, no. 3, pp. 28–31, 2014.

[36] F. Remondino, L. Barazzetti, F. Nex, M. Scaioni, and D. Sarazzi, "UAV photogrammetry for mapping and 3D modeling–current status and future perspectives," *International Archives of the Photogrammetry, Remote Sensing and Spatial Information Sciences*, vol. 38, no. 1, p. 22, 2011.

[37] F. Ono, H. Ochiai, K. Takizawa, M. Suzuki, and R. Miura, "Performance

analysis of wireless relay network using network coding and UAS," in *IEEE Globecom Workshops*, (Georgia, US), pp. 1409–1414, Dec. 2013.

[38] S. Erik, "Counter narcotics missions for unmanned aerial vehicles," tech. rep., DTIC Document, 2000.

[39] E. Jakob, S. Jürgen, and C. Daniel, "Camera-based navigation of a low-cost quadrocopter," in *International Conference on Intelligent Robots and Systems (IROS)*, (Algarve, Portugal), pp. 2815–2821, Oct. 2012.

[40] V. Artale, G. Barbaraci, C. Milazzo, C. Orlando, and A. Ricciardello, "Dynamic analysis of a hexacopter controlled via LQR-PI," in *AIP Conference Proceedings*, vol. 1558, (Rhodes, Greece), pp. 1212–1215, Sept. 2013.

[41] A. Sung, C. Cheol, S. Kang, J. Son, B. L. Lee, and K. Han, "Multirotor type unmanned aerial vehicle available for adjusting direction of thrust," May 2016. US Patent App. 15/148,445.

[42] S. Inkyu and C. Peter, "Estimation and control for an open-source quadcopter," in *Proceedings of the Australasian Conference on Robotics and Automation*, (Melbourne, Australia), Dec. 2011.

[43] I. Sa and P. Corke, "System identification, estimation and control for a cost effective open-source quadcopter," in *IEEE International Conference on Robotics and Automation*, (Minnesota, US), pp. 2202–2209, May 2012.

[44] Y. S. Young, L. Zongli, and A. Paul, "Introduction to rotor dynamics," in *Control of Surge in Centrifugal Compressors by Active Magnetic Bearings*, pp. 17–55, Springer, 2013.

[45] M. Bernard, K. Takeo, and T. M. Brian, *System identification modeling of a model-scale helicopter*. Carnegie Mellon University, The Robotics Institute, 2000.

[46] A. Maziar, S. Agostino, M. Mammone, M. Nelson, and T. Zhou, "Classification of unmanned aerial vehicles," tech. rep., University of adelaide australia, 2006.

[47] P. Vasile, B. Mircea, and L. Andrei, "Innovative solutions and UAS limits," *Review of the Air Force Academy*, vol. 26, no. 2, pp. 51–58, 2014.

[48] E. W. Frew and T. X. Brown, "Airborne communication networks for small unmanned aircraft systems," *Proceedings of the IEEE*, vol. 96, no. 12, pp. 2008–2027, 2008.

[49] T. Andre, K. A. Hummel, A. P. Schoellig, E. Yanmaz, M. Asadpour, C. Bettstetter, P. Grippa, H. Hellwagner, S. Sand, and S. Zhang, "Application-driven design of aerial communication networks," *IEEE Communications Magazine*, vol. 52, pp. 129–137, May 2014.

[50] F. Eurocontrol, "Communications operating concept and requirements for the future radio system (COCR)," tech. rep., Eurocontrol/FAA, 2007.

[51] K. J. Hayhurst, J. M. Maddalon, P. S. Miner, M. P. DeWalt, and G. F. McCormick, "Unmanned aircraft hazards and their implications for regulation," in *ieee/aiaa Digital Avionics Systems Conference*, (Oregon, US), pp. 1–12, Oct. 2006.

[52] E. Yanmaz, M. Quaritsch, S. Yahyanejad, B. Rinner, H. Hellwagner, and C. Bettstetter, "Communication and coordination for drone networks," in *Ad Hoc Networks*, pp. 79–91, Springer, 2017.

[53] A. J. Mohammad, V. Frost, S. Zaghloul, G. Prescott, and D. Braaten, "Multichannel iridium communication system for polar field experiments," in *IEEE International Geoscience and Remote Sensing Symposium*, vol. 1, (Anchorage, Alaska), p. 124, Sept. 2004.

[54] J. Engel, L. Sturm, and D. Cremers, "Accurate figure flying with a quadrocopter using onboard visual and inertial sensing," *Imu*, vol. 320, p. 240, 2012.

[55] M. e. Grisworld, "Spectrum management: Key to the future of unmanned aircraft systems?(maxwell paper, number 44)," tech. rep., DTIC Document, 2008.

[56] E. Yanmaz, R. Kuschnig, and C. Bettstetter, "Achieving air-ground communications in 802.11 networks with three-dimensional aerial mobility," in *IEEE INFOCOM*, (Turin, Italy), pp. 120–124, Apr. 2013.

[57] N. H. Motlagh, M. Bagaa, and T. Taleb, "UAV-based IoT platform: A crowd surveillance use case," *IEEE Communications Magazine*, vol. 55, pp. 128–134, Feb. 2017.

[58] C. Evans-Pughe, "Bzzzz zzz [ZigBee wireless standard]," *IEE Review*, vol. 49, pp. 28–31, Mar. 2003.

[59] J. S. Lee, Y. W. Su, and C. C. Shen, "A comparative study of wireless protocols: Bluetooth, UWB, ZigBee, and Wi-Fi," in *33rd Annual Conference of the IEEE Industrial Electronics Society (IECON)*, (Taipei, Taiwan), pp. 46–51, Nov. 2007.

[60] A. Shaw and K. Mohseni, "A fluid dynamic based coordination of a wireless sensor network of unmanned aerial vehicles: 3-D simulation and wireless communication characterization," *IEEE Sensors Journal*, vol. 11, pp. 722–736, Mar. 2011.

[61] M. Franceschinis, C. Pastrone, M. A. Spirito, and C. Borean, "On the performance of ZigBee pro and ZigBee IP in IEEE 802.15.4 networks," in *International Conference on Wireless and Mobile Computing, Networking and Communications (WiMob)*, (Lyon, France), pp. 83–88, Oct. 2013.

[62] N. Ahmed, S. S. Kanhere, and S. Jha, "On the importance of link characterization for aerial wireless sensor networks," *IEEE Communications Magazine*, vol. 54, pp. 52–57, May 2016.

[63] D. Perez, I. Maza, F. Caballero, D. Scarlatti, E. Casado, and A. Ollero, "A ground control station for a multi-UAV surveillance system," *Journal of Intelligent & Robotic Systems*, vol. 69, no. 1-4, pp. 119–130, 2013.

[64] R. S. Stansbury, M. A. Vyas, and t. A. Wilson, "A survey of UAS technologies for command, control, and communication (C3)," *Journal of Intelligent & Robotic Systems*, vol. 54, no. 1, pp. 61–78, 2009.

[65] L. Reynaud, T. Rasheed, and S. Kandeepan, "An integrated aerial telecommunications network that supports emergency traffic," in *The 14th International Symposium on Wireless Personal Multimedia Communications (WPMC)*, (Brest, France), pp. 1–5, Oct. 2011.

[66] P. Pace and G. Aloi, "Disaster monitoring and mitigation using aerospace technologies and integrated telecommunication networks," *IEEE Aerospace and Electronic Systems Magazine*, vol. 23, pp. 3–9, Apr. 2008.

[67] E. Xargay, V. Dobrokhodov, I. Kaminer, A. M. Pascoal, N. Hovakimyan, and C. Cao, "Time-critical cooperative control of multiple autonomous vehicles: Robust distributed strategies for path-following control and time-coordination over dynamic communications networks," *IEEE Control Systems*, vol. 32, pp. 49–73, Oct. 2012.

[68] S. Morgenthaler, T. Braun, Z. Zhao, T. Staub, and M. Anwander, "UAVNet: A mobile wireless mesh network using unmanned aerial vehicles," in *IEEE Globecom Workshops*, (California, US), pp. 1603–1608, Dec. 2012.

[69] X. Cai, A. Gonzalez-Plaza, D. Alonso, L. Zhang, C. B. Rodrguez, A. P. Yuste, and X. Yin, "Low altitude uav propagation channel modelling," in *11th European Conference on Antennas and Propagation (EUCAP)*, (Paris, France), pp. 1443–1447, Mar. 2017.

[70] R. Amorim, H. Nguyen, P. Mogensen, I. Z. Kovcs, J. Wigard, and T. B.

Srensen, "Radio channel modeling for UAV communication over cellular networks," *IEEE Wireless Communications Letters*, vol. 6, pp. 514–517, Aug. 2017.

[71] D. W. Matolak and R. Sun, "Air-ground channel characterization for unmanned aircraft systems: The near-urban environment," in *IEEE Military Communications Conference*, (Florida, US), Oct. 2015.

[72] N. Schneckenburger, T. Jost, D. Shutin, and U. C. Fiebig, "Line of sight power variation in the air to ground channel," in *European Conference on Antenna and Propagation*, (Davos, Switzerland), pp. 1–5, Apr. 2015.

[73] E. Yanmaz, R. Kuschnig, and C. Bettstetter, "Channel measurements over 802.11a-based UAV-to-ground links," in *IEEE GLOBECOM Workshops (GC Wkshps)*, (texas, US), pp. 1280–1284, Dec. 2011.

[74] C. m. Cheng, P. h. Hsiao, H. T. Kung, and D. Vlah, "Performance measurement of 802.11a wireless links from UAV to ground nodes with various antenna orientations," in *International Conference on Computer Communications and Networks*, (Virginia, US), pp. 303–308, Oct. 2006.

[75] N. Goddemeier and C. Wietfeld, "Investigation of air-to-air channel characteristics and a UAV specific extension to the rice model," in *IEEE Globecom Workshops (GC Wkshps)*, (California, US), pp. 1–5, Dec. 2015.

[76] B. Y. Muneer and D. Nour, "Flying ad-hoc networks: Routing protocols, mobility models, issues," *International Journal of Advanced Computer Science and Applications(IJACSA)*, vol. 7, no. 6, 2016.

[77] Y. Zhou, J. Li, L. Lamont, and C. A. Rabbath, "Modeling of packet dropout for UAV wireless communications," in *International Conference on Computing, Networking and Communications (ICNC)*, (hawaii, US), pp. 677–682, Jan. 2012.

[78] R. Khanduri and S. S. Rattan, "Performance comparison analysis between IEEE 802. 11a/b/g/n standards," *International Journal of Computer Applications*, vol. 78, no. 1, 2013.

[79] S. Waharte, N. Trigoni, and S. Julier, "Coordinated search with a swarm of UAVs," in *IEEE Annual Communications Society Conference on Sensor, Mesh and Ad Hoc Communications and Networks Workshops*, (Rome, Italy), pp. 1–3, June 2009.

[80] J. Navia, I. Mondragon, D. Patino, and J. Colorado, "Multispectral mapping in agriculture: Terrain mosaic using an autonomous quadcopter UAV," in *International Conference on Unmanned Aircraft Systems (ICUAS)*, (Virginia, US), pp. 1351–1358, June 2016.

[81] I. G. R. Shaw, "Predator empire: The geopolitics of US drone warfare," *Geopolitics*, vol. 18, no. 3, pp. 536–559, 2013.

[82] H. Granbohm and J. Wiklund, "GPRS- general packet radio service," *Ericsson Review*, vol. 76, no. 2, pp. 82–88, 1999.

[83] S. Chandrasekharan, K. Gomez, A. Al-Hourani, S. Kandeepan, T. Rasheed, L. Goratti, L. Reynaud, D. Grace, I. Bucaille, T. Wirth, and S. Allsopp, "Designing and implementing future aerial communication networks," *IEEE Communications Magazine*, vol. 54, pp. 26–34, May 2016.

[84] B. Lee, J. Lee, Y. J. Lee, and S. Sung, "Development of cellular data network enabled autonomous rotary UAV," in *International Conference on Control, Automation and Systems (ICCAS 2013)*, (Gwangju, South Korea), pp. 719–722, Oct. 2013.

[85] E. Teng, J. D. Falcao, C. Dominguez, F. Mokaya, P. Zhang, and B. Iannucci, "Aerial sensing and characterization of three-dimensional rf fields," *Univ. at Buffalo, cse. buffalo. edu, accessed: Sep*, 2016.

[86] S. Qazi, A. S. Siddiqui, and A. I. Wagan, "UAV based real time video surveillance over 4G LTE," in *International Conference on Open Source Systems Technologies (ICOSST)*, (Lahore, Pakistan), pp. 141–145, Dec. 2015.

[87] A. Furuskar, S. Mazur, F. Muller, and H. Olofsson, "EDGE: enhanced data rates for GSM and TDMA/136 evolution," *IEEE Personal Communications*, vol. 6, pp. 56–66, June 1999.

[88] J. F. Huber, D. Weiler, and H. Brand, "UMTS, the mobile multimedia vision for IMT 2000: a focus on standardization," *IEEE Communications Magazine*, vol. 38, pp. 129–136, Sept. 2000.

[89] J. Bergman, M. Ericson, D. Gerstenberger, B. Göransson, J. Peisa, and S. Wager, "HSPA evolution–boosting the performance of mobile broadband access," *Ericsson Review*, vol. 85, no. 1, pp. 32–37, 2008.

[90] C. Ball, T. Hindelang, I. Kambourov, and S. Eder, "Spectral efficiency assessment and radio performance comparison between LTE and WiMAX," in *International Symposium on Personal, Indoor and Mobile Radio Communications PIMRC*, (Cannes, France), pp. 1–6, Dec. 2008.

[91] D. Martín-Sacristán, J. F. Monserrat, J. Cabrejas-Peñuelas, D. Calabuig, S. Garrigas, and N. Cardona, "On the way towards fourth-generation mobile: 3GPP LTE and LTE-advanced," *EURASIP Journal on Wireless Communications and Networking*, vol. 2009, p. 4, 2009.

[92] Z. Sun, P. Wang, M. C. Vuran, M. A. Al-Rodhaan, A. M. Al-Dhelaan, and I. F. Akyildiz, "Bordersense: Border patrol through advanced wireless sensor networks," *Ad Hoc Networks*, vol. 9, no. 3, pp. 468–477, 2011.

[93] M. Alzenad, A. El-Keyi, and H. Yanikomeroglu, "3-D placement of an unmanned aerial vehicle base station for maximum coverage of users with dif-

ferent QoS requirements," *IEEE Wireless Communications Letters*, vol. 7, pp. 38–41, Feb. 2018.

[94] X. Wang, A. Chowdhery, and M. Chiang, "SkyEyes: Adaptive video streaming from UAVs," in *Proceedings of the 3rd Workshop on Hot Topics in Wireless*, (New York, USA), pp. 2–6, Oct. 2016.

[95] Q. Wu, L. Liu, and R. Zhang, "Fundamental trade-offs in communication and trajectory design for UAV-enabled wireless network," *IEEE Wireless Communications*, vol. 26, pp. 36–44, Feb. 2019.

[96] S. Verdu, *Multiuser detection.* Springer, 1998.

[97] Y. Zeng, R. Zhang, and T. J. Lim, "Wireless communications with unmanned aerial vehicles: opportunities and challenges," *IEEE Communications Magazine*, vol. 54, pp. 36–42, May 2016.

[98] R. Sun and D. W. Matolak, "Initial results for airframe shadowing in L- and C-band air-ground channels," in *2015 Integrated Communication, Navigation and Surveillance Conference (ICNS)*, pp. X1–1–X1–8, Apr. 2015.

[99] S. Andradóttir, "A global search method for discrete stochastic optimization," *SIAM Journal on Optimization*, vol. 6, no. 2, pp. 513–530, 1996.

[100] R. S. Sutton and A. G. Barto, *Reinforcement learning: An introduction.* MIT press, 2018.

[101] Y. Cai, F. R. Yu, J. Li, Y. Zhou, and L. Lamont, "MAC performance improvement in UAV ad-hoc networks with full-duplex radios and multi-packet reception capability," in *IEEE International Conference on Communications (ICC)*, (Ontario, Canada), pp. 523–527, June 2012.

[102] M. R. Ramli, J.-M. Lee, and D.-S. Kim, "Hybrid mac protocol for UAV-assisted data gathering in a wireless sensor network," *Internet of Things*, p. 100088, Aug. 2019.

[103] Q. Yang and S. Yoo, "Optimal UAV path planning: Sensing data acquisition over IoT sensor networks using multi-objective bio-inspired algorithms," *IEEE Access*, vol. 6, pp. 13671–13684, Mar. 2018.

[104] M. A. Araghizadeh, P. Teymoori, N. Yazdani, and S. Safari, "An efficient medium access control protocol for WSN-UAV," *Ad Hoc Networks*, vol. 52, pp. 146–159, 2016.

[105] X. Ma, R. Kacimi, and R. Dhaou, "Fairness-aware uav-assisted data collection in mobile wireless sensor networks," in *International Wireless Communications and Mobile Computing Conference (IWCMC)*, (Paphos, Cyprus), pp. 995–1001, Sept. 2016.

[106] X. Ma, R. Kacimi, and R. Dhaou, "Adaptive hybrid mac protocols for UAV-assisted mobile sensor networks," in *IEEE Annual Consumer Communications Networking Conference (CCNC)*, pp. 1–4, Jan 2018.

[107] D. Ho and S. Shimamoto, "Highly reliable communication protocol for WSN-UAV system employing TDMA and PFS scheme," in *IEEE GLOBECOM Workshops (GC Wkshps)*, (Texas, US), pp. 1320–1324, Dec. 2011.

[108] C. Y. Tazibt, M. Bekhti, T. Djamah, N. Achir, and K. Boussetta, "Wireless sensor network clustering for uav-based data gathering," in *Wireless Days*, (Porto, Portugal), pp. 245–247, Mar. 2017.

[109] D. Ho, E. I. Grtli, P. B. Sujit, T. A. Johansen, and J. B. Sousa, "Cluster-based communication topology selection and uav path planning in wireless sensor networks," in *International Conference on Unmanned Aircraft Systems (ICUAS)*, (Georgia, US), pp. 59–68, May 2013.

[110] C. Zhan, Y. Zeng, and R. Zhang, "Energy-efficient data collection in UAV enabled wireless sensor network," *IEEE Wireless Communications Letters*, vol. 7, pp. 328–331, June 2018.

[111] A. Vldu, C. Grumzescu, I. Bica, and V. Patriciu, "Energy considerations for data gathering protocol in wireless sensor networks using unmanned aerial vehicles," in *International Conference on Communications (COMM)*, (Bucharest, Romania), pp. 237–240, June 2016.

[112] H. Li, L. Wang, S. Pang, and M. Towhidnejad, "A cross-layer design for data collecting of the UAV-wireless sensor network system," in *12th IEEE International Conference on Embedded and Ubiquitous Computing*, (Milano, Italy), pp. 242–249, Aug. 2014.

[113] W. Wang, C. Dong, H. Wang, and A. Jiang, "Design and implementation of adaptive MAC framework for UAV ad hoc networks," in *International Conference on Mobile Ad-Hoc and Sensor Networks (MSN)*, (Hefei, China), pp. 195–201, Dec. 2016.

[114] C. Lin, H. T. Kung, T. Lin, S. J. Tarsa, and D. Vlah, "Achieving high throughput ground-to-UAV transport via parallel links," in *IEEE ICCCN*, (Hawaai, US), pp. 1–7, July 2011.

[115] T. Ho, M. Medard, R. Koetter, D. R. Karger, M. Effros, J. Shi, and B. Leong, "A random linear network coding approach to multicast," *IEEE Transactions on Information Theory*, vol. 52, pp. 4413–4430, Oct. 2006.

[116] T. D. Ho and J. Park, "Novel multiple access scheme for wireless sensor network employing unmanned aerial vehicle," in *Digital Avionics Systems Conference*, (Utah, US), pp. 1–8, Oct. 2010.

[117] S. Sotheara, N. Aomi, T. Ando, L. Jiang, N. Shiratori, and S. Shimamoto, "Effective data gathering protocol in WSN-UAV employing priority-based contention window adjustment scheme," in *IEEE Globecom Workshops (GC Wkshps)*, (Texas, US), pp. 1475–1480, Dec. 2014.

[118] A. Jiang, Z. Mi, C. Dong, and H. Wang, "CF-MAC: A collision-free MAC

protocol for UAVs ad-hoc networks," in *IEEE Wireless Communications and Networking Conference*, (Doha, Qatar), pp. 1–6, Apr. 2016.

[119] S. Say, H. Inata, and S. Shimamoto, "A hybrid collision coordination-based multiple access scheme for super dense aerial sensor networks," in *IEEE Wireless Communications and Networking Conference*, (Doha, Qatar), pp. 1–6, Apr. 2016.

[120] A. I. Alshbatat and L. Dong, "Adaptive MAC protocol for UAV communication networks using directional antennas," in *International Conference on Networking, Sensing and Control (ICNSC)*, (Illinois, US), pp. 598–603, Apr. 2010.

[121] A. I. Alshbatat and L. Dong, "Performance analysis of mobile ad hoc unmanned aerial vehicle communication networks with directional antennas," *International Journal of Aerospace Engineering*, vol. 2010, 2011.

[122] P. Zhan, K. Yu, and A. L. Swindlehurst, "Wireless relay communications with unmanned aerial vehicles: Performance and optimization," *IEEE Transactions on Aerospace and Electronic Systems*, vol. 47, pp. 2068–2085, July 2011.

[123] F. Jiang and A. L. Swindlehurst, "Optimization of UAV heading for the ground-to-air uplink," *IEEE Journal on Selected Areas in Communications*, vol. 30, pp. 993–1005, June 2012.

[124] C. Dixon and E. W. Frew, "Optimizing cascaded chains of unmanned aircraft acting as communication relays," *IEEE Journal on Selected Areas in Communications*, vol. 30, pp. 883–898, June 2012.

[125] C. Dixon, *Controlled mobility of unmanned aircraft chains to optimize network capacity in realistic communication environments.* PhD thesis, University of Colorado at Boulder, 2010.

[126] S. Gil, M. Schwager, B. J. Julian, and D. Rus, "Optimizing communication in air-ground robot networks using decentralized control," in *IEEE International Conference on Robotics and Automation*, (Alaska, US), pp. 1964–1971, May 2010.

[127] K. H. Kim, K. G. Shin, and D. Niculescu, "Mobile autonomous router system for dynamic (re)formation of wireless relay networks," *IEEE Transactions on Mobile Computing*, vol. 12, pp. 1828–1841, Sept. 2013.

[128] J. Chen and D. Gesbert, "Optimal positioning of flying relays for wireless networks: A LOS map approach," in *IEEE ICC*, (Paris, France), pp. 1–6, May 2017.

[129] J. Lyu, Y. Zeng, and R. Zhang, "Cyclical multiple access in UAV-aided communications: A throughput-delay tradeoff," *IEEE Wireless Communications Letters*, vol. 5, pp. 600–603, Dec. 2016.

[130] J. Lyu, Y. Zeng, R. Zhang, and T. J. Lim, "Placement optimization of UAV-mounted mobile base stations," *IEEE Communications Letters*, vol. 21, pp. 604–607, Mar. 2017.

[131] S. Rohde and C. Wietfeld, "Interference aware positioning of aerial relays for cell overload and outage compensation," in *IEEE Vehicular Technology Conference (VTC Fall)*, (Quebec, Canada), pp. 1–5, Sept. 2012.

[132] S. Zhang, Y. Zeng, and R. Zhang, "Cellular-enabled UAV communication: A connectivity-constrained trajectory optimization perspective," *IEEE Transactions on Communications*, vol. 67, pp. 2580–2604, Mar. 2019.

[133] L. Xie, J. Xu, and R. Zhang, "Throughput maximization for UAV-enabled wireless powered communication networks," *IEEE Internet of Things Journal*, vol. 6, pp. 1690–1703, Apr. 2019.

[134] L. Shi, Y. Hu, J. Xu, Y. Shi, and X. Ding, "The mobile base station strategy for wireless networks with successive interference cancellation," *IEEE Access*, vol. 7, pp. 88570–88578, June 2019.

[135] L. Shi, J. Zhang, Y. Shi, X. Ding, and Z. Wei, "Optimal base station placement for wireless sensor networks with successive interference cancellation," *Sensors*, vol. 15, no. 1, pp. 1676–1690, 2015.

[136] A. Fotouhi, M. Ding, and M. Hassan, "Flying drone base stations for macro hotspots," *IEEE Access*, vol. 6, pp. 19530–19539, Mar. 2018.

[137] E. Kalantari, H. Yanikomeroglu, and A. Yongacoglu, "On the number and 3d placement of drone base stations in wireless cellular networks," in *IEEE Vehicular Technology Conference (VTC-Fall)*, (Montreal, QC, Canada), pp. 1–6, Sept. 2016.

[138] H. Shakhatreh, A. Khreishah, J. Chakareski, H. B. Salameh, and I. Khalil, "On the continuous coverage problem for a swarm of UAVs," in *IEEE 37th Sarnoff Symposium*, (New Jersey, US), pp. 130–135, Sept. 2016.

[139] M. Mozaffari, W. Saad, M. Bennis, and M. Debbah, "Drone small cells in the clouds: Design, deployment and performance analysis," in *IEEE GLOBECOM*, (California, US), pp. 1–6, Dec. 2015.

[140] A. A. Nasir, H. D. Tuan, T. Q. Duong, and H. V. Poor, "UAV-enabled communication using NOMA," *IEEE Transactions on Communications*, vol. 67, pp. 5126–5138, July 2019.

[141] B. Galkin, J. Kibilda, and L. A. DaSilva, "Deployment of UAV-mounted access points according to spatial user locations in two-tier cellular networks," in *Wireless Days (WD)*, (Toulouse, France), pp. 1–6, Mar. 2016.

[142] M. Mozaffari, W. Saad, M. Bennis, and M. Debbah, "Optimal transport theory

for power-efficient deployment of unmanned aerial vehicles," in *IEEE ICC*, pp. 1–6, 2016.

[143] Y. Zeng, J. Xu, and R. Zhang, "Energy minimization for wireless communication with rotary-wing UAV," *IEEE Transactions on Wireless Communications*, vol. 18, pp. 2329–2345, Apr. 2019.

[144] Y. Zeng and R. Zhang, "Energy-efficient UAV communication with trajectory optimization," *IEEE Transactions on Wireless Communications*, vol. 16, pp. 3747–3760, June 2017.

[145] Y. Sun, D. Xu, D. W. K. Ng, L. Dai, and R. Schober, "Optimal 3D-trajectory design and resource allocation for solar-powered UAV communication systems," *IEEE Transactions on Communications*, vol. 67, pp. 4281–4298, June 2019.

[146] D. Yang, Q. Wu, Y. Zeng, and R. Zhang, "Energy tradeoff in ground-to-UAV communication via trajectory design," *IEEE Transactions on Vehicular Technology*, vol. 67, pp. 6721–6726, July 2018.

[147] V. Dao, H. Tran, S. Girs, and E. Uhlemann, "Reliability and fairness for UAV communication based on non-orthogonal multiple access," in *IEEE ICC Workshops*, (Shanghai, China), pp. 1–6, May 2019.

[148] M. F. Sohail, C. Y. Leow, and S. Won, "Non-orthogonal multiple access for unmanned aerial vehicle assisted communication," *IEEE Access*, vol. 6, pp. 22716–22727, Apr. 2018.

[149] S. Barghi, H. Jafarkhani, and H. Yousefi'zadeh, "MIMO-assisted MPR-aware MAC design for asynchronous WLANs," *IEEE/ACM Transactions on Networking*, vol. 19, pp. 1652–1665, Dec. 2011.

[150] M. Gowda, N. Roy, R. R. Choudhury, and S. Nelakuditi, "Compressing back-

off in CSMA networks," in *IEEE 24th International Conference on Network Protocols (ICNP)*, (Singapore), pp. 1–10, Nov. 2016.

[151] A. Mukhopadhyay, N. B. Mehta, and V. Srinivasan, "Design and analysis of an acknowledgment-aware asynchronous MPR MAC protocol for distributed WLANs," *IEEE Transactions on Wireless Communications*, vol. 12, pp. 2068–2079, May 2013.

[152] A. Ksentini, A. Nafaa, A. Gueroui, and M. Naimi, "Determinist contention window algorithm for IEEE 802.11," in *International Symposium on Personal, Indoor and Mobile Radio Communications*, vol. 4, (Berlin, Germany), pp. 2712–2716 Vol. 4, Sept. 2005.

[153] Y. Edalat and K. Obraczka, "Dynamically tuning ieee 802.11's contention window using machine learning," in *22nd International ACM Conference on Modeling, Analysis and Simulation of Wireless and Mobile Systems*, (Florida, US), pp. 19–26, Nov. 2019.

[154] A. H. Y. Abyaneh, M. Hirzallah, and M. Krunz, "Intelligent-cw: Ai-based framework for controlling contention window in WLANs," in *IEEE International Symposium on Dynamic Spectrum Access Networks (DySPAN)*, (New Jersey, US), pp. 1–10, Nov. 2019.

[155] P. X. Zheng, Y. J. Zhang, and S. C. Liew, "Multipacket reception in wireless local area networks," in *International Conference on Communications (ICC)*, vol. 8, (Istanbul, Turkey), pp. 3670–3675, June 2006.

[156] F. Babich and M. Comisso, "Theoretical analysis of asynchronous multipacket reception in 802.11 networks," *IEEE Transactions on Communications*, vol. 58, pp. 1782–1794, June 2010.

[157] P. X. Zheng, Y. J. Zhang, and S. C. Liew, "Analysis of exponential backoff

with multipacket reception in wireless networks," in *Proceedings of Conference on Local Computer Networks*, (Florida, USA), pp. 855–862, Nov. 2006.

[158] S. Nagaraj, D. Truhachev, and C. Schlegel, "Analysis of a random channel access scheme with multi-packet reception," in *IEEE Globecom*, pp. 1–5, Nov. 2008.

[159] Y. J. Zhang, "Multi-round contention in wireless LANs with multipacket reception," *IEEE Transactions on Wireless Communications*, vol. 9, pp. 1503–1513, Apr. 2010.

[160] S. Zhou and Z. Niu, "Distributed Medium Access Control with SDMA Support for WLANs," *IEICE Transactions on Communications*, vol. 93, pp. 961–970, 2010.

[161] R. Liao, B. Bellalta, and M. Oliver, "DCF/USDMA: Enhanced DCF for uplink SDMA transmissions in WLANs," in *International Wireless Communications and Mobile Computing Conference (IWCMC)*, (Limassol, Cyprus), pp. 263–268, Aug. 2012.

[162] W. L. Huang, K. B. Letaief, and Y. J. Zhang, "Joint channel state based random access and adaptive modulation in wireless LANs with multi-packet reception," *IEEE Transactions on Wireless Communications*, vol. 7, pp. 4185–4197, Nov. 2008.

[163] Y. Zhang, M. Zhang, C. Fu, J. Li, and F. Shu, "Design and analysis of an energy-efficient CSMA protocol for asynchronous multiple-packet reception," *IEEE Access*, vol. 5, pp. 6483–6491, Mar 2017.

[164] Y. Zhang, A. Gong, Y. Lo, J. Li, F. Shu, and W. S. Wong, "Generalized $p$ -persistent CSMA for asynchronous multiple-packet reception," *IEEE Transactions on Communications*, vol. 67, pp. 6966–6979, Oct. 2019.

[165] G. Sachdeva and G. S. Sharvani, "Design and implementation of an efficient and adaptive asynchronous MPR MAC protocol for WLAN," in *Fifth International Conference on Advanced Computing Communication Technologies*, (Haryana, India), pp. 595–601, Feb. 2015.

[166] C. Chen, S. Hou, and S. Wu, "A novel analytical model for asynchronous multi-packet reception MAC protocol," *IEEE Communications Letters*, vol. 21, pp. 1289–1292, June 2017.

[167] J. Zhang, Z. Dziong, F. Gagnon, and M. Kadoch, "Multiuser detection based MAC design for ad hoc networks," in *International Conference on Heterogeneous Networking for Quality, Reliability, Security and Robustness & Workshops*, (Vancouver, Canada), pp. 1–7, Aug. 2007.

[168] J. Zhang, Z. Dziong, F. Gagnon, and M. Kadoch, "Receiver initiated MAC design for ad hoc networks based on multiuser detection," in *International ICST Conference on Heterogeneous Networking for Quality, Reliability, Security and Robustness*, (Hong Kong), pp. 1–7, July 2008.

[169] B. P. Crow, I. Widjaja, J. G. Kim, and P. T. Sakai, "IEEE 802.11 wireless local area networks," *IEEE Communications Magazine*, vol. 35, pp. 116–126, Sept. 1997.

[170] G. D. Celik, G. Zussman, W. F. Khan, and E. Modiano, "Mac for networks with multipacket reception capability and spatially distributed nodes," *IEEE Transactions on Mobile Computing*, vol. 9, pp. 226–240, Feb. 2010.

[171] H. Chen, F. Yu, H. C. B. Chan, and V. C. M. Leung, "A novel multiple access scheme over multi-packet reception channels for wireless multimedia networks," *IEEE Transactions on Wireless Communications*, vol. 6, pp. 1501–1511, Apr. 2007.

[172] G. D. Celik, G. Zussman, W. F. Khan, and E. Modiano, "MAC for networks with multipacket reception capability and spatially distributed nodes," in *IEEE INFOCOM - Conference on Computer Communications*, pp. 1436–1444, Apr. 2008.

[173] D. Truhachev, S. Nagaraj, and C. Schlegel, "Throughput/reliability tradeoffs in spread spectrum multi-hop ad-hoc wireless networks with multi-packet detection," in *International Conference on Communications*, pp. 1–5, June 2009.

[174] R. Gau, "Modeling the slotted nonpersistent CSMA protocol for wireless access networks with multiple packet reception," *IEEE Communications Letters*, vol. 13, pp. 797–799, October 2009.

[175] Y. Cai, F. R. Yu, J. Li, Y. Zhou, and L. Lamont, "Medium access control for unmanned aerial vehicle (uav) ad-hoc networks with full-duplex radios and multipacket reception capability," *IEEE Transactions on Vehicular Technology*, vol. 62, pp. 390–394, Jan 2013.

[176] M. Mollanoori and M. Ghaderi, "On the performance of successive interference cancellation in random access networks," in *IEEE Communications Society Conference on Sensor, Mesh and Ad Hoc Communications and Networks (SECON)*, (Seoul, South Korea), pp. 461–469, June 2012.

[177] M. Kontik and S. C. Ergen, "Distributed medium access control protocol for successive interference cancellation-based wireless ad hoc networks," *IEEE Communications Letters*, vol. 21, pp. 354–357, Feb. 2017.

[178] S. Lv, X. Wang, and X. Zhou, "Link scheduling in wireless networks with successive interference cancellation," in *International Conference on Mobile Ad-hoc and Sensor Networks*, (Hangzhou, China), pp. 61–67, Dec. 2010.

[179] O. Goussevskaia and R. Wattenhofer, "Scheduling wireless links with successive interference cancellation," in *International Conference on Computer Communications and Networks (ICCCN)*, (Munich, Germany), pp. 1–7, July 2012.

[180] A. Sankararaman and F. Baccelli, "CSMA k-SIC; A class of distributed MAC protocols and their performance evaluation," in *IEEE Conference on Computer Communications*, (Kowloon, Hong Kong), pp. 2002–2010, Apr. 2015.

[181] F. Uddin and S. Mahmud, "Carrier sensing-based medium access control protocol for WLANs exploiting successive interference cancellation," *IEEE Transactions on Wireless Communications*, vol. 16, pp. 4120–4135, June 2017.

[182] M. F. Uddin, "Throughput performance of NOMA in WLANs with a CSMA MAC protocol," *Wireless Networks*, vol. 25, no. 6, pp. 3365–3384, 2019.

[183] M. F. Uddin, "Energy efficiency maximization by joint transmission scheduling and resource allocation in downlink NOMA cellular networks," *Computer Networks*, vol. 159, pp. 37–50, 2019.

[184] E. Balevi, F. T. A. Rabee, and R. D. Gitlin, "ALOHA-NOMA for massive machine-to-machine IoT communication," in *IEEE ICC*, (Missouri, US), pp. 1–5, May 2018.

[185] Z. Ding, L. Dai, and H. V. Poor, "MIMO-NOMA design for small packet transmission in the internet of things," *IEEE Access*, vol. 4, pp. 1393–1405, Apr. 2016.

[186] M. Elkourdi, A. Mazin, E. Balevi, and R. D. Gitlin, "Enabling slotted Aloha-NOMA for massive M2M communication in IoT networks," in *IEEE 19th Wireless and Microwave Technology Conference (WAMICON)*, (Florida, US), pp. 1–4, Apr. 2018.

[187] A. Mazin, M. Elkourdi, and R. D. Gitlin, "Comparison of slotted aloha-NOMA and CSMA/CA for M2M communications in IoT networks," in *2018 IEEE 88th Vehicular Technology Conference (VTC-Fall)*, (Illinois, US), pp. 1–5, Aug. 2018.

[188] A. Dalili Shoaei, M. Derakhshani, and T. Le-Ngoc, "A NOMA-enhanced reconfigurable access scheme with device pairing for M2M networks," *IEEE Access*, vol. 7, pp. 32266–32275, Mar. 2019.

[189] J. Yang, L. Feng, H. Liang, T. Jin, and F. Xu, "A novel SDN design to support SIC for WiFi networks," in *IEEE International Conference on Computer and Communication Systems (ICCCS)*, (Singapore), pp. 549–553, Feb. 2019.

[190] T. Tandai, H. Mori, K. Toshimitsu, and T. Kobayashi, "An efficient uplink multiuser MIMO protocol in IEEE 802.11 WLANs," in *International Symposium on Personal, Indoor and Mobile Radio Communications*, pp. 1153–1157, Sept. 2009.

[191] A. Ettefagh, M. Kuhn, C. Eşli, and A. Wittneben, "Performance analysis of distributed cluster-based MAC protocol for multiuser MIMO wireless networks," *EURASIP Journal on Wireless Communications and Networking*, no. 1, p. 34, 2011.

[192] T. W. Kuo, K. C. Lee, K. C. J. Lin, and M. J. Tsai, "Leader-contention-based user matching for 802.11 multiuser MIMO networks," *IEEE Transactions on Wireless Communications*, vol. 13, pp. 4389–4400, Aug. 2014.

[193] K. Tan, H. Liu, J. Fang, W. Wang, J. Zhang, M. Chen, and G. M. Voelker, "SAM: Enabling practical spatial multiple access in wireless LAN," in *Annual International Conference on Mobile Computing and Networking*, pp. 49–60, Sept. 2009.

[194] S. Wu, W. Mao, and X. Wang, "Performance study on a CSMA/CA-based

MAC protocol for multi-user MIMO wireless LANs," *IEEE Transactions on Wireless Communications*, vol. 13, pp. 3153–3166, June 2014.

[195] H. Jin, B. C. Jung, H. Y. Hwang, and D. K. Sung, "Performance comparison of uplink WLANs with single-user and multi-user MIMO schemes," in *IEEE Wireless Communications and Networking Conference*, (Nevada, US), pp. 1854–1859, Mar. 2008.

[196] T. H. Lin and H. T. Kung, "Concurrent channel access and estimation for scalable multiuser MIMO networking," in *Proceedings of IEEE INFOCOM*, (Turin, Italy), pp. 140–144, Apr. 2013.

[197] D. Jung, R. Kim, and H. Lim, "Asynchronous medium access protocol for multi-user MIMO based uplink WLANs," *IEEE Transactions on Communications*, vol. 60, pp. 3745–3754, Dec. 2012.

[198] T. Kim, T. Song, W. Kim, and S. Pack, "Phase-divided MAC protocol for integrated uplink and downlink multiuser MIMO WLANs," *IEEE Transactions on Vehicular Technology*, vol. 67, pp. 3172–3185, Apr. 2018.

[199] S. Zhou and Z. Niu, "Distributed medium access control with SDMA support for WLANs," *IEICE transactions on communications*, vol. 93, no. 4, pp. 961–970, 2010.

[200] B. W. Ke, Y. J. Zhang, and S. C. Liew, "Media access control with spatial correlation for MIMO ad hoc networks," in *IEEE International Conference on Communications*, pp. 3660–3665, June 2007.

[201] K. Higuchi and A. Benjebbour, "Non-orthogonal multiple access (NOMA) with successive interference cancellation for future radio access," *IEICE Transactions on Communications*, vol. 98, pp. 403–414, Oct. 2015.

[202] M. F. Uddin, "Throughput analysis of a CSMA based WLAN with succes-

sive interference cancellation under rayleigh fading and shadowing," *Wireless Networks*, vol. 22, pp. 1285–1298, May 2016.

[203] I. Berenguer, X. Wang, and V. Krishnamurthy, "Adaptive MIMO antenna selection via discrete stochastic optimization," *IEEE Transactions on Signal Processing*, vol. 53, pp. 4315–4329, Nov. 2005.

[204] A. Masadeh, Z. Wang, and A. E. Kamal, "Reinforcement learning exploration algorithms for energy harvesting communications systems," in *IEEE ICC*, (Missouri, US), May 2018.

[205] C. Bishop, *Pattern Recognition and Machine Learning.* Springer-Verlag New York, 2006.

[206] S. Cho, "SINR-based MCS level adaptation in CSMA/CA wireless networks to embrace IoT devices," *Symmetry*, vol. 9, no. 10, p. 236, 2017.

[207] M. Tarique and M. T. Hasan, "Impact of nakagami-m fading model on multi-hop mobile ad hoc network," *International Journal of Computer Applications*, vol. 26, no. 2, pp. 5–12, 2011.

[208] D. Yuan, V. Angelakis, L. Chen, E. Karipidis, and E. G. Larsson, "On opimal link activation with interference cancellation in wireless networking," *IEEE Transactions on Vehicular Technology*, vol. 62, pp. 939–949, Feb. 2013.

[209] C. Andrieu, N. de Freitas, A. Doucet, and M. I. Jordan, "An introduction to MCMC for machine learning," *Machine Learning*, vol. 50, pp. 5–43, Jan 2003.